AFRPシート緊張接着によるRC梁の曲げ補強法の開発に関する実験的研究

EXPERIMENTAL STUDY ON DEVELOPMENT OF STRENGTHENING METHOD FOR RC BEAMS REINFORCED WITH PRE-TENSIONED AFRP SHEET

by

Abdel Aziz Mohamed Ali Ibrahim Abdel Aziz

A Dissertation Submitted for the Division
of
Civil and Environmental Engineering
in
Partial Fulfillment of the Requirements for the Degree
of
Doctor of Philosophy of Engineering

Muroran Institute of Technology
Muroran, JAPAN
September, 2011

ACKNOWLEDGEMENTS

The research was carried out under the supervision of Dr. Norimitsu Kishi, Professor of Chair of Structural Mechanics, Muroran Institute of Technology, Muroran, Japan. His motivation, encouragement, dedication, positive mind, and valuable advice made it a very exciting and invigorating experience.

The author likes to extend thanks and sincere appreciation to Dr. Norimitsu Kishi, for his generous and articulate guidance and encouragement in conducting this research. The author also acknowledges gratitude to all members of the Final Examination Committee: for their helpful suggestions.

The author also thanks Dr. Kurihashi, Dr. Komuro, and all graduate students for their assistance during this study.

Grateful appreciation is extended to the ministry of high education, Egypt, for awarding Scholarship throughout the whole period of the graduate study.

I would like to thank my mother and my wife for their rate of confidence and encouragement throughout my graduate studies.

TABLE OF CONTENTS

LIST OF TABLES

LIST OF FIGURES

ABSTRACT

Nowadays, Fiber Reinforced Polymer (FRP) sheet bonding method has been rapidly introduced for reinforcing and/or retrofitting of the existing Reinforced Concrete (RC) structures. Due to bonding normal FRP sheet onto the tension-side surface of the RC members, the effects due to bonding the FRP sheet can be expected after rebar yielding. However, cracking and rebar yielding loads cannot be much improved. Recently, in order to increase not only the ultimate load-carrying capacity of the RC members but also cracking and rebar yielding loads, pre-tensioned FRP sheet bonding method has been developed. In the previous studies, metal system was applied as anchoring devices of the sheet. Even though the premature failure at the ends of the sheet can be prevented by applying the metallic anchoring system, the installation of the system into RC members is not easy task because of its heavy weight. Also, stainless steel must be used to be anti-corrosive when FRP sheet is applied. Then, in order to easily apply the pre-tensioned FRP sheet bonding method for reinforcing RC members, the anchoring system should be simplified without any dropping of anchoring performance.

From this point of view, here, a flexural reinforcing method using pre-tensioned AFRP sheet without metallic device was proposed. In this method, to distribute the concentrated anchoring stresses of pre-tensioned AFRP sheet, the base cross-directional non-pre-tensioned AFRP sheet was bonded to the concrete surface around the anchoring area. In addition, to decrease gradients of bonding stresses near the anchoring area, a strain relaxation polymer (with low young's modulus) was used as a bonding material. The applicability of the method was discussed by conducting four-point loading test of the flexural reinforced RC beams with pre-tensioned AFRP sheet and comparing the experimental results with the numerical ones. The analytical portion of the research is employed to describe the flexural behavior of the all tested beams. A multi-section method was applied to analytically estimate the load-displacement relation and the axial strain distribution of AFRP sheet used for flexural

reinforcing each RC beam. This research is divided into three studies as follows;

(1) Strengthening Study of RC beams; this study examined the behavior of flexural pre-tensioned AFRP strengthening systems without anchoring device, hence investigate the effectiveness and feasibility of a proposed anchoring method. The variables used in the experimental program included the pre-tension force ratio introduced to the AFRP sheet (0, 20, and 40%) and the main reinforcement steel ratio (0.79 and 1.24%). From this study, the results show that the proposed anchoring method is effective and feasible because the load-carrying capacity increased considerably. A good agreement between experimental and analytical methods was achieved up to ultimate state with somewhat a perfect bonding between the AFRP sheet and concrete surface.

(2) Strengthening Study of pre-cracked RC beams; this study investigated the load-carrying behavior of pre-cracked RC beams strengthened with pre-tensioned sheet compared to non-pre-cracked ones. Pre-tension force ratio introduced to the AFRP sheet (0 and 40%) and level of prior loading (Level 1 is up to main rebar yielding; Level 2 is up to average point between main rebar yielding and ultimate load) were taken as variables. From this study, it is observed that due to introducing pre-tension force into the sheet, flexural capacity and durability of the pre-cracked RC beams can be improved and the width of cracks can be decreased. This implies that a new anchoring method is effective and feasible. Numerical results can better match the experimental results for non-pre-cracked beams but not for pre-cracked beams subjected to high prior loading because the existing cracks and the stiffness of putty used for flattening the bonding surface were not considered in numerical analysis.

(3) Repair Study of pre-cracked RC beams; this study examined the effectiveness of pre-tensioned AFRP systems to restore capacity of repaired pre-cracked RC beams reinforced with pre-tensioned sheet. Pre-tension force ratio introduced to the AFRP sheet (0 and 40%), with/without existing cracks and with/without repairing the cracks by injection epoxy resin were taken as variables. From this study, it can be concluded that : 1) flexural load-carrying capacity of the pre-cracked RC beams can be significantly improved by bonding the pre-tensioned AFRP sheet onto the tension-side surface;2) by repairing the existing cracks, the sheet rupture can be prevented because the opening of cracks and also large strains occurring in the sheet due to the opening can be rationally restrained; and 3) numerical results can better match the experimental results for non-pre-cracked beams but not for pre-cracked ones.

CHAPTER 1

INTRODUCTION

1.1 General

Repair and strengthening of Reinforced Concrete (RC) structures and bridges are major challenges facing structural engineers. Most of the infrastructure is usually subjected to overload, which causes a structure failure at a load level below its capacity. So that overload should be taken into consideration in the retrofitting RC structures. Moreover, these structures that have been built more than several decades ago may need to be strengthened and upgraded to meet the current service load demands. Several methods of strengthening RC structures using various materials have been studied and applied in the retrofitting field. The most recent type of material used is Fiber Reinforced Polymer (FRP) reinforcement. FRP has proven to be an excellent strengthening material for the retrofitting of RC structures compared to other traditional strengthening materials. Thus, FRP material is increasingly attracting the attention of civil engineers worldwide because of such favorable performance characteristics as high strength-to-weight ratio, resistance to corrosion, and magnetic neutrality. There are many methods for repair and strengthening of existing structures. A method that is appropriate for particular structure may not necessarily be appropriate for another. The common methods for the strengthening and repair of RC structures are:

1- Surface treatment methods;
2- Injection as a repair technique;
3- Jacketing;
4- External reinforcement;
5- Post-tensioning;
6- Fiber-reinforced polymer material.

In this research, FRP sheet is chosen to be tested as a strengthening and repair method and to investigate the effectiveness and feasibility of using a new anchoring method without anchoring devices at the end of the pre-tensioned FRP sheet. FRP sheet is considered a new structural material, which is under investigation to replace reinforcing steel. The following are the advantages of this method compared to others:

1- High strength to weight ratio for FRP;

2- The increase in weight of the structure after repair or strengthening is negligible;

3- High resistance against corrosion;

4- Ease application by hand-lay-up;

5- Does not need very high experience;

6- The short period of execution;

7- In most cases, it does not need complete vacation of the building;

8- No need for high technology.

These advantages can overcome the relatively high cost of the material. Also, some disadvantages of using FRP for strengthening and repair must be taken into account. They are lower modulus of elasticity of FRP as compared to steel, and linear behavior of FRP materials, which can lead to brittle failure.

This study examines the behavior of RC beams reinforced with FRP sheet. Due to deficiencies in the built environment, engineers may be asked to retrofit or upgrade the capacity of an existing concrete structural member. This could be a result of new demands on the structure, or a repair of damage from an unforeseen event. A possible capacity timeline of a structure is shown in **Fig.1.1**, illustrating the philosophy behind structural repair and strengthening. Three structural deficiencies are shown. The first is a result of problems with the as-built condition of the structure, either from a design or construction flaw. Important reinforcement could have been mistakenly omitted, the design cross-sectional dimensions may not have been properly constructed, or perhaps the regular service loading of the structure exposed flaws in the design process. The second structural deficiency shown in **Fig.1.1** is the result of an accident which impairs the ability of the structure to safely carry load, resulting from an impact event, fire, etc. The third structural

deficiency may result when the demand on the structure is changed by the owner. Strengthening is then required to upgrade the capacity to meet new loading demands.

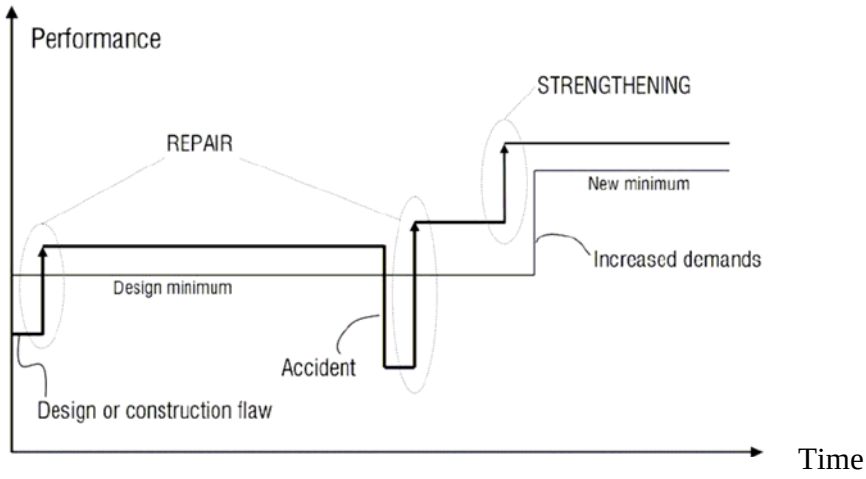

Fig.1.1 Repair/strengthening philosophy (Carolin 2003)

Retrofits are possible using the traditional building materials of concrete and steel. The cross-section of the structural element can be increased, or steel plates can be bolted or adhesively affixed to the structure to increase capacity. In some cases of structural repair after an accident, the internal reinforcing can be spliced back together to restore the capacity. Each of these techniques is costly, and some perform poorly under service conditions. The main benefit of using FRP materials for the strengthening of existing structures is the lightweight nature of the composite materials, which makes the use of extensive scaffolding (required in the installation of steel plates) unnecessary.

This research study was initiated by a desire to more fully understand the behavior of RC beams repaired or strengthened with pre-tensioned FRP sheet with a new anchoring method without metal devices. There have been only a few studies which have examined the behavior of retrofitted RC beams using pre-tensioned FRP sheet bonding method, and most of the studies focusing on using non-pre-tensioned FRP sheet or pre-tensioned FRP sheet with metal system.

By bonding non-pre-tensioned FRP sheet onto the tension-side surface of the RC members, the load-carrying capacity of the members can be increased, but cracking and rebar yielding loads cannot be much increased (El-Hatcha et al. 2004). However, these loads can be increased by introducing pre-tension force into the FRP sheet (Wight et al 2001. and Kishi et al. 2009). Sang et al. (2008) and Dong et al. (2009) independently investigated reinforcing effects of pre-tensioned Carbon FRP (CFRP) sheet on flexural behavior of the RC beams. In these studies, they applied a metal system as anchoring devices of the sheet. Even though the premature failure at the ends of the sheet can be prevented by applying the metallic anchoring system, the installation of the system into RC members is not an easy task because of its heavy weight. Also, stainless steel must be used to be anti-corrosive when CFRP sheet is applied. Then, in order to easily apply the pre-tensioned FRP sheet bonding method for reinforcing RC members, the anchoring system should be simplified without dropping the anchoring performance.

From this point of view, here, a flexural reinforcing method using pre-tensioned Aramid FRP (AFRP) sheet was proposed. In this method, a simple anchoring system without metallic device was applied. The applicability of the method was discussed by conductinga four-point loading test of the flexural reinforced pre-cracked RC beams with bonding pre-tensioned AFRP sheet and comparing the experimental results with the numerical ones.

1.2 Objective and scope of research

The aim of this research is to develop a rational flexural reinforcing method for strengthening RC beams using a pre-tensioned AFRP sheet with a new proposed anchoring method. In this method, to distribute the concentrated anchoring stresses of pre-tensioned AFRP sheet, the base cross-directional non-pre-tensioned AFRP sheet was bonded to the concrete surface around the anchoring area. In addition, to decrease gradients of bonding stresses near the anchoring area, a strain relaxation polymer (with low young’s modulus) was used as a bonding material. An applicability of the proposed method for anchoring pre-tensioned AFRP sheet was investigated by conducting a static four-point loading test. In addition, a multi-section method was employed to analytically predict the flexural

behavior of the tested beams.

The objectives of this research are threefold. First, to investigate the overall structural behavior of pre-tensioned FRP Strengthened RC beam, effectiveness and feasibility of using a simple anchoring method without metal system is studied. The second objective is to study the applicability of using pre-tensioned FRP sheet bonding method to strengthen pre-cracked RC beams. The third objective of this research is to investigate the flexural behavior of pre-tensioned FRP bonding method by repaired pre-cracked RC beams.

A total of 20 RC beams were tested in the course of this research; 8 as part of a Strengthening Study of RC beams, 5 as part of a Strengthening Study of pre-cracked RC beams, and 7 as part of the Repair Study of pre-cracked RC beams.

-The Strengthening Study of RC beams, whose experimental program will be described in Chapter 6 of this dissertation, examined the behavior of flexural pre-tensioned AFRP strengthening systems. The variables examined in the experimental program included the pre-tension force ratio introduced to the AFRP sheet (0, 20, and 40%) and the main reinforcement steel ratio (0.79 and 1.24%).

-The Strengthening Study of pre-cracked RC beams, whose experimental program will be described in Chapter 7, investigated the load-carrying behavior of pre-cracked RC beams strengthened with pre-tensioned sheet compared to non-pre-cracked ones. Pre-tension force ratio introduced to the AFRP sheet (0 and 40%) and level of prior loading (Level 1 is up to main rebar yielding; Level 2 is up to average point between main rebar yielding and ultimate load) were taken as variables.

-The Repair Study, whose experimental program will be described in Chapter 8, examined the effectiveness of pre-tensioned AFRP systems to restore the capacity of pre-cracked RC beams repaired with pre-tensioned sheet. In this study, pre-tension force ratio introduced to the FRP sheet (0 and 40%), with/without existing cracks and with/without repairing the cracks were taken as variables.

The analytical portion of the research is employed to describe the flexural behavior of all tested beams and for comparison with the experimental results. A multi-section method was applied to analytically estimate the load-displacement relation and the axial strain

distribution of AFRP sheet used, flexural reinforced by each RC beam with different ratios of pre-tension stress in the sheet and the main reinforcement steel ratio.

1.3 Outline of thesis

This thesis consists of nine chapters followed by references as follows:

Chapter 1: Introduction.

This chapter contains historical remarks, advantages and disadvantages of the FRP, the importance of using FRP in strengthening and repair existing concrete structures, objectives of the thesis, and the main content of the thesis.

Chapter 2: Contains a literature review of experimental and analytical programs using non-pre-tensioned and pre-tensioned FRP and failure mechanisms of the beams strengthened with FRP. This chapter also includes full historical review for the composite materials, their different types, shapes and methods of production.

Chapter 3: Presents previous and a new proposed anchoring method of bonding pre-tensioned FRP sheet, as well as the used pre-tensioning process.

Chapter 4: Describes experimental tests on RC beams strengthened or repaired with FRP sheet. The choice of the test parameters and detailed description of the different test specimens used is included. The preparation of the specimens and the properties of the materials used are also presented. At the end of this chapter, a detailed description of the different setups, loading and measuring devices for the different types of experiments is also given, as well as the method of testing each different parameter.

Chapter 5: Presents analytical approach, assumptions, constitutive law of the used material and application method.

Chapter 6, 7, and 8: Contains discussion and analysis of experimental and analytical results of the tested RC beams. The results include load-deflection, axial strain distribution curves of the sheet, and failure loads and crack patterns.

Chapter 9: Contains summary and conclusions in detail for all studies explained in Chapters 6.7, and 8.

CHAPTER 2

BACKGROUND AND LITERATURE REVIEW

2.1 Introduction

Flexural strengthening/repair using FRP materials can improve dramatically the overall performance of existing structures. Large increases in ultimate load are possible, and in many cases the ductility of the original system can be maintained with proper detailing of the FRP retrofit. In addition to maintaining ductility, the original failure mode of the structural system (crushing of concrete) can be preserved with certain FRP designs.

Due to deficiencies in the built environment, many universities and research organizations have pursued the challenge to repair or strengthen existing structures with pre-tensioned FRP materials in flexure. This chapter provides a summary of the literature in the field of flexural FRP repair or strengthening of concrete structures. Topics in this section include: 1) Non-pre-tensioned FRP strengthening/repair of concrete structures, 2) Pre-tensioned FRP strengthening/repair of concrete structures, 3) The use of near surface mounted (NSM) FRP reinforcement, 4) FRP systems and failure mechanism, and 5) Definition of FRP material.

2.2 Strengthening concrete structures with non-pre-tensioned FRP strips

FRP strips have been widely applied to the strengthening and upgrading of structurally inadequate concrete structures because of their unique advantages such as high strength-to-weight ratio and considerably good resistance to corrosion over the conventional steel bars and plates. The existing applications of FRP reinforcement in buildings, bridges and tunnel linings have demonstrated that the FRP bonding technique is remarkably efficient. Some research efforts on this topic carried out are outlined as follows:

The use of fibers to increase the strength of various buildings and structures is an ancient technology – utilized when people first started using straw in clay bricks for residential walls and roofs (Nanni 1999). These early uses saw the advantage of using two materials with different material properties. After World War II, the use of FRP was mainly confined to the military for boat hulls, submarine parts and aircraft components. Once it became economically feasible, industry took advantage of the excellent properties of FRP materials, manufacturing everything from fishing poles and bicycle frames to architectural components and bath tubs. In the 1960's, FRP began to be used in structural applications mainly as a result of its non-corrosive properties. Bridge deck slabs, sea walls, and floor slabs in aggressive chemical environments were reinforced with Glass FRP as an alternative to epoxy coated reinforcing (ACI 440 1996). Strengthening buildings and bridges using FRP was first used as an alternative to the bonding of steel plates to the soffits of RC beams (Oehlers 1990). FRP strengthening gained popularity in Europe and Japan in the 1980's as a result of the high strength to weight ratio and easy installation of FRP materials. Throughout the 1990s, the use of FRP in North America, Europe and Asia has continued to become more prevalent with many repair and strengthening projects completed. The number of companies manufacturing FRP products has also increased, with numerous companies producing FRP sheets, reinforcing bars and pultruded laminates. The primary reason that RC beams are no longer commonly strengthened in flexure with externally bonded steel plates is simply because of the difficulty in installation. It is still widely believed that corrosion is a serious problem, but a study of RC beams strengthened with externally bonded steel plates by Swamy et al. (1995) proved otherwise through the experimental testing of the beams after 12 years of environmental exposure. The authors observed increases in the flexural strength of the beams over time in every case.

Yeong-Soo and Chadon (2003) investigated flexural behavior of RC beams strengthened with CFRP laminates at different levels of sustaining load. Results of the experiments and model predictions showed that sustaining load levels at the time of strengthening have more influence on deflections of beams at yielding and at ultimate stage than on the ultimate strength of the beam.

Federico et al. (2003) studied an analysis of FRP composite grid RC beams. This study focuses on the use of explicit finite element analysis tools to predict the behavior of FRP composite grid RC beams subjected to four-point bending. A comparison of the proposed approach with the experimental data indicated that the procedure provides a good lower bound for conservative predictions of load-carrying capacity.

Ayman et al. (2001) showed that an externally bonded CFRP laminates are a feasible and economical alternative to traditional methods for strengthening and stiffening deficient RC and PC girders. Good agreement is found between theory and experimental results of concrete T-beams strengthened with varying amounts of CFRP laminates.

Laura et al. (2001) studied bond of FRP laminates to concrete. It is concluded that failure occurred in the concrete- adhesive interface, with very little or no sign of damage in the concrete surface. The number of plies used to make CFRP laminate affected the bond failure load, but the average of the ultimate loads of specimens strengthened with 2-ply was only 1.5 times that of specimens strengthened with 1-ply.

Teng et al. (2001) presented an experimental study on RC cantilever slabs bonded with GFRP strips. The results showed that: 1) although all the GFRP-strengthened slabs experienced debonding of FRP strips, some of them eventually failed by FRP rupture, 2) from the viewpoint of ductility, debonding leads to more ductile behavior of the slab.

Zhishen and Jun (2003) focused on the study of concrete cracking behavior and interfacial debonding fracture in FRP-strengthened concrete beams. An experimental program is systematically reviewed according to the observed failure modes, in which it is found that the interfacial debonding may propagate either within the adhesive layer or through concrete layer in the vicinity of bond interface. The results showed that; 1) Imperfection of FRP–concrete bond with low interfacial bond strength and interfacial fracture energy is one major factor to cause the premature debonding in adhesive layer, 2) If concrete is relatively brittle with low fracture energy, interfacial debonding mainly happens through interfacial concrete adjacent to the bond interface.

Thanasis (1998) studied shear strengthening of RC beams using epoxy-bonded FRP composites. The paper deals with the application of FRP laminates or fabrics as shear

strengthening materials for RC beams. From the results, it is shown that the effectiveness of the technique increases almost linearly with the FRP axial rigidity and reaches a maximum, beyond which it varies very little.

Sergio et al. (2001) investigated flexural capacity of RC beams using CFRP composites. Results indicate that strengthening configurations involving techniques such as placement of transverse straps along the composite laminates or bonding the composites on the side surface of the specimens controlled debonding and provided a more ductile failure mode than placement on the bottom surface of the beams.

Osman et al. (2001) described an application of FRP laminates to strengthen an aging RC T-beam bridge. Load tests results revealed that, after installation of the laminates, main rebar stresses were moderately reduced, concrete stresses (flexural and shear) moderately increased, and transverse live-load distribution to the beams slightly improved under service loads.

Houssam and Gerardo (2001) studied the effect of surface preparation on the bond interface between FRP sheets and concrete members. Results show that surface treatment by water jet produces a better bonding strength than surface treatment by sander.

Zhang et al. (2005) presented a numerical prediction method for flexural behavior of RC beams reinforced with FRP sheet. From applying the discrete cracks pattern proposed in this paper, it was confirmed that the load-carrying capacity and failure mode of the RC beams can be better predicted numerically.

Kishi et al. (2005) developed a numerical analysis method by using a three-dimensional elasto-plastic finite element method to simulate the load-carrying capacity of RC beams failed in the FRP sheet peel-off mode. Comparisons between analytical and experimental results confirm that the proposed numerical analysis method is appropriate for estimating the load-carrying capacity and failure behavior of RC beams flexurally reinforced with a FRP sheet.

Mikami et al. (2000) established a rational flexural strengthening method on RC members with FRP sheet. The results obtained from these experiments are: 1) FRP sheet is delaminated from concrete surface due to peeling action of concrete blocks which are

generated by developing flexural and diagonal cracks; and 2) the maximum bending moment of the strengthened RC beams is not affected by FRP sheet material and interval of two-point loading.

Kishi et al. (2007) investigated the influences of rebar yielding on sheet debonding of FRP sheet bonded on the tension-side surface of the RC beams. The results showed that, in case of using rebar with yield point as main rebar, flexural reinforcing effects of FRP sheet can be increased corresponding to an increase in number of sheet piles. On the other hand, in case using rebar without yielding point, if the upper concrete cover has not reached at ultimate state with compression failure mode, FRP sheet may be peeled-off from its end accompanying with the concrete cover before the reinforcing effects due to bonding FRP sheet is generated;

Kurihashi et al. (2002) established a rational flexural strengthening design procedure for RC beams in case using FRP sheet. The results showed that: 1) Failure mode of T-shape RC beams strengthened with AFRP sheet is divided two types apart: sheet Debonding Failure (DF) type and Flexural Compressive Failure (FCF) type; 2) The smaller rebar ratio under keeping sheet volume ratio constant and/or the larger value of sheet volume ratio under keeping the value of rebar ratio constant, the more remarkably the RC beams are failed with DF type.

Sawada et al. (2003) developed a rational sheet debond-controling method for Debonding Failure (DF) type RC beams, proposing U-shape jacketing method. Results obtained from this study were as follows: (1) jacketing with AFRP sheet in the area of half lower height of neutral axis and rebar yield area in the equi-shear span, RC beams can be upgraded upto the point of analytical ultimate state; and (2) not jacketing in U-shape but bonding FRP sheet only on the side-surface of the rebar yield area in the equi-shear span, debonding of flexural strengthening FRPs can be also controlled.

Zhang et al. (2003) investigated influence of material properties of FRP sheet on load-carrying capacity and failure behavior of flexural strengthened RC beams. From this study, it can be observed that in case using FRP sheet with high axial stiffness, FRP sheet will be peeled-off rapidly due to diagonal crack occurred near loading-points in the

equi-shear span, and midspan deflection tends to be small comparing with that of the cases using FRP sheet with low axial stiffness.

Zhang et al. (2007) provided some basic experimental data for investigating the effects of bonding configurations of the FRP sheet on shear load-carrying capacity and failure behavior of the RC beams reinforced with FRP sheet in shear. From this study, the results showed that in case of RC beams reinforced with FRP sheet in U-shape jacketing method, shear load-carrying capacity of the beams is affected by bonding height of the sheet. A higher bonding height of FRP sheet leads to a greater shear load-carrying capacity.

Süleyman et al. (2010) compared the analysis results of footbridges using steel and CFRP materials. Three dimensional finite element model of the footbridge is created by SAP2000 software using both steel and CFRP materials. It is seen from the analyses result that CFRP is more effective than steel.

Osman et al. (2010) presented a numerical study for strengthening flat slab using CFRP. The CFRP sheets and plates were externally bonded to the slab tension face. Analytical study showed that most of the studied codes design expressions varied in predicting the capacity observed in the tests. The using of CFRP Sheets or plates in strengthening flat slabs led to significant improvement in the flexural capacity and less improvement in the punching capacity.

Ramadan et al. (2010) investigated the effect of external strengthening technique using CFRP sheets on the behavior of RC box girders. Results showed an increase in ultimate and crack loads, good improvement in the response in loads capacity, deflections, and effectiveness of the present suggested technique.

2.3 Strengthening/repair of pre-cracked concrete structures with non-pre-tensioned FRP strips

The use of FRP strips is a more innovative technique that has the potential to not only restore the ultimate strength of the damaged concrete structures, but also withstand the repetitive service loadings that all structures members undergo. Several experimental studies have examined the use of FRP to repair/strengthen pre-cracked concrete structures

as follows;

Saadatmanesh and Ehsani (1990) performed a parametric study to examine the effect of different design material properties and quantities on the strength of glass FRP retrofitted beams. An effective way of eliminating the corrosion problem is to replace steel plates with corrosion-resistant synthetic materials such as fiber composites. Strengthening concrete beams with epoxy bonded GFRP plates appears to be a feasible way of increasing the load carrying capacity of existing bridges.

Mohsen et al. (2001) presented results of an experimental investigation on the effectiveness of flexural strengthening with epoxy-bonded, CFRP laminates. The girders were preloaded up to 65, 85, and 117% of control yield moment and locked and strengthened with two layers of CFRP wraps before resuming the loading up to failure. The results demonstrate the feasibility of rehabilitating and strengthening damaged RC structures with CFRP wrap while the structures are under service load.

Grace et al. (1999) studied the behavior of RC beams strengthened with various types of FRP laminates. Each beam was initially loaded above its cracking load. It is concluded that, in addition to the longitudinal layers, the fibers oriented in the vertical direction forming a U-shape around the beam cross-section significantly reduce beam deflections and increase beam load-carrying capacity.

Aging conditions are described for slandered concrete cylinders wrap with the same E-glass and aramid woven fabric reinforcement, and emarginated with the same epoxy resin employed to repair three deteriorated pier columns in a highway bridge in West Virginia (Lopiz et al. 1999). The results show that confinement of concrete columns with FRP wrap increases the strength and ductility of the structure.

One common repair technique is to splice the steel prestressing strands; however, this was found to perform poorly during fatigue, and in many cases it was unable to restore the ultimate strength of the girder (Zobel and Jirsa 1998). The use of FRP materials is a more innovative technique that has the potential to not only restore the ultimate strength of the damaged girder, but withstand the repetitive service loadings that all bridge girders undergo.

In Alabama, one span of a reinforced concrete bridge was chosen to repair damage due to aging (Stallings et al. 2000). The results of these load tests demonstrated that the FRP repair system reduced girder deflections ranging between 2 to 12 percent, as well as reducing rebar stresses by an average of 8 percent. The usage of CFRP plates to repair and strengthen RC bridge girders was successfully verified by field loading tests.

Three separate PC bridges were repaired with CFRP systems in repair projects sponsored by the Missouri Department of Transportation. In the first project, eleven prestressed concrete bridge girders located on a bridge in Independence, MO were impact damaged due to an over height vehicle and repaired with CFRP wet lay-up sheets (Schiebel et al., 2001). Detailing of the CFRP repair system followed industry standards and provided transverse U-wraps at 400 mm spacing and extension of the CFRP well away from the damaged concrete area. In the second project, PC bridge girder was repaired in-situ with CFRP wet lay-up sheets after damage due to impact ruptured two prestressing strands (Tumialan et al. 2001). Following current industry standards, the CFRP repair system was successfully installed by a contractor. Field testing was not performed, however the repaired girder is performing well in service. A third project sponsored by the Missouri DOT, repaired impact damage caused by a contractor who struck a girder during construction of a new bridge (Di Ludovico et al. 2003). Two prestressing strands were ruptured and a significant loss of concrete occurred. The concrete section was restored and the girder repaired using CFRP sheets in both the longitudinal and transverse directions. Load testing was not performed on the repaired section, but the girder is currently performing well under traffic loading.

The Iowa Department of Transportation has sponsored several research projects that involved the use of CFRP to repair impact-damaged PC bridge girders. In the first project, several over height impacts damaged all the girders on a bridge (Klaiber 1999). CFRP sheets were added in the transverse direction to prevent debonding. Load tests after the CFRP installation indicated that the repaired girder exhibited 27 percent less deflection than the damaged girder. In a second project sponsored by the Iowa DOT, a bridge was load tested before and after the installation of a CFRP repair system. The researchers concluded that flexural strengthening of impact-damaged PC girders is possible when up to 15% of

the strands are severed.

An experimental project was sponsored by the Florida Department of Transportation to create guidelines, standard practices, and experimental data for the repair of impact-damaged bridge girders using CFRP systems (Green et al. 2004). The researchers concluded that FRP can be used to restore a significant portion of the strength capacity of an impact-damaged girder, however they observed that proper detailing at termination points is critical to any FRP system.

Di Ludovico et al. (2005) tested three 11 m PC bridge girders, with a 810 mm composite cast-in-place slab monotonically to failure to assess the flexural behavior of repaired damaged sections with CFRP wet lay-up laminates. The results show that the CFRP system can restore the ultimate capacity and stiffness of the original girder, but the two repaired girders could not match the original serviceability.

El-Tawil and Okeil (2002) conducted a parametric study of PC bridge girders flexurally rehabilitated with CFRP laminates. Three levels of damage were examined corresponding to a 10, 20 and 30 percent nominal loss of prestressing strands. They proposed using a reliability index of 3.75. This is slightly more conservative than American Association of State Highway and Transportation Officials Load Resistance Factor Design (AASHTO LRFD) mandated value for PC girders to account for the brittle nature of CFRP rupture, which was the failure mode for the girders they analyzed.

Mahmoud et al. (2010) investigated the effectiveness of using CFRP sheets for the repair of pre-cracked RC beams due to flexural failure. Twelve RC beams, including ten beams were pre-cracked and repaired with CFRP sheets at two different levels of preload (50% and 83% of their ultimate capacity). The results indicated that the gain in the ultimate flexural strength is more significant for beams strengthened with two plies of CFRP sheets. Also, the results showed that the preload level has not any considerable effect on the flexural capacity or mode of failure of the repaired beams.

2.4 Strengthening of concrete structures with pre-tensioned FRP strips

Although bonding an FRP strips to a beam can increase its ultimate strength, the sheet does not significantly change the cracking load or the behavior of the beam under service loads. However, by prestressing the sheet, the material is used more efficiently since it contributes to the load-bearing capacity under both service and ultimate conditions. It closes cracks, delays the opening of new ones, and can restore prestress to a system that has suffered a loss of internal prestressing. A beam strengthened with prestressed sheets may also attain higher ultimate loads than one strengthened with non-prestressed sheets because the failure mode of the strengthened beam may change. Since the sheets are fully bonded over their length to the lower face of the concrete girder, they provide excellent control of cracks and contribute more strength enhancement than unbonded tendons. Although many topics have been investigated thus far, the application of prestressed FRP sheets is limitedly reported. Triantaflllou and Deskovic (1991) described the short-term mechanical behavior of a novel prestressing technique. The technique involves external bonding of pre-tensioned FRP composite sheets on the tension zones of structural elements. Analytical models are developed describing the maximum achievable prestress level so that the FRP-prestressed system does not fail near the anchorage zones. It is found that the method's efficiency is improved by increasing the thickness of the adhesive layer and/or increasing the area fraction of the composite material, efficiency being defined as the level of prestress at the bottom fiber of the member.

Later, to verify their analytical model, Triantafillou et al. (1992) studied the effect of prestressed CFRP sheet on RC beams. They found that the prestressed CFRP sheets significantly improved the serviceability and shear capacity of the strengthened beams due to their confinement effects. A reasonable agreement was achieved between their model and the obtained experimental results. It was also found that excellent flexural behaviour was obtained in terms of strength, stiffness, and ductility.

Taljesten (1997) carried out a research in the area of plate bonding, i.e., the problems that can arise when concrete members need to be strengthened using prestressed FRP plates. The results showed that the stresses are very large at the end of the plate, but the quickly

diminish as we move nearer the center of the beam. The magnitude of the stresses is influenced not only by geometrical and material parameters of the beam, but also by the adhesive and the strengthening material. The performed study showed a good agreement with finite element analysis.

A similar study was conducted by Quantrill and Hollaway (1998). The prestressing technique employed was developed and refined on smaller-scale 1.0m length specimens before being applied to larger 2.3m length beams studied with two levels of prestressed CFRP plate (ranging from 17.5% - 41.7% of the CFRP plate tensile strength). The main conclusions drawn from the work indicated that the technique of prestressing advanced composite plates prior to bonding to RC beams has the potential to provide a more ancient solution to strengthening problems.

Wight et al. (2001) conducted an experimental project to evaluate the effectiveness of prestressed CFRP sheets for strengthening RC beams. A prestressing level of 200MPa in the CFRP sheet was examined. Serviceability and ultimate conditions are considered in the theoretical prediction of beam behavior, including the effects of multiple layer prestressing and external loading. The bonding of prestressed FRP sheets to the tensile face of concrete beams improved both the serviceability and the ultimate behavior of the RC beams. Therefore, prestressing of CFRP sheets to strengthen RC structures was an effective and practical method.

Sang et al. (2008) evaluated the flexural behavior of RC beams strengthened with prestressed CFRP plates. The results show that; 1) the non-prestressed specimens fail by spalling of the CFRP plate from the RC beam, while prestressed specimens fail due to CFRP plate failure, 2) surface bonding with a CFRP plate without prestressing increases the ultimate load of a specimen as much as 20.6%, and strengthening with prestressed CFRP plate increases the ultimate load as much as 46.7%–243.0%.; and 3) the initial cracking is considerably delayed as prestressing level increases, whereas concrete compressive strength and tensile steel reinforcement ratio are not effective for the delay of initial cracking.

Dong et al. (2009) tested 13 FRP-strengthened RC beams in flexure and used the finite element method for analysis. The various variables included bonding or no bonding of the FRP, the anchorage system, the amount of prestressing, and the span length. The flexural test results and analytical predictions for the CFRP-strengthened beams showed very good agreement in terms of the debonding load, yield load, and ultimate load. The ductility of the beams strengthened with CFRP plates having the anchorage system was considered high if the ductility index was above 3.

New techniques for applying prestressed CFRP sheets have been proposed and include use of apparatus to reduce the prestress at the end of the sheet and avoid the need for permanent anchors (Stoecklin and Meier 2001 and 2003). In this method, the prestressing force can be reduced gradually towards both ends of the FRP strip. This increases the development length of the prestressing force such that the occurrence of shear stresses remains within the limitations of the shear strength of concrete. This can be achieved by using a purposely developed pre-tensioning device, which allows the CFRP strips to be debonded the concrete structure using a stepwise approach.

However, in short PC beams, the results of the experiments showed that the gradient anchorages method was not effective because gradient anchorage was in the region of high shear stresses from loading as well as initial prestress (Aram et al. 2008). This method would be more effective for large span beams, like bridge girders, with enough of an uncracked zone (anchorage length) or smaller shear stresses from loading (Czaderski and Motavalli 2007).

Ferrier et al. (2001) studied the mechanical behavior of RC element strengthened with external prestressed composite plates taking material properties and composite prestress level as variables. In this study, FRP plate was anchored using FRP U-shape around the pre-tensioned sheet ends. The results indicated that the use of prestressed externally bonded composite is effective method to increase the efficiency of external reinforcement and allowed increasing the composite strain level under structure loading. Moreover, using FRP U-shape resulted in avoiding slippage and peeling off the composite plate.

Kim et al. (2008 a,b) presented the flexural behavior of RC beams strengthened with

prestressed CFRP sheets using nonmetallic anchor systems. The study showed that the developed nonmetallic anchors are more effective in resisting peeling-off cracks compared to the permanent steel anchors and the beams strengthened with the nonmetallic anchors provide comparable load-carrying capacity with respect to the steel anchored control beam.

Piyong et al. (2008 a,b) used nonmetallic anchorages (by warping FRP in a U-shape around the pre-tensioned sheet ends). In this research, a mechanical device for prestressing CFRP sheet was developed, in which prestressing is applied by manual torque wrench without the need for power-operated hydraulic jack. The results showed that the device was efficient and the load-carrying behavior of the beams reinforced with pre-tensioned CFRP sheet considerably increased, compared to control ones.

Recently, pre-tensioned FRP sheets bonding method has been proposed to effectively increase crack-opening load and yield load of the rebar for retrofitting and/or reinforcing existing RC beams with FRP sheets. Also, this kind of reinforcing method for RC structures has been noted and an effective anchoring method for the pre-tensioned AFRP sheets into RC beams was experimentally conducted (Ikeda et al. 2007). The authors concluded that cracking, yielding, ultimate loads increased considerably due to introducing pre-tension force in the FRP sheet.

Shang et al. (2005) presented the experimental results of flexural behaviour of five RC beams strengthened by prestressed-CFRP. Based on the results obtained from the experimental tests, the following conclusions can be reached; (1) Compared to the non-prestressed-CFRP method, the prestressed-CFRP method can significantly increase the cracking load and flexural stiffness and therefore reduce deflection at working load level; and (2) A failure mode of rupture of the prestressed-CFRP sheet (rather than de-bonding) is achievable and hence lead to a full utilization of the CFRP's high tensile strength. In short, the use of prestressed-CFRP sheet is a feasible and effective method to strengthen concrete structures.

Kim et al. (2008c) studied the flexural behavior of two-way reinforced concrete slabs externally strengthened with prestressed or non-prestressed CFRP sheets. A nonlinear three-dimensional finite-element analysis is conducted to predict the flexural behaviors of the

slabs. An increase in the load-carrying capacity of 25 and 72% is achieved for the slabs strengthened with non-prestressed and prestressed CFRP sheets, respectively, in comparison to the unstrengthened slab.

Wu et al. (2009) investigated the flexural behavior of a new FRP deck system, which consists of a series of pultruded FRP tubes post-tensioned together in the direction of traffic. Tests and analysis showed that failure mode, stiffness and capacity of the deck depend on FRP material properties, tube size, span length, interface bond and prestress level. Longer span decks fail in bending, whereas shorter span decks suffer from local shear failure due to stress concentrations at the corner of the tubes. Panel action is generally improved with higher prestressing or by epoxy bonding of the sides of the tubes. Prestressing provides additional redundancy and reserved strength.

Wu et al. (2006) described poly-p-phenylene benzobisoxazole (PBO) Prestressing Upgrading Technique (PPUT) briefly to strengthen a full-scale PC girder. The results showed that; (1) Reasonable strain distribution monitoring results can be achieved by the polynomial curve fitting technology, especially in the case of the Point Fixed bonding method(PF), (2) Both Overall Bonding (OB) and PF installation methods for optic fiber sensing are capable of tensional strain measurement for concrete and PBO sheets, and (3) The proposed multi-layer end anchoring system for relieving shear stress concentration at PBO sheet ends is efficient to avoid the debonding between the concrete surface and the prestressed PBO sheets.

Lee et al. (2002) studied the use of post-tensioned, nonlaminated, CFRP straps as external shear reinforcement for concrete. It was found that the ultimate load capacity of the strengthened beams was significantly higher than that of the control specimen. Nonlaminated prestressed CFRP straps represent efficient and durable reinforcing elements for infrastructure applications. A concrete beam strengthened with CFRP straps exhibited a significantly higher load capacity than an unstrengthened beam.

Diab et al. (2009) discussed experimental results of the short and long-term behavior of the anchorage zones of externally bonded prestressed FRP sheets. Using different layers of FRP sheet, the prestress level of FRP sheets varied from 20% to 40% of the guaranteed tensile

strength. The experimental observation was conducted in an outdoor environment and lasted about twenty months when temperatures were in the 7-30 °C range. The effective bonding length was found to increase to 50% due to creep of the adhesive layer. The anchored end of the FRP sheets using steel plates and anchor bolts is an effective solution to enhance the bond capacity of FRP-concrete interface for short and long-term loading.

Zhou et al. (2010) have developed a brand-new method for externally anchored FRP sheet prestress strengthening, which makes full use of the features of Wave-Shaped-Gear-Grip (WSGG) anchors by fixing both ends and then fastening the middle to force FRP sheets to elongate geometrically and generate a pretension. They concluded that the externally anchored FRP straps prestressing strengthening technology makes full use of the features of WSGG anchors. It uses the operational technique of fixing both ends and then fastening the middle to perform prestress stretching and anchoring of FRP straps. The prestress technique has been proved to be practicable, very simple and convenient.

Mortazavi et al. (2003) presented the results from experiments on a new strengthening technique for concrete columns that uses expansive materials to apply lateral pre-tensioning. The level of pre-tensioning is controlled by using different amounts expansive agent. It is shown that jacketing columns by pre-tensioned FRP materials can increase the load-bearing capacity up to 30% compared with conventional wrapping and up to more than 2 times compared with unconfined concrete.

Rousakis et al. (2003) executed a consequent investigation on concrete cylinders of 5 different strengths and confinements with 3 different prestress levels. The results showed that prestress of the confining device elevates the transition zone, which has importance for the stability of confined concrete columns. The ultimate load is not affected by the degree of prestress. The normalized increase in ultimate load by prestressed confinement decreases with higher concrete strength.

Zhou et al. (2007) investigated the effect of releasing pretension, analytically and experimentally, for flexural members externally bonded with prestressed FRP laminate or near-surface-mounted with prestressed FRP plate or rod. The comparison between the analytical and the measured results showed the analyses in this paper are rational and

correct. If higher prestress is needed, in girders for example, mechanical anchorage such as bolt fastening should be provided to prevent premature debonding from occurring at the ends of the prestressed laminate.

2.5 Strengthening/repair of pre-cracked concrete structures with pre-tensioned FRP strips

El-Hacha et al. (2003 and 2004) developed a technique for strengthening damaged PC T-beams using prestressed CFRP sheet. The feasibility and effectiveness of using bonded prestressed CFRP sheets to strengthen pre-cracked concrete beams at both room (+22°C) and low (-28°C) temperatures have been investigated experimentally. Materials and prestress changes due to temperature variations that would affect and cause changes in flexural behavior were studied. The beams were subjected to loads exceeding the cracking strength by almost 10%. The external load was then removed, residual deflections were observed after unloading, and the beams were subjected to their own dead weight. The strengthened beams showed significant increases in flexural stiffness and ultimate capacity as compared to the control-unstrengthened beams. The flexural behavior of the strengthened beams was not adversely affected by short-term exposure to reduced temperature (-28°C).

Kim et al. (2008d) investigated the flexure of RC beams strengthened with prestressed CFRP sheets. PC beams are constructed and a significant loss of prestress is simulated by reducing the reinforcement ratio to observe the strengthening effects. The beams were precracked and a significant reduction of the internal reinforcement was made. The prestressed CFRP sheets result in less localized damage in the strengthened beam and the level of the prestress in the sheets significantly contributes to the ductility and cracking behavior of the strengthened beams. Consequently, the recommended level of prestress to the CFRP sheets is 20% of the ultimate design strain with adequate anchorages.

Kim et al. (2008e) described detailed flexural behavior, including live load distributions. The bridge has been damaged by frequent impact from heavy trucks, and repaired using prestressed CFRP sheets. They concluded that the prestressed CFRP sheets contributed to

recovering the load-carrying capacity of the damaged exterior girder to the undamaged state; however, no significant differences were found in the change of deflection of the exterior girder (approximately 5%) under the undamaged, damaged, and repaired states.
Kim et al. (2008f) performed a sound repair on a 40 year old four-span prestressed concrete girder bridge with an innovative strengthening method using prestressed CFRP sheets. This application is the first North American field application of its type. An adequate repair design is conducted based on AASHTO LRFD and the Canadian Highway Bridge Design Code. The following conclusions are drawn: (1) an adequate anchor system was necessary to apply a high level of prestress to CFRP sheets, and (2) the flexural load-carrying capacity of the damaged bridge was fully recovered to the level of the undamaged state by applying prestressed CFRP sheets on the tensile side of the girder. Serviceability, especially crack control, was also improved after the repair.
Wu et al. (2003) investigated the effectiveness of poly-p-phenylene benzobisoxazole (PBO) Prestressing Upgrading Technique (PPUT), which is used to retrofit RC beams under fatigue loading using prestressed PBO fiber sheets PFS. The results showed that RC beam strengthened with prestressed PFS following the P-PUT method exhibits satisfactory fatigue performance. The yield and ultimate loads increase due to the additional cracking occurring under fatigue loading.
Mukherjee and Rai (2009) presented the results of an experimental study to investigate the flexural behavior RC beams that have reached their ultimate bearing capacities and then retrofitted with externally prestressed CFRP laminates. The damage in the beams started with bending cracks in the central region of the beam. After unloading the permanent deformations in al the specimens have been recorded. The results indicate that the flexure performance of the rehabilitated beams were far superior to that of the fresh RC beams. The beams had higher failure loads and lower deflections.
Wight et al. (2003) investigated effectiveness of externally bonded non-prestressed and prestressed CFRP sheet for strengthening the damaged spans of continuous, multiple-span beams. The beams were damaged by severely damaging one of the two beams, which caused light damaged in the second span. The results showed that both prestressed and non-

prestressed CFRP sheets are suitable method for restoring flexural strength and stiffness of the beams but the prestressed sheets are more effective at strengthened damaged beams.

One promising means of increasing the capacity of existing shear-deficient beams is to strengthen the structure using external prestressed CFRP straps (Kesse and Lee 2007). Two beams were pre-cracked to a load level of 70% of the unretrofitted ultimate load capacity before being unloaded and strengthened with one five layer or two 10-layer straps. The results demonstrate that the interaction between the strap spacing, the initial prestress force, and the strap stiffness has an important influence on the strengthened behavior. A limited amount of preexisting damage seemed to affect the overall beam stiffness but not the ultimate load capacity.

Hung et al. (2005) studied the strengthening of RC beams using Prestressed Glass FRP (PGFRP). CFRP has recently become popular for use as repair or rehabilitation material for deteriorated RC structures, but because CFRP material is very stiff, the difference in CFRP sheet and concrete material properties is not favorable for transferring the prestress from CFRP sheets to RC members. Glass FRP (GFRP) sheets with Modulus of Elasticity quite close to that of concrete were chosen in this study. T and ⊥-shaped beams were used as the under-strengthened and over-strengthened beams. The GFRP sheets were prestressed to one-half their tensile capacities before being bonded to the T- and ⊥-shaped RC beams. The PGFRP sheets also enhanced the load-carrying capacity. The test results indicated that T-shaped beams with GFRP sheets increased in load-carrying capacity by 55% while the same beams with PGFRP sheets could increase load-carrying capacity by 100%. The ⊥-shaped beams with GFRP sheets could increase load-carrying capacity by 97% while the same beams with PGFRP sheets could increase the load-carrying capacity by 117%.

El-Hatcha et al. (2003b) tested three one-way slabs and three large-scale RC T-beams to investigate the effectiveness of using prestressed CFRP sheets to strengthen concrete beams subjected to fatigue loading. The loading was very severe with amplitude of loading from a small preload to a load from 90-100% of the yield load of the steel reinforcement. The results showed that the prestressed sheet relieved the stresses present in the internal reinforcement steel and were much more effective at extending the fatigue life, increasing

the strength system and improving the serviceability of the beams than non-prestressed sheet.

2.6 Strengthening of concrete structures with near surface mounted FRP (NSM FRP)

At present, FRP sheet bonding method and/or tension-side surface overlaying method with concrete have been applied for reinforcing the existing RC slabs and beams. However, applying those reinforcing methods, concrete surface of those existing RC members will be perfectly covered with sheet and/or overlaid concrete. As the results, following drawbacks are pointed out: 1) It is impossible to do a visual inspection of crack developed due to degradation of concrete; and 2) Anti-fatigue capacity of existing concrete tends to be decreased due to undrained water infiltrated in concrete and so on. As one of the methods for figuring out of those drawbacks, near-surface mounting method of FRP rod has been proposed.

Debonding failures in externally bonded FRP strengthening systems led to development of NSM FRP strengthening technique, which utilizes more of the ultimate tensile strength of the FRP material prior to failure. The concept of NSM is straightforward: first a groove is sawcut into the concrete surface; next the groove is filled halfway with two part structural epoxy. Then, a FRP bar or strip is placed inside the groove, and then the groove is completely filled with epoxy material as shown schematically in **Fig. 2.1.** The use of NSM FRP bars and strips are emerging as an alternative technology to externally bonded FRP laminates. Advantages of using NSM systems include the possibility of anchoring the bars/strips into adjacent members, shorter installation time, and an attractive finished appearance.

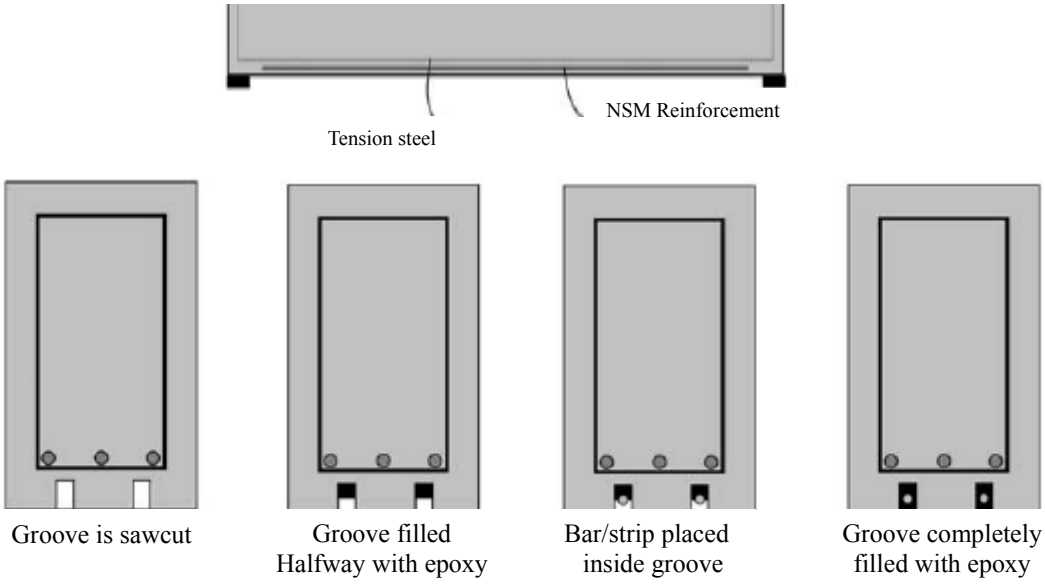

Fig. 2.1 NSM Reinforcement

Kish et al. (2005b) investigated an enhancement of flexural load-carrying capacity of the existing RC members reinforced with NSM FRP rods and debonding behavior of those FRP rods. In this study, the axial stiffness is varied in three levels of magnitude. The results obtained from this study are as follows: 1) It is experimentally observed that the similar reinforcing effects of AFRP rods/sheet can be expected if axial stiffness of reinforcing materials is similar to each other; and 2) The failure mode of the RC beams can be predicted using an empirical equation for the RC beams reinforced with bonding FRP sheet.
Carolin et al. (2001) tested a series of concrete beams strengthened with NSM CFRP strips. Test results demonstrated the effectiveness of the NSM technique compared to the externally bonded technique. They recommended replacing the epoxy used in bonding the strips to the surrounding concrete, with cement mortar to improve the work environment on site.
Hassan and Rizkalla (2002) investigated the feasibility of using different strengthening techniques as well as different types of FRP for strengthening prestressed concrete bridge decks in flexure. Large-scale models of a prestressed concrete bridge deck were tested to

failure. Test results showed that the efficiency of near surface mounted CFRP strips was three times that of the externally bonded strips.

Hassan and Rizkalla (2003 & 2004) presented experimental and analytical investigations to evaluate bond characteristics of NSM CFRP bars and strips. The influence of the groove dimensions, groove spacing and the limited adhesive cover was investigated. They concluded that the tensile stresses at the concrete-adhesive interface, as well as at the FRP-adhesive interface, are highly dependent on the groove dimensions and control the mode of failure of near surface mounted FRP bars and strips. They recommended widening of the groove to minimize the induced tensile stresses at the concrete-epoxy interface and increase the debonding loads of NSM bars.

El-Hacha and Rizkalla (2004) examined the static behavior of four beams strengthened with either NSM bars or strips. The failure of a T-beam specimen strengthened with NSM bars was due to epoxy split failure along the NSM groove, at an applied load less than two beams strengthened with NSM strips of a similar axial stiffness which failed due to FRP rupture. A T-beam strengthened with GFRP strips failed due to concrete split failure along the NSM groove. Compared to beams strengthened with externally bonded FRP of similar axial stiffness, the results show that the NSM strengthening technique utilizes more of the tensile strength of the FRP material and is therefore more effective.

Yost et al. (2004) studied the structural performance of retrofitted concrete flexural members using a near surface mounted CFRP method. They reported an increase of 30% and 78% in the yield load and ultimate strength compared to the values for the control beam, respectively. They also found that the bond strengths between the CFRP reinforcement, the epoxy and the adjacent concrete were adequate to develop the full tensile capacity of the CFRP reinforcement.

Barros and Fortes (2005) and Barros et al. (2006) investigated the effectiveness of CFRP laminates as a NSM for structural strengthening. They examined different variables which are number of CFRP laminate, different steel reinforcement ratios, and different depths of the cross-section. It was found that an increase of 91% as an average was obtained. It is also reported that a high deformability of the strengthened RC beams was assured and an

increase in the rigidity of the beam of 28% corresponding to the serviceability limit state analysis.

Aidoo et al. (2006) conducted a full-scale experimental investigation on repairing of RC interstate bridge using CFRP materials. Three types of strengthening methods were investigated externally bonded, NSM, and powder actuated fasteners. All methods showed an increase in the load-carrying capacity of the girders. They reported that in particular, the externally bonded and NSM CFRP methods behaved better than the powder actuated fastener method, although the NSM showed a significantly higher ductility and was explained to be due to the better bond chrematistics.

The use of prestressed NSM FRP to strengthen RC beams under static loadings was examined by Nordin and Täljsten (2006). It was found that using prestressed quadratic CFRP rods increased the cracking, yield and ultimate loads of the strengthened beams with respect to the reference beam. Based on their monotonic test results, they concluded that the fatigue life of RC beams strengthened with prestressed NSM CFRP material might be improved. Also, they concluded that, the combination of a higher cracking load and smaller crack widths would enhance the durability of the structure. Furthermore, the force transfer between the structures and CFRP rod worked well in the laboratory conditions without a need for a mechanical anchor device.

2.7 Failure Mechanism of beams reinforced with FRP strips

In recent years, it has been common to bond FRP strips to the tension-side surface of existing RC members in situ to increase the flexural load-carrying capacity. In such flexural reinforcing, it is well known that failure mode of the reinforced structure differs by axial stiffness (cross-sectional area X Young's modulus) and bonding length of the reinforcing FRP sheet. To date, five failure modes have been identified: (1) sheet rupture, (2) concrete compression failure, (3) concrete cover delamination failure from the sheet end along the main rebar, (4) FRP sheet delamination failure, and (5) FRP sheet peel-off failure due to opening of a critical diagonal crack (CDC) in the equi-shear span (Triantafillou and Plevris 1992, Zhang et al. 2005, and Kishi et al. 2005a) as shown in **Figs.2.2 and 2.3.** The first

failure mode is caused when the tensile strength of FRP material is less than shear strength of the concrete beam. However, the second failure mode (concrete crushing) occurs due to concentration of stresses at loading points at upper zone. The third failure mode may be expected in the following two cases: (1) when the flexural load-carrying capacity of the beams exceeds the shear load-carrying capacity due to flexural over-reinforcing with the FRP sheet; and (2) when the sectional bending capacity at the end of the FRP sheet is smaller than the applied bending moment. In the former case, the failure can be controlled by reducing the volume of the FRP sheet. In the latter case, the failure may be restrained by increasing the bonding length of the FRP sheet so as to bring the sectional bending capacity to a value greater than the applied bending moment. The fourth failure mode may result from shear failure of the bonding interface between the FRP sheet and concrete under pure bending. FRP sheet peel-off failure (the fifth failure mode) may occur in the case of RC beams reinforced with moderate volume and enough bonding length of the FRP sheet. In this failure mode, FRP sheet peel-off will be initiated at the tip of the CDC and developed towards the supporting point accompanied by the widening of CDC.

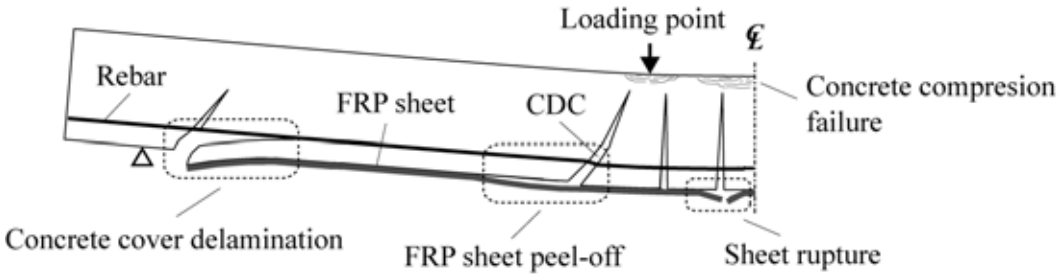

Fig.2.2 Schematic diagram for failure modes of beams reinforced with FRP sheet (Zhang et al. 2005)

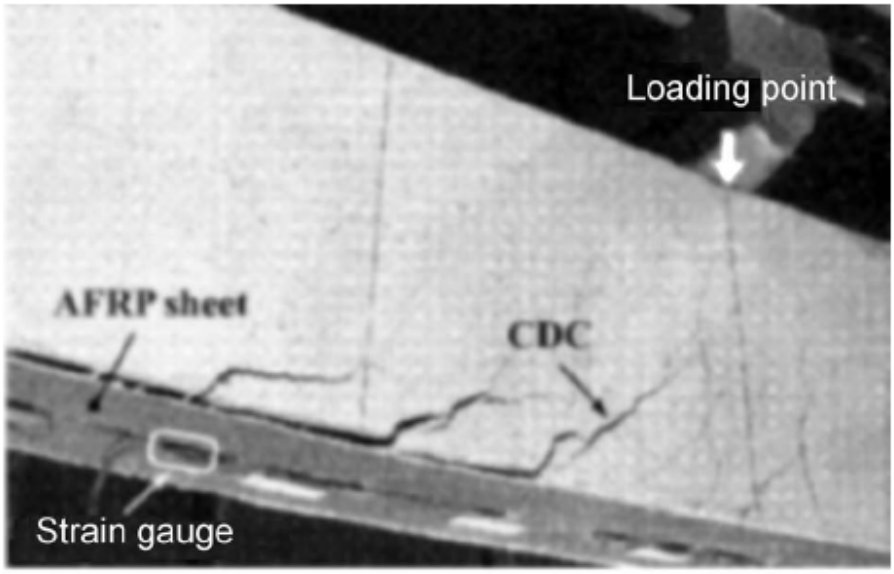

Fig.2.3 Sheet peel-off due to critical diagonal crack (CDC) (Kishi et al.2005a)

Kurihashi et al. (2002) conducted the static loading test on various rectangular RC beams strengthened with FRP sheet and investigating the load-carrying behavior of strengthened RC beams including sheet-debonding mechanism. Consequently, it has been clear that' 1) two types of failure mode of the RC beams are experimentally confirmed: sheet-debonding failure (DF) type and flexural-compression failure (FCF) type, in which DF type beams are failed due to FRP sheet being debonded before surcharged load reaches analytical ultimate point, but FCF type beams are failed due to FRP sheet debonding after getting to the analytical ultimate point with the upper cover concrete crashing; and 2) FRP sheet is debonded due to a peeling action of concrete blocks formed at the lower cover concrete near loading point in the shear-span area irrespective of failure mode.

Renata et al. (2008) mentioned that FRP delamination failure mode at midspan occurred with concrete cover layer adhered to FRP when width of FRP sheet is small (50mm) and without concrete cover layer when width of FRP sheet is big (120mm) as shown in **Fig.2.4**.

(a) (b)

Fig. 2.4 FRP Delaminarion failure mode (a) without concrete cover, and (b) with concrete cover (Renata et al. 2008)

Aram et al. (2007) described two types of FRP debonding failure modes, as shown in **Fig. 2.5** as follows: the first is plate bending debonding, which starts from end of FRP plate and then spread in the concrete, either at a cut-off point of plate (plate end shear failure(1)) or at last crack (anchorage failure at last crack(2)). The second mode of failure is mid-span debonding, which occurs in the shear span (shear crack (3)) or in pure bending span (flexural crack (4)) after that it propagates towards the end of plate. In general, FRP debonding occurs when the beam subjected to high tensile and bond shear stresses developed in concrete near adhesive layer. The weakest part in the bond surface is the concrete layer close to the surface. So, FRP debonding occurs when interfacial stresses can not be sustained by the concrete and debonding initiates in the regions of high stress concentration (at the end of FRP plate or around shear and flexural cracks).

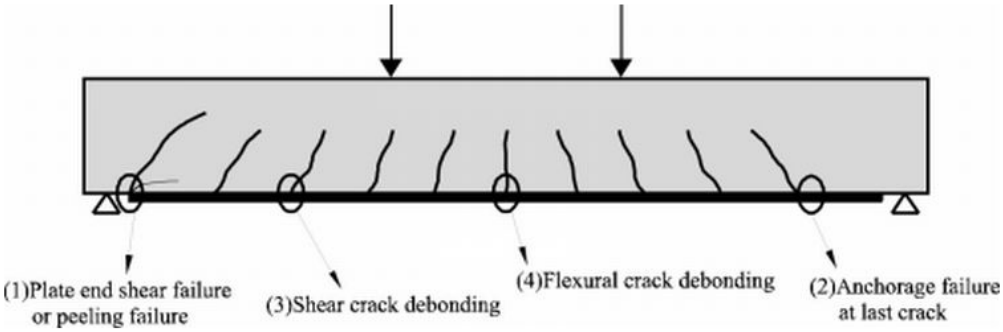

Fig. 2.5 Debonding failure modes of FRP strengthened RC beams (Aram et al. 2007)

Own (2006) described in details the five different failure mechanisms have been identified for RC/PC strengthened with FRP: 1) crushing of concrete, 2) FRP rupture, 3) shear failure, 4) plate-end (PE) debonding, and 5) intermediate crack (IC) debonding. Flexural failure is defined as either concrete crushing, or FRP rupture. Bond failure occurs either due to PE debonding or IC debonding. A figure illustrating the location of the five types of failure is given in **Fig. 2.6** for the loading configuration. Bond failure in FRP strengthened RC or PC girders propagates in one of two directions: from the FRP termination point (PE debonding), or from the intermediate flexural cracks (IC debonding). Shear failure occurs when the shear resistance of the beam from the concrete, steel and/or FRP materials is lower than that of the applied shear force. Flexural failure, defined as crushing of concrete or rupture of FRP, can often occur in FRP strengthened RC/PC members. Numerous situations may arise where designing a CFRP strengthened RC/PC member results in crushing of concrete. FRP rupture is commonly encountered in beams which are strengthened with FRP having a low axial stiffness, or having a large amount of transverse anchorage provided for debonding mitigation.

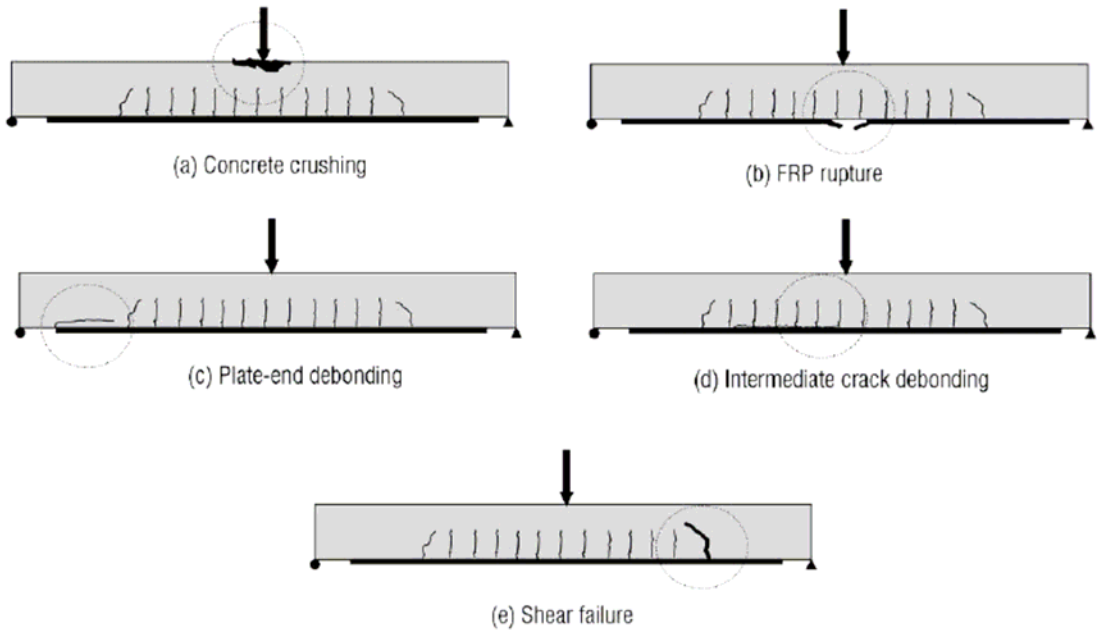

Fig. 2.6 Failure modes of FRP strengthened RC structures (Own 2006)

2.8 Definition of fiber reinforced polymer (FRP)

FRP is a term used for advanced composite materials when they are used for engineering applications. FRP materials have been used in a variety of industries, such as aerospace, automotive, shipbuilding, chemical processing, etc, for many years. Their high strength-to-weight ratio and excellent resistance to electromechanical corrosion make them attraction materials for structural applications. Many of structural engineers are generally not familiar with the basic properties of this material. The fibrous composite is obtained when the polymer matrix (epoxy, vinylester or polyester resins) impregnates the fibers (glass, carbon, graphite or aramid). The properties of the laminates depend on the amount and orientation of fiber as shown in **Fig.2.7**. The permanent deformations of fibers under short-term loading are relatively negligible, but they exhibit brittle tension failure modes. The matrix has generally poor mechanical properties, as the behavior of polymer is dependent on time. The tensile strength of the composite laminate is the most important when used in repair and it can be high compared to concrete or steel. The following is a brief description of some fibers, resins and combinations of the two in the form of FRP.

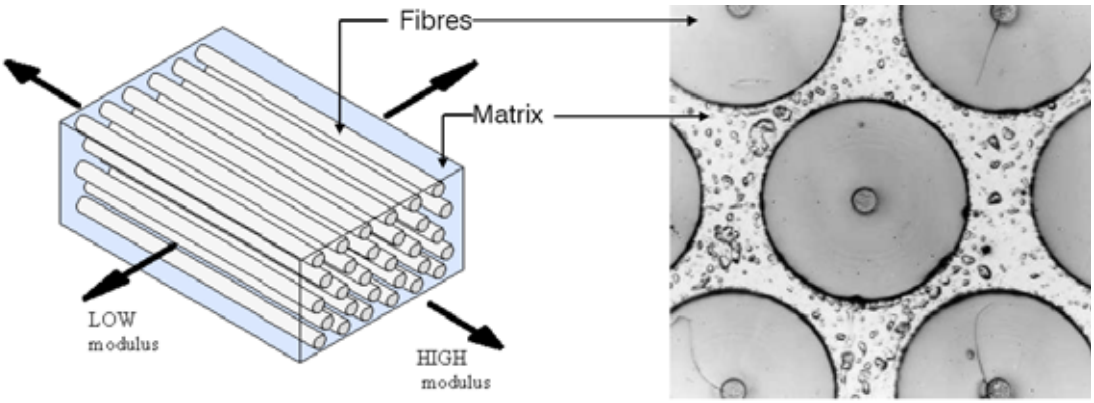

Fig. 2.7 Components of composite materials

2.8.1 Fiber

Fibers are either inorganic, as the case of carbon fibers or glass fibers, or organic as the case of aramid fibers. They are characterized by their high tensile strength, low elastic modulus and the fact that they are linearly elastic to failure. Nanni (1992). Fibers are made of very thin continuous filaments, and therefore, are quite difficult to be individually manipulated. For this reason, they are commercially available in different shapes (**Fig. 2.8**). A brief description of the most used is summarized as follows:

• Monofilament: basic filament with a diameter of about 10 μm.

• Tow: untwisted bundle of continuous filaments.

• Yarn: assemblage of twisted filaments and fibers formed into a continuous length that is suitable for use in weaving textile materials.

• Roving: a number of yarn or tows collected into a parallel bundle with little or no twist.

By combining a number of tows or yarns together, a tape is obtained, where tows or yarns can be simply arranged side by side or sewed or fastened on a bearing. The classification of fibers is directly taken from that traditionally used for textile fibers. The stress versus strain behavior of typical FRP and steel FRP (SRP) and traditional building materials used in tension: mild steel reinforcing and high strength steel used in prestressing strands, are presented in **Fig.2.9** (ACI 1996). In addition, **Table 2.1** shows properties of commn high-strength (Larralde and Hamid 1994)

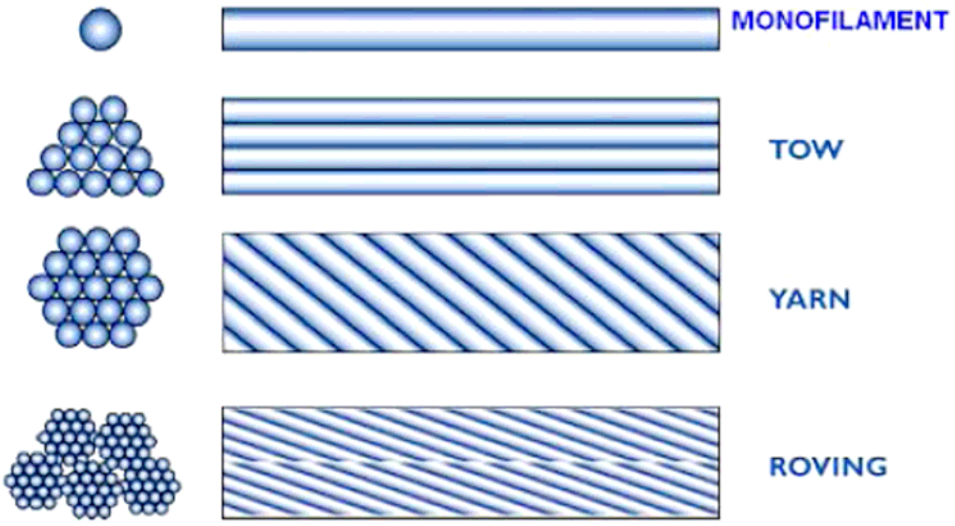

Fig. 2.8 Most used shape of fibers

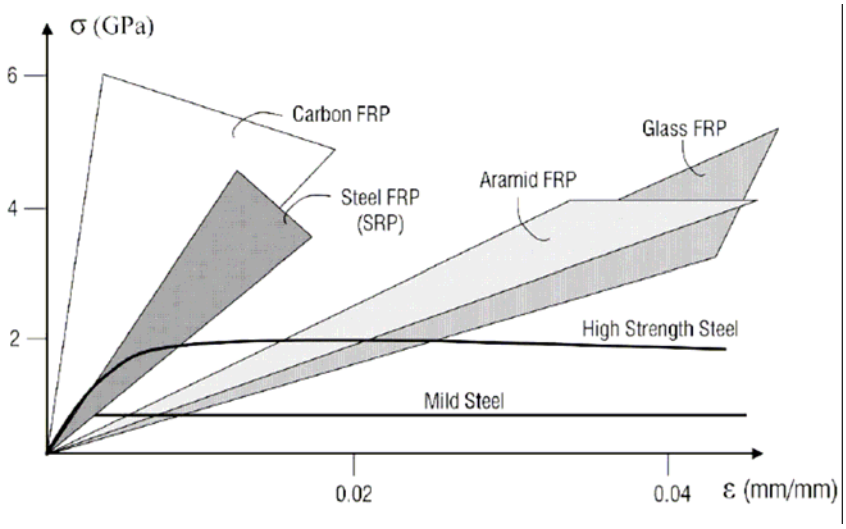

Fig.2.9 Stress-strain characteristics of steel, FRP, SRP materials (ACI Committee 1996)

Table 2.1 Properties of Common High-Strength Fibers (Larralde and Hamid 1994)

Fiber	Modulus of Elasticity (GPa)	Tensile Strength (Mpa)	Poisson's Ratio	Specific Gravity
Glass				
E-Glass	73.5	3500	0.3	2.5
S-Glass	868	4655	0.3	2.5
Carbon/Graphite				
T40	287	5740	0.2	1.8
ACP	217	3500	0.3	1.8
CELION	241	3150	0.3	1.8
Silicon Carbide				
SCS-6	420	2500	0.17	3.1
Nicalon	105	1421	0.2	2.6
FP	385	1400	0.3	3.9
Aramid				
Kevlar	119	1750	0.3	1.44

2.8.1.1 Carbon fibers

Carbon fibers have the property of elastic conductivity but are still magnetically neutral. Compared to glass fiber, carbon fibers have much higher tensile strength (up to 5600 MPa), as well as a high elastic modulus ranging from 270 to 750 GPa. The difference in mechanical properties between the different fibers depends upon their molecular arrangement of the carbon atoms and the number of defects present. In the formation of fiber, a temperature of more than 1000˚C is necessary, which increase the cost of the product. In general, the low-modulus carbon fiber have lower specific gravities, lower cost,

higher tensile strengths and higher tensile strains to failure than the high-modulus fibers (Abdelrahman and Rezkallah 1999).

2.8.1.2 Glass Fibers

Glass fibers are the most commonly used types of fibers. They are available and economically cheaper than carbon and aramid fibers. Glass fibers are electrically and magnetically neutral. Glass fiber strength is easily affected by moisture, sustained load and high alkali environments. The extent of degradation due to these factors depends upon the chemical composition of the glass fibers. There are several types of glass fiber. But here, we will concentrate on two types of glass fibers: E-Glass and S-Glass. E -Glass is the most widely used glass fiber as it is the least expensive. The ultimate axial tensile strength ranges between 2500 MPa to 3500 MPa with an elastic modulus of about 73 GPa. S-Glass has better mechanical properties than E-Glass with an ultimate tensile strength of about 4000 MPa and an elastic modulus of about 86 GPa (ACI report 1995).

2.8.1.2 Aramid Fibers

Aramid is a word that srands for pory-para-phenyleneterephthalamide. These are organic fibers produced from a liquid crystal polymer. Three commercially well known aramid fibers are Kevlar, Twaron and Technora. Their mechanical properties fall between those of glass and those of carbon fibers, with an ultimate tensile strength up to 3900 MPa and a tensile elastic modulus of up to 130 GPa. The aramid fibers are easily affected by strong acids and bases as well as ultraviolet radiation (ACI report 1995).

2.8.2 Matrix Resins

Matrix polymers in FRP have many purposes. The first is to bind fibers together and produce a more even distribution of stresses. Secondly, the matrix provides compressive and shear strength and protects the fibers from lateral pressure and abrasion. And thirdly, the matrix protects the fibers from environmental conditions such as moisture, acid and alkali attack as well as ultraviolet radiation. The most widely used matrix resins in the

production of FRP are thermosetting polymers. (Moukwa1996). **Fig.2.10** shows the stress-strain relation for fiber, matrix and the resulting FRP material. The most widely used thermosetting polymers for the production of FRP are polyester, vinylester and epoxy resins.

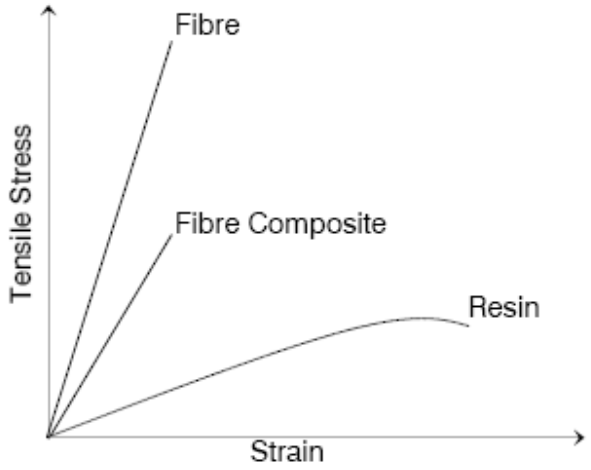

Fig. 2.10 Stress-strain relationship of fibers,
matrix and FRP (ACI Committee 1996).

2.8.2.1 Polyester Resins

Polyester resins are used mainly in the construction, marine and automotive industries. They have poor impact and mechanical properties and high curing shrinkage. Typically, polyester resins have good adhesion between fibers and resin, are easy to process, can withstand temperatures greater than 150 C˚, and have low cost. Polyesters have tensile strengths in the range of 45 to 190 MPa, tensile elastic modulus between 2.5 and 12 GPa, ultimate tensile elongation between to 3%, and coefficient of thermal expansion as 120x10 exp-6 /C˚ (ACI report 1995).

2.8.2.2 Vinylester Resin

The properties of vinylester include tensile strength in the range of 40 to 100 MPa, tensile elastic modulus of 3 to 5 GPa, ultimate tensile elongation of 1 to 7%, coefficient of thermal expansion between 80 to 160exp-6 /C˚, and heat distortion temperature of 120 to 140˚C .Vinylester are more expensive than polyesters but provide increased mechanical and chemical performance. Vinylesters have good fatigue and impact resistance, are flexible, and are resistant to acids and alkalis. For these reasons, many researchers believe that vinylester should be used as matrix resins for FRP bars, tendons and laminates. However, vinylesters can be attacked by moisture, ultraviolet radiation and high temperatures, although not to the same extent as polyesters (ACI Report 1995).

2.8.2.3 Epoxy Resin

Epoxy resins are widely used in aircraft, aerospace and defense industries. They have low shrinkage compared to polyester resins, excellent fatigue resistance, good strength, excellent mechanical properties, and good adhesion to variety of fibers. Epoxy resins are widely recognized as having better resistance to acids, alkalis, and ultraviolet radiation than both vinylesters and polyesters. But some epoxies are sensitive to moisture, although still less permeable than polyesters. Other disadvantages include high cost and low impact strength. Also, some epoxies can cause rashes on skin when exposed to it; therefore, must be handled with care. The tensile strength of epoxy resin ranges from of 50 to 100 MPa, tensile modulus of 3 to 6 GPa, ultimate tensile elongation of 2 to 8 %, and heat distortion temperature of 120 to 200 C˚ (Moukwa 1996).

2.9 SUMMARY

This chapter discussed some of the previous work done in the field of research of the FRP sheet. The first part of this chapter discussed the different experimental works on the RC beams strengthened/repaired with non-pre-tensioned or pre-tensioned AFRP sheet. The cracking behavior and deflection, the ultimate behavior and flexure capacity, and the bond strength were discussed. It could be concluded that the AFRP sheet in general with a lower

elastic modulus than steel are less stiff. The ultimate capacities of the RC beams strengthened with AFRP sheet were bigger than those for the control RC beams. This led to the conclusion that there was no stress problem in the AFRP strengthened RC beams, but only there was a deflection and serviceability problem.

However, Prestressing the FRP sheet/plates prior to bonding has the following advantages:

- Provides stiffer behavior as at early stages most of the concrete is in compression and therefore contributing to the moment of resistance.
- Crack formation in the shear span is delayed and the cracks when they appear are more finely distributed and narrower (crack widths are also a matter of bond properties).
- Closes cracks in structures with pre-existing cracks.
- Improves serviceability and durability due to reduced cracking.
- Improves the shear resistance of member as the whole concrete section will resist the shear, provided that the concrete remains uncracked.
- The same strengthening is achieved with smaller areas of stressed strips compared with unstressed strips.
- With adequate anchorage, prestressing may increase the ultimate moment of resistance by avoiding failure modes associated with peeling-off at cracks and the ends of the strips.
- The neutral axis remains at a lower level in the prestressed case than in the unstressed one.
- Resulting in greater structural efficiency.
- Prestressing significantly increases the applied load at which the internal steel begins to yield compared to a non-stressed member.

In the second part of this chapter, the general history and the definition of the FRP sheet were discussed. From this part it could be concluded that the mechanical and physical properties of the Aramid Fibers fall between those of glass and those of carbon fibers. On the other hand, the Aramid Fibers are more flexible, and thus the most popular type of composites in Japan.

CHAPTER 3

A new anchoring method of bonding FRP sheet

3.1 Introduction

This chapter presents background for previous anchoring methods of pre-tensioned FRP material (metal system and non-metallic anchorages), advantages and disadvantages of these anchorage methods .In additions, pervious prestressing methods are explained briefly and the used prestressing method in this research will be mentioned in detail. Finally, the proposed anchoring method without anchoring devices in this present study will be explained and its advantages will be mentioned.

3.2 Previous anchoring methods of pre-tensioned FRP material

The rehabilitation of deteriorated or understrength concrete structures with bonded FRP material is becoming an accepted method of strengthening concrete structures throughout the world. The structures strengthened with FRP sheet exhibit many advantages over structures strengthened with conventional steel materials such as less susceptibility to corrosion, minimal increase of permanent dead load, significant increases in load-carrying capacity, and good fatigue resistance. FRP sheets are widely used for external strengthening due to its high modulus and strength, and may be used more effectively by applying prestress. The expected benefits of the prestressed FRP sheets include the effective use of the material strength, restored prestressing, and improved serviceability (i.e., increased cracking loads, closure of existing cracks, and reduced deflections. An active load-carrying mechanism occurs which ensures that some of the dead load of the structure is carried by the prestressed FRP sheets (El-Hacha et al. 2004; Wight et al. 2001); whereas,

nonprestressed sheets only support additional live loads. Despite these advantages, only limited research, regarding the application of prestressed FRP sheets, has been reported to date. This is primarily because of the additional labor required and issues concerning the anchors. To apply prestress to FRP sheets, adequate anchorage must be provided to resist a high level of prestressing force. However, anchoring of the end zones has been one of the biggest problems when concrete structures are strengthened with prestressed CFRP laminates or sheets. Due to limited shear strength of concrete, the high shear stresses at the ends of prestressed FRP strips can not be transferred into the structure as shown in **Fig.3.1.** Thus, it has been necessary to mechanically anchor the strips at the ends to prevent premature peeling failures with the following previous methods.

1-Metallic anchoring system

Different techniques using bolted metal plates have been tested as well as decreasing the thickness of the CFRP at the ends to lower the stresses in the concrete-CFRP interface. The results have proven effective multilayer application of CFRP has been tested to achieve a different prestressing profile on the concrete beam (Wight et al. 2001 and El-hatch et al. 2004). Steel anchors are commonly used as in the following studies:

Quantrill and Hollaway (1998) used prestressed CFRP plates to strengthen RC beams of 1.0 and 2.3 m span with prestress levels ranging from 17.5 to 41.7% of the strip ultimate strength with anchoring metal system. In this system, for the 1.0 m length beams, a CFRP plate width of 80 mm was used, whereas for the larger-scale 2.3 m beams, strengthening were achieved through the use of 90 mm wide plates. A plate longer than the length of the RC beam in question was used. Aluminum tabs were used to provide stress distribution in the plate end regions. These were bonded to both faces of the plate at each end and were 2 mm thick, 130 mm long for both beam sizes, and full plate width. Each end was then sandwiched between two steel plates 9mm thick of the dimensions as shown in **Fig.3.2**.

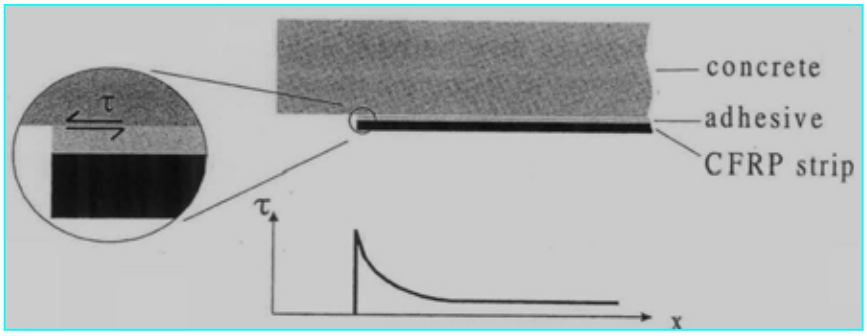

(a) Shear stress peak at the end of prestressed FRP strip

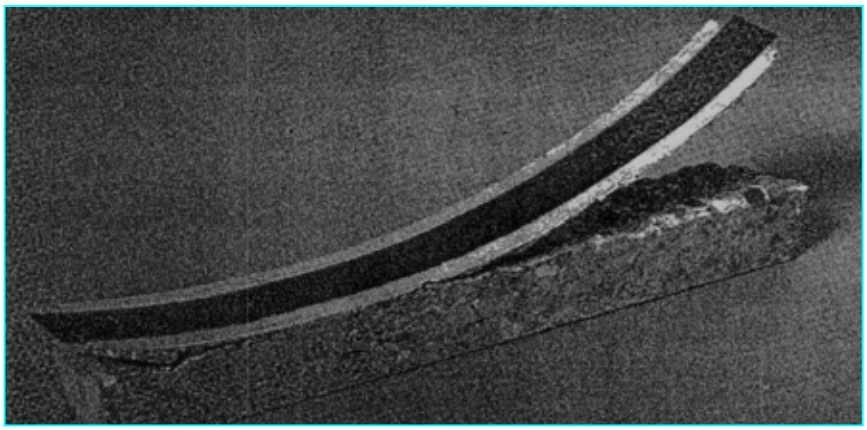

(b)Premature failure of prestressed FRP strip without anchorage

Fig.3.1 Problems due to applying prestressing to FRP material (Stöcklin and Meier 2001 and 2003)

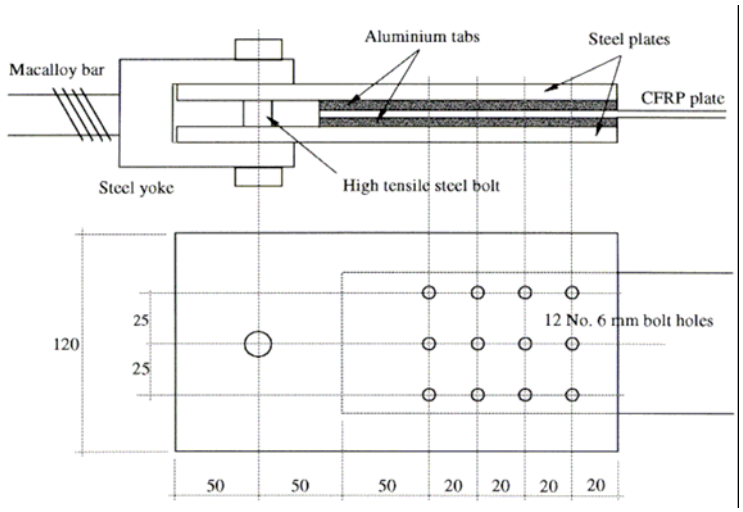

Fig.3.2 Assembly of anchorage system (Quantrill and Hollaway1998).

Wight et al. (2001) also studied, experimentally, the post strengthening of concrete beams with prestressed FRP strips. The mechanical anchorage system used for the RC beams is shown in **Fig.3.3**. The mechanical anchorage system consisted of steel roller anchors bonded to the sheets and steel anchor assemblies fixed to the beam. The roller anchors that gripped the sheet consisted of two stainless-steel rollers bonded to each end of the sheet. The rollers were 32 mm in diameter, 380 mm long, and the central 300 mm was knurled to improve bond performance. At least three days prior to prestressing operations, the sheet was wrapped 2.5 times around the roller, and a two-part epoxy was applied to bond the sheet to the rollers.

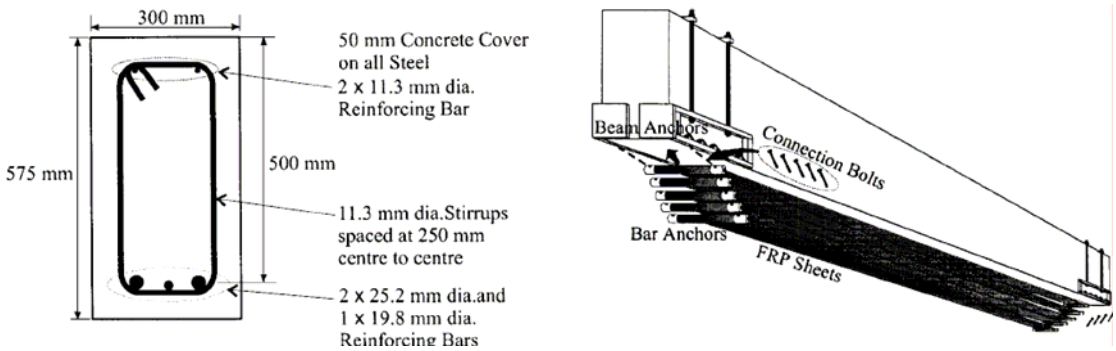

Fig.3.3 Mechanical anchorage system and cross-section of the beam (Wight et al. 2001).

El-Hacha et al. (2003and 2004) studied the strengthening of pre-cracked PC beams using prestressed CFRP strips under short- and long-term loading, and exposure to both room and low temperatures. The designed metal anchorage system consisted of a movable flat steel plate anchor at jacking end, a fixed steel angle anchor at the dead end, brackets and steel rods.

Dong et al. (2009) provided RC beams with prestressed CFRP plates anchored to the tension face in order to obtain the required strengthening capacity. As shown in **Fig.3.4**, an anchorage system is necessary for fixing the prestressed CFRP plates. The rough surface of the anchorage system is processed, and then fixed to the beam with anchor bolts. In order to

prevent a load concentration, the anchorage system of the CFRP plate was attached to a GFRP tab.

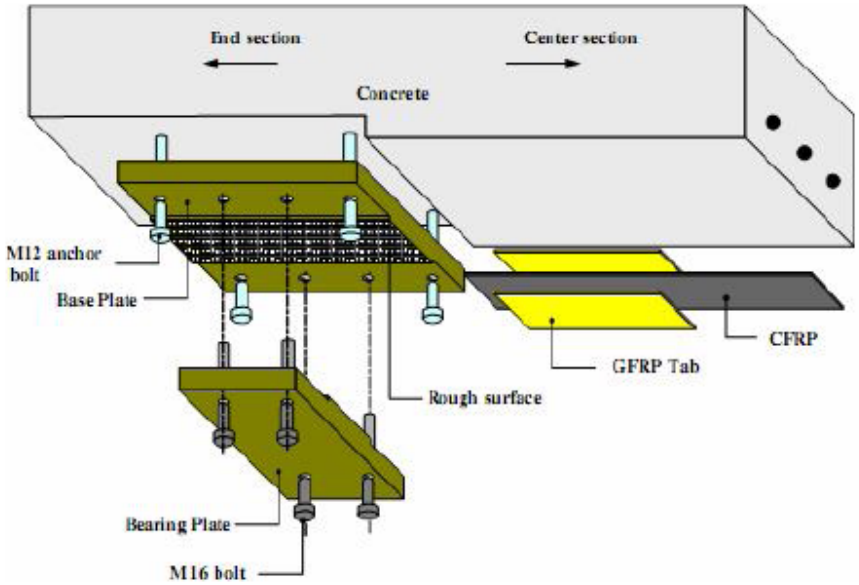

Fig.3.4 Detail of the anchorage system (Dong et al. 2009)

Sang et al. (2009) used hilti bolts (HST-M 16/140) for anchoring the base plate and they were bonded into the concrete beam using boring and epoxy-filling. In order to install a base plate of the anchoring device shown in **Fig.3.5**, the dust in the anchor bolt-hole is removed by air pressure.

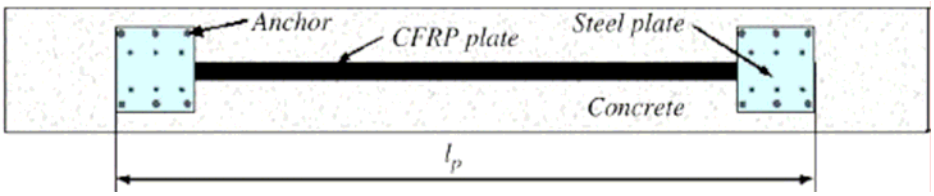

Fig.3.5 Beams specimen and the anchorage system (Sang 2008)

2- Gradually anchored prestressed FRP strips using a stepwise approach

All of the previously mentioned references investigated the application of prestressed CFRP strips by mechanical anchorage system. However, the presence of permanent anchors minimizes the likelihood of premature peeling-off failure of the bonded FRP sheets. The permanent metallic anchor system, mounted in the strengthened beam, increases dead load and may present aesthetic and durability problems including corrosion.

Thus, it may be desirable to remove the steel anchors after complete curing of the strengthening system provided that neither significant losses of the sustained prestress nor a premature failure occurs. Some researches presented strengthening method by replacing the metallic anchorage with nonmetallic FRP anchors for RC/PC beams using prestressed FRP sheets as following:

An anchorage system was developed at the Swiss Federal Laboratories for Materials Research (Empa) without using any mechanical devices for anchoring of the end parts of the CFRP strips (Stöcklin and Meier 2001and 2003) as shown in **Fig.3.6**. With this method, the prestressing force is reduced gradually toward both ends of the strip in steps via heating which cures the adhesive (see **Fig.3.7**). In comparison to other FRP prestressing techniques, the stressing procedure is the same, with the addition of the heating work step which has the advantage of no anchorage devices (corrosion) and a better quality of adhesive.

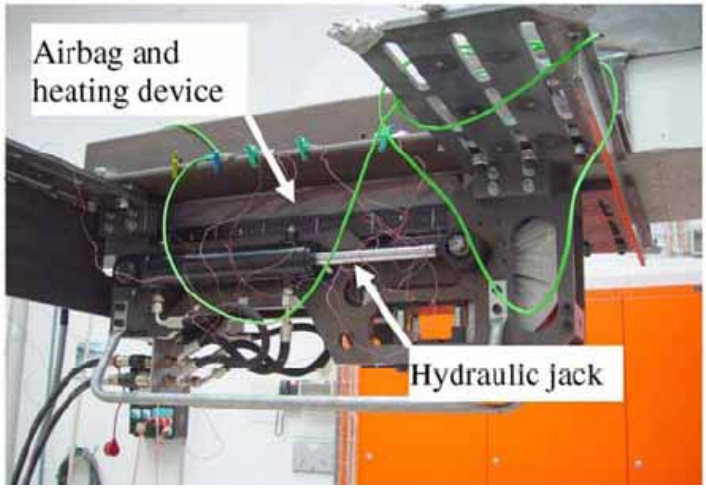

Fig.3.6 General gradual anchoring using a stepwise approach
(Stöcklin and Meier 2001and 2003)

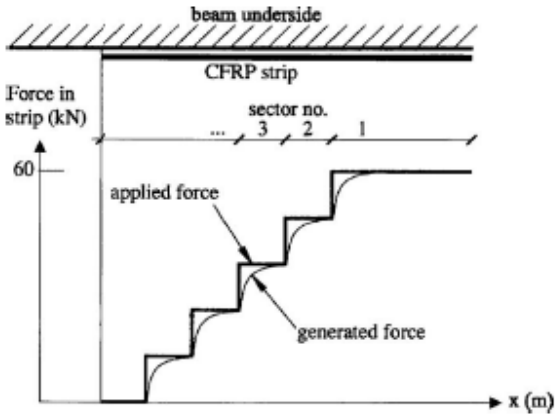

Fig.3.7 Force gradient at plate end
(Czaderski and Motavalli 2007 and Aram et al. 2008).

At Empa, a project for the strengthening of large-scale prestressed concrete bridge girders with prestressed CFRP strips anchored using gradient method was performed (Czaderski and Motavalli 2007). The results showed that Empa device is effective in the long span beams.

In addition, Aram et al. (2008) carried out a new set of small scale tests, which aims at further investigation the debonding of prestressed CFRP strips anchored with the gradient method. The existing prestressing and heating device developed at Empa to produce gradient anchorage was used. The authers proved that Empa device is not effective in short span beams due to high shear stresses generated in short span.

3-Non-metallic anchoring system using FRP U-wrap

Ferrier et al 2004, Piyong et al 2008, and Kim et al. (2008a,b) developed non-metallic anchor systems replace the permanent steel anchorage. Kim et al. (2008a,b) tested nine doubly reinforced concrete beams with various types of nonmetallic anchor systems such as non-anchored U-wraps, mechanically anchored U-wraps, and CFRP sheet-anchored U-wraps as shown in **Fig.3.8**. The study shows that the developed nonmetallic anchors are more effective in resisting peeling-off cracks compared to the permanent steel anchors and

the beams strengthened with the nonmetallic anchors provide comparable load-carrying capacity with respect to the steel anchored control beam. With this technique, the replaced FRP anchors can effectively minimize the loss of prestress when the metallic anchors are removed. The nonmetallic anchors can also preclude premature peeling-off failure of the longitudinally prestressed FRP sheets as shown in **Fig.3.9**. However, sliding and the sheet peeling-off between the FRP U-wrap and longitudinal pre-tensioned FRP occurred.

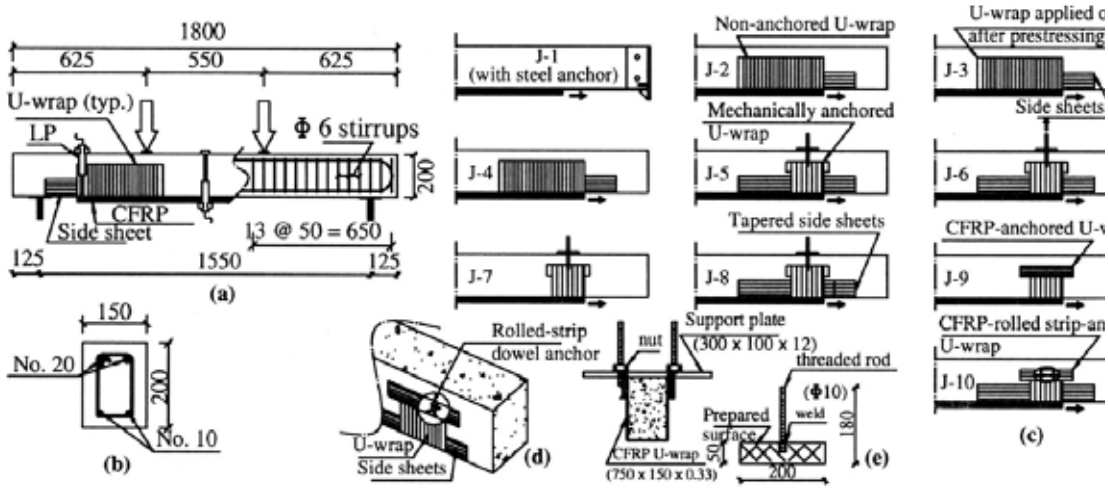

Fig.3.8 Beam details: (a) test setup; (b) cross section; (c) various anchors; (d) dowel anchor (J-10); and (e) mechanical anchorage for U-wraps (Kim et al. 2008a,b).

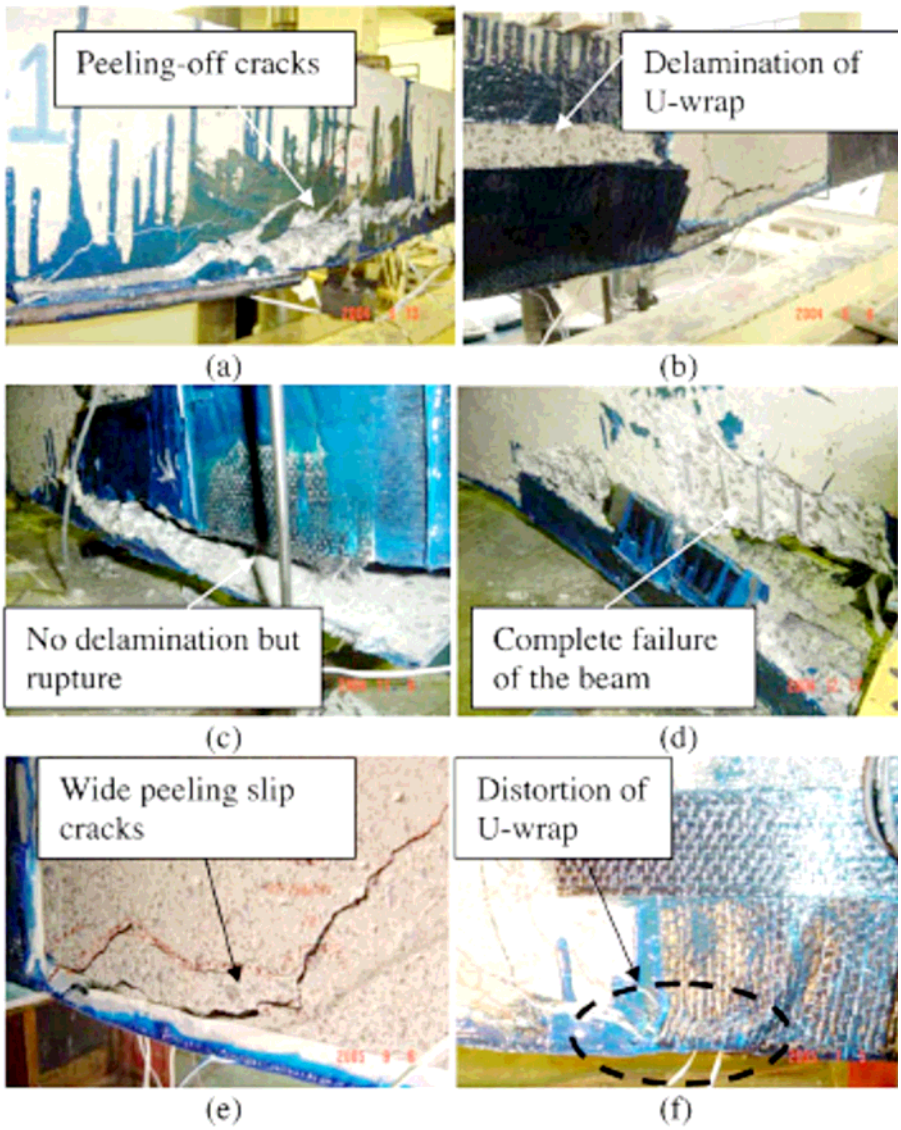

Fig.3.9 Failure modes of the beams shown in Fig.3.7: (a) J-1 with permanent metallic anchor; (b) J-2 with nonanchored U-wraps; (c) J-5 with mechanically anchored U-wraps; (d) J-6 with mechanically anchored prestressed U-wraps; (e) J-7 without side sheets; and (f) J-9 with CFRP-sheet anchor and without side sheets (Kim et al. 2008a,b).

From this point of view, in the present study, a new anchoring method without anchoring devices is proposed to avoid these disadvantages of previous methods (Sawada et al. 2009, Abdel Aziz et al. 2010a and b, and Kurihashi et al. 2010), which will be explained in details later in this chapter.

3.3 Prestressing method of FRP material

3.3.1 Existing prestressing methods

Strengthening of RC members with a prestressing FRP system is generally classified into three methods:

1- Indirectly prestresses the sheet/plate by cambering the flexural members.

2- Pre-tension is introduced directly to the sheet/plate by jacking against an external reaction frame

3- Pre-tension is introduced to the sheet/plate by jacking directly to the strengthened beam itself.

- The first method was proposed by Saadatmanesh and Ehsani (1991), in which stressing in the FRP system was achieved by initially cambering the beam upward with the use of hydraulic jack (**Fig 3.10)**. The FRP plates then are attached to the lower face of the beam. After the epoxy adhesive was properly cured, the jacking force is removed. As the beam deflects under its own self-weight and sustained dead load, a tensile stress is transferred to the FRP plate. Advantages of the system are that it does not require the usage of specialized prestressing mechanical devices, the FRP system can be extended to the ends of the strengthened member, and the prestressed FRP system can be easily anchored at the ends of the FRP sheets or plates. Some of the disadvantages associated with this method are that it is labor intensive, only low level of prestressing can be induced in the plates, it is not easy to achieve the desired level of prestressing in the plates or sheets, and the reacting floor or foundation must be capable of sustaining the applied vertical loads.

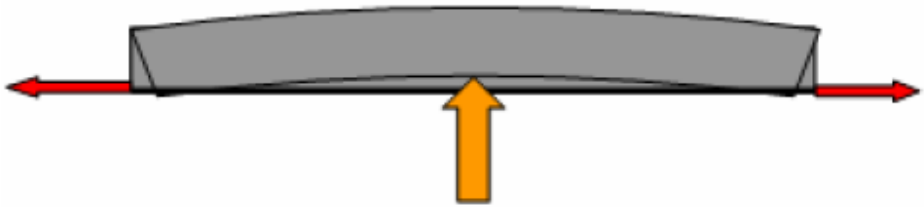

'Fig.3.10 Prestresses the sheet by cambering the flexural members
(Saadatmanesh and Ehsani 1991)

-The second method applies direct tension to the sheet by jacking against an external reaction frame has been carried out by some researchers (Triantafillou et al. 1992, and Piyong et al. 2008). For this method, Piyong et al. (2008) proposed a new mechanical device, made of one steel beam for prestressing FRP sheets. As presented in **Fig.3.11**, the mechanical device consist of one continuous steel beam comprising two anchorage and two loading region. The anchorage region consists of removable and fixed steel plate to anchorage the CFRP. The loading region consists of (1) one steel strip to support and achieve the desired prestress in CFRP sheets, (2) two threaded rods welded to the steel strip and used to raise the steel strip in order to create a prestressing force. An attractive feature of this device is that the prestressing was achieved with a manual torque wrench without the need for using power-operated hydraulic jacks or any other type of sophisticated equipment. In typical prestressing applications, transfer of the prestressing is achieved under high strain rates, which increases the propensity for end debonding at low prestressing levels. This issue can be mitigated by the proposed device because the prestressing release is achieved under low strain rates. For higher prestressing levels in which debonding of the CFRP sheets cannot be prevented solely by controlling the strain rate at transfer, U-wraps can be easily installed at the ends of the prestressing FRP system. Some disadvantages of this device are 1) the presence of the anchorage and loading regions may not permit the prestressed sheet to extend to the very end of the strengthened RC beam; and 2) the length of FRP system may be limited because of deformations within the device itself (Piyong Yu et al. 2008).

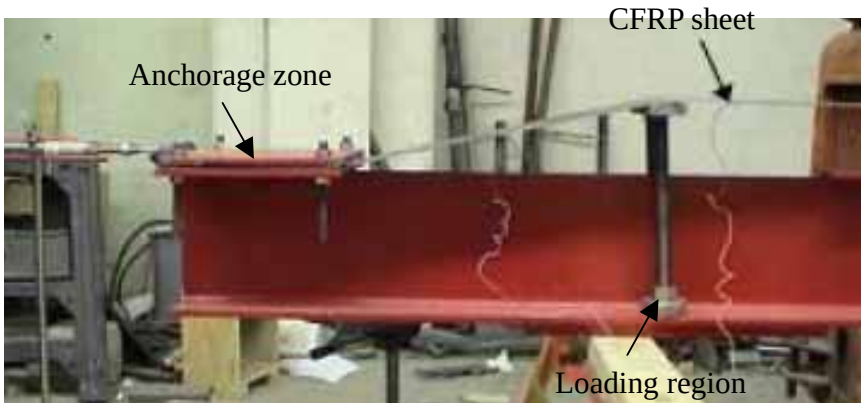

Fig.3.11 Prestressing the sheet by jacking directly against reaction frame (Pivong et al. 2008)

- In the third method designated as the direct method, the FRP sheets or plates are first anchored at one end (dead anchor) and then tensioned from the other end (live anchor) using a power-operated hydraulic jack as shown in **Fig.3.12**. According to this method, the FRP sheets or plates must be anchored to the beam itself at either end. The dead end is first anchored before stressing and the live end is subsequently anchored after the stress is applied to the FRP system.

Fig.3.12 Prestressing the sheet by jacking directly to the strengthened beam itself.

Quantrill and Hollaway (1998) presented the sequence of procedures followed in preparing the prestressed beams as shown in **Fig.3.13**. Each concrete beam was positioned bond surface up beneath the CFRP plate. The FRP plate was then stressed to the required level and the concrete beam lifted with jacks up to the level of the taut plate (a) Dead weight was applied to the upper face of the FRP plate (b); in practice, a pressure bag may be used to support the external plate during bonding. After the adhesive had cured, steel clamps were installed at each end of the beam to ensure adequate anchorage of the FRP plate ends upon

release of the prestress. The load applied to the CFRP plate was then reduced to zero, the prestress being transferred to the beam by the cured adhesive bond layer, and the plate was cut through to isolate the beam.

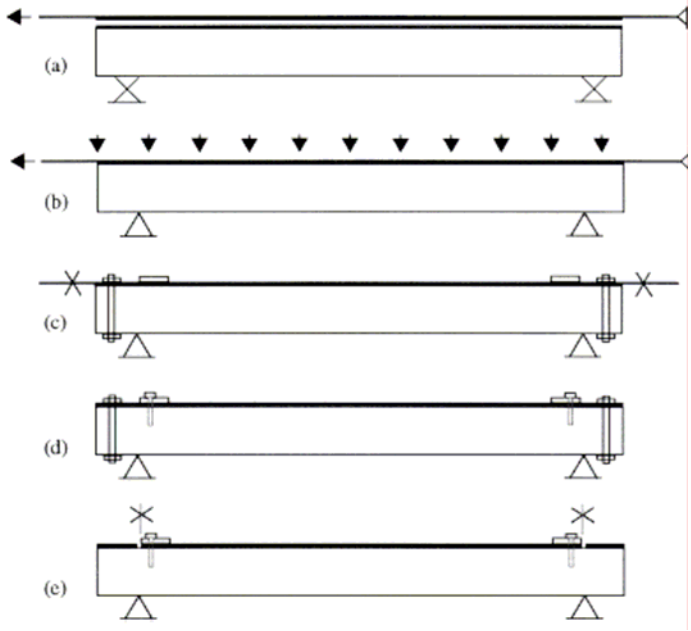

Fig.3.13 Sequence of prestressing operations (Quantrill and Hollaway1998).

Wight et al. (2001) and El-Hacha et al. (2003 and 2004) showed that to prestress the sheets, the roller at one end of the FRP sheet was fixed to the beam (dead end) and the roller at the other end was movable (jacking end). During prestressing, the movable roller was attached by steel prestressing strands to a hydraulic jack that reacted against the beam. The prestress was applied to the sheet, and the sliding roller was then attached, in its extended position, to a second permanent anchorage assembly as shown in **Fig.3.3**. Subsequent layers were added to the beam, using the same technique, until all layers were attached. When subjected to a prestress, the FRP sheet tended to separate itself from the beam surface to which it was to be bonded. This separation was caused by imperfections in the tension face of the beam or camber in the member. To bring the sheet into contact with the beam surface, a force was applied to the sheet perpendicular to the beam surface by weights.

Stochlin and Meier (2001and 2003) developed prestressing device as shown in **Fig.3.14**, in which to generate a gradually anchored and prestressed CFRP strips, a stepwise approach is used as follows: The CFRP strip is clamped and prestressed and then converted with adhesive. The device is temporarily mounted to the structure. The middle part of the strip is bonded. Then, the force is marginally reduced, and the following areas are bonded. The force is reduced further and the adjacent areas are bonded. This procedure is repeated until there is no remaining prestressing force at the ends of the strip. Aftre that, the prestressing device can be removed immediately. The adhesive is completely cured using a heating device.

Kim et al. (2008a,b) introduced the prestress force to FRP sheet by mounting the assembled end-cap anchors at both ends of the beams; then the fully cured CFRP sheets, bonded onto the jacking plates, were placed into the end-cap anchors to be prestressed, as shown in **Fig.3.15**. One side of the jacking plate was firmly fixed on the end-cap anchor; on the other hand, the other jacking end was allowed to move longitudinally for prestressing.

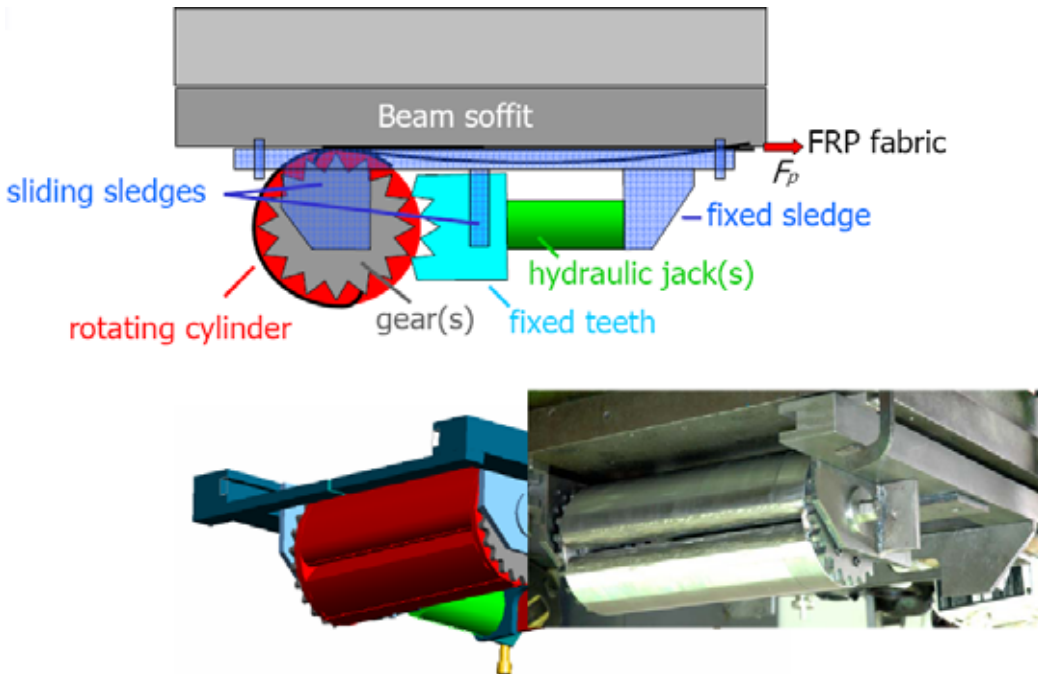

Fig.3.14 Prestressing device developed by Stochlin and Meier (2001and 2003).

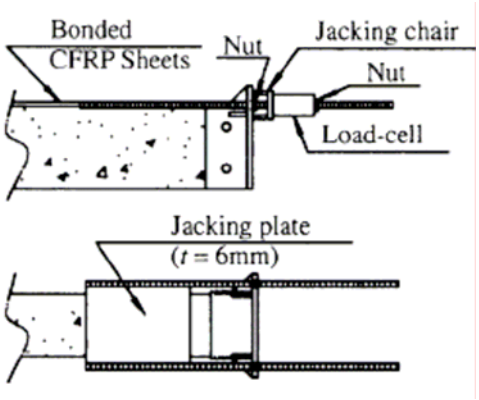

Fig.3.15 Prestressing operation (Kim et al. 2008a,b).

Sang et al. (2008) and Dong et al. (2009) applied the prestressing to CFRP plates by jacking the prestressing device using an oil jack as shown in **Figs.3.16 and 3.17,** respectively. Oil jack is connected to the installation anchor plate. After the prestressing, the epoxy adhesive is injected to between the CFRP plate and the bottom concrete additionally. Then, the CFRP is fixed on the installation plate in front of the oil-jack. The base plate of anchor used to fix the CFRP plate prevents slippage using a surface curvature, which increases the friction force.

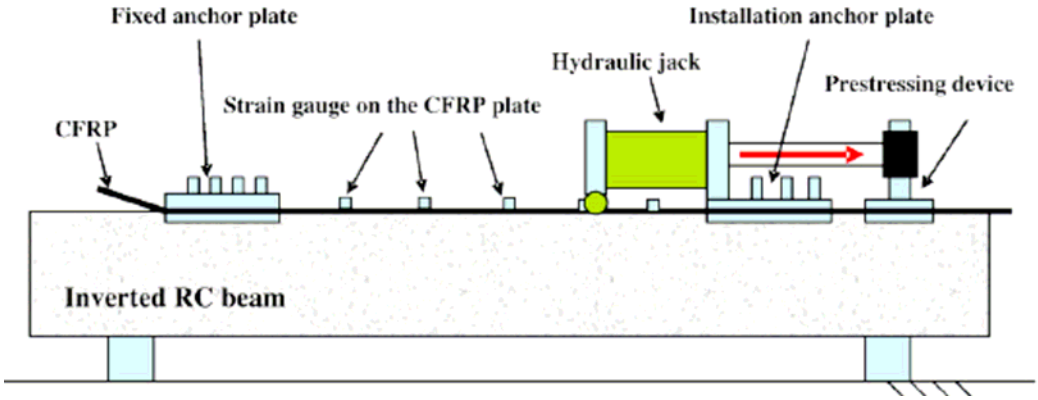

Fig.3.16 Prestressing system of CFRP plate (Sang et al. 2008).

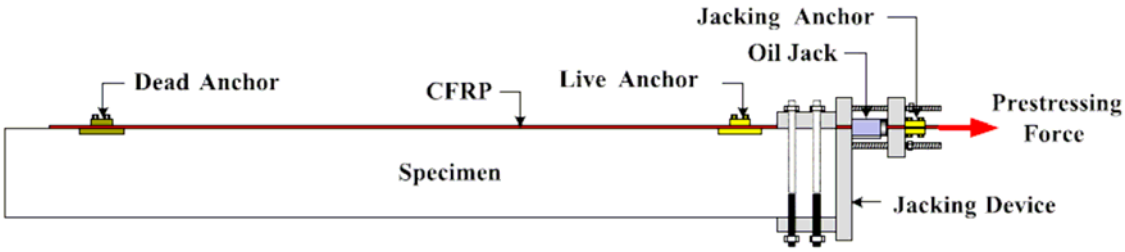

Fig.3.17 Prestressing device (Dong et al. 2009).

3.3.2 The used prestressing method in the current study

In the present study, the third method designated as the direct method was used, in which pre-tension force is introduced to the AFRP sheet by jacking directly to the strengthened beam itself. The advantages of the direct tensioning method include its ease of application on site. For example, this method was recently applied on site to strengthen the Main Street Bridge-Overpass No. 4, Winnipeg, Man., Canada (Kim et al. 2004, 2006; Kim 2006). This application was particularly the first North American site application using prestressed CFRP sheets. In the current study, according to this method, AFRP sheet was first anchored temporarily at one end (dead end) and then tensioned from the other end (live anchor) using a power-operated hydraulic jack as shown in **Figs.3.18 and 3.19**. After the adhesive had cured, the sheet ends upon release of the prestress because the load applied to the AFRP sheet was then reduced to zero. Therefore, the prestress being transferred to the beam by the cured adhesive bond layer, and the sheet was cut through to isolate the beam.

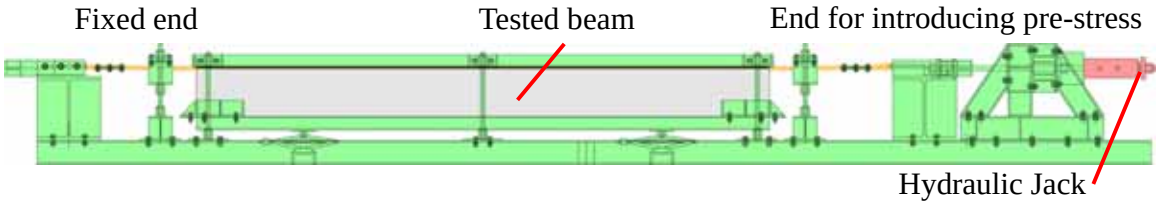

Fig.3.18 Schematic of prestressing device

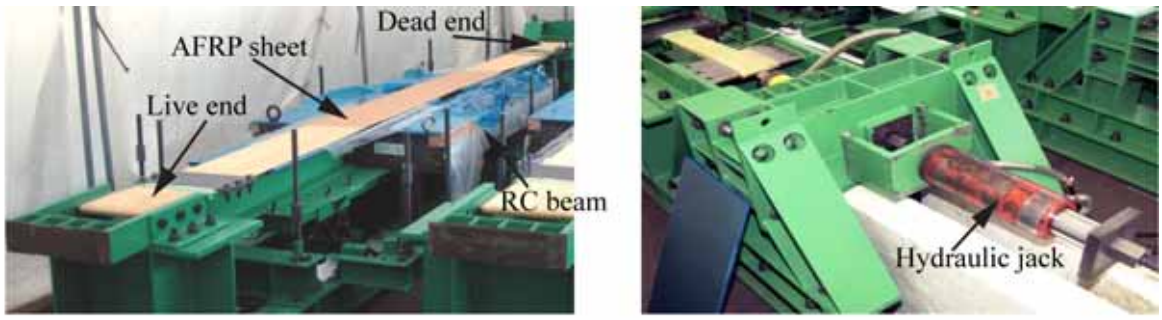

a) Preparation of bonding AFRP sheet b) Set of hydraulic jack

Fig.3.19 View of prestressing device and bonding AFRP sheet

3.4 A new anchoring bonding method of AFRP sheet developed in this research

Anchoring of the end zones has been one of the biggest problems when concrete structures are strengthened with prestressed FRP sheet. In many instances, anchorage systems serve as a permanent anchorage to the FRP system leading to a costly solution due to the high costs associated with fabricating the specialized prestressing anchors and plates (Wight et al. 2001, El-Hatcha et al 2003, and Dong et al. 2009). To achieve a cost-effective solution, these anchorages can be optionally removed for usage in further applications. If left in place, permanent steel anchors are likely to be exposed to significant weathering or galvanic corrosion due to contact with the FRP material. Also, the anchors may need to be removed for aesthetics reasons, leading to potential debonding of the prestressing sheets or plates. To avoid premature debonding, it may be necessary to install U-wraps before removal of the anchors and plates (Kim et al. 2008a,b). Because of the presence of these

anchors and plates, however, the U-wraps must be placed away from the ends of the prestressed FRP system. Other disadvantages that can be associated with this method are that it tends to be laborious, and the beam surface must be properly treated before drilling for installation of the anchors. Moreover, sliding and the sheet peeling-off between the FRP U-wrap and longitudinal pre-tensioned FRP occurred. Thus, in the current study, a proposed anchoring method without anchoring devices (i.e., there are no metallic or non-metallic anchorages to be used) is developed to avoid these disadvantages of previous methods.

In this research, the AFRP sheet used for flexural reinforcing was bonded on the tension-side surface with 300 mm wide, leaving a 50 mm between the supporting point and the sheet end to prevent shear failure at supporting zones. For bonding the pre-tensioned AFRP sheet to the cross-directional AFRP sheet, bond for strain relaxation was used, which has a 150 % strain capacity and a young's modulus of 1/60 times smaller than that of the normal epoxy-resin. Epoxy-resin-type putty was used to adjust the horizontal level between the cross-directional AFRP sheet and the bonding surface of the RC beam as shown in **Fig.3.20**.

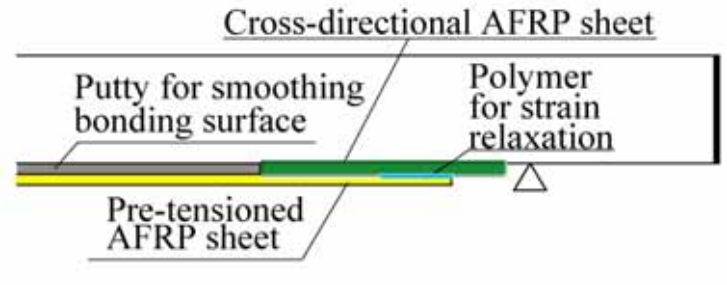

Fig.3.20 A proposed anchoring method of bonding AFRP sheet

Steps of a proposed bonding method of AFRP sheet

The AFRP sheet was bonded using a new proposed method based on the following procedure (Kishi et al. 2009), in which a schematic diagram of each step is shown in **Fig.3.21**:

(1) A grit-blasting bonding surface of the RC beam was applied to improve the bonding capacity and then the entire bonding area was coated with a primer to smoothen the rough concrete surface;

(2) The cross-directional AFRP sheet of 450 mm length was fixed at the ends of the main AFRP sheet used for flexural reinforcing, to widely disperse the concentrated anchoring stresses not only in the axis direction of the beam but also in the width direction (**Fig. 3.21a**);

(3) The level difference between the cross-directional AFRP sheet and the concrete surface was smoothened by filling with the putty material (its thickness was approximately 7 mm) (**Fig. 3.21b**);

(4) To apply pre-tensioning, the sheet was first anchored temporarily at one end (dead end) by warping the sheet around the steel plate and the other end was left as a live end attached to hydraulic jack. The AFRP sheet was then pre-cast by impregnation in epoxy-resin and curing;

(5) During one day, normal epoxy-resin was applied on the bonding surface of the RC beam, except for 200 mm from each end of the AFRP sheet bonded with a strain relaxation polymer to decrease the gradient of bonding stress near the anchoring. Subsequently, a pre-tension force was imposed into the AFRP sheet using a power-operated hydraulic jack immediately from the live end and the AFRP sheet was bonded to the surface by applying some pressure; (**Fig. 3.21c**); and

(6) After curing the epoxy, the pre-tension force was released by cutting the ends of the AFRP sheet in order to induce the force into the AFRP sheet. Consequently, the effect of pre-tensioning transferred to RC beam.

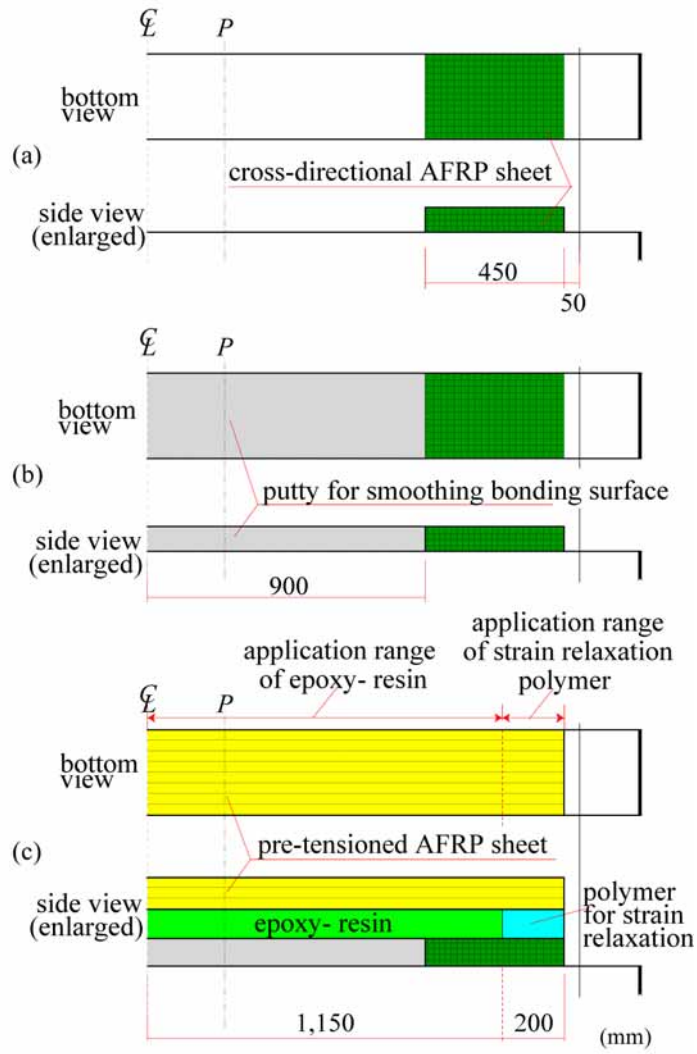

Fig.3.21 Schematic of a proposed bonding method of AFRP sheet

3.5 Summary

Adequate anchorage must be provided to resist a high level of prestressing force in the sheets because anchoring of the end zones has been one of the biggest problems when concrete structures are strengthened with prestressed FRP sheet. Due to limited shear strength of concrete, the high shear stresses at the ends of prestressed FRP strips can not be transferred into the structure. Thus, it has been necessary to mechanically anchor the strips at the ends to prevent premature peeling failures. However, the presence of permanent anchors minimizes the likelihood of premature peeling-off failure of the bonded FRP sheets. The permanent metallic anchor system, mounted in the strengthened beam, increases dead load and may present aesthetic and durability problems including corrosion. Thus, it may be desirable to remove the steel anchors after complete curing of the strengthening system provided that neither significant losses of the sustained prestress nor a premature failure occurs. With this technique, the replaced FRP anchors can effectively minimize the loss of prestress when the metallic anchors are removed. The nonmetallic anchors can also preclude premature peeling-off failure of the longitudinally prestressed FRP sheets. However, sliding and the sheet peeling-off between the FRP U-wrap and longitudinal pre-tensioned FRP occurred. From this point of view, in this present study, a new anchoring method without anchoring devices is proposed to avoid these disadvantages of previous methods.

CHAPTER 4

Experimental program

4.1 Introduction

This chapter presents the outline of experimental program of specimens used in this research. In additions, properties of the used material (concrete, steel reinforcement and FRP sheet), loading method and measurement items are explained. Finally, measurement system flow chart and measurement equipments (load cell, strain gauges, and laser sensor) used in this present study will be described.

4.2 Outline of specimens

A total of 20 RC beams were tested in the course of this research; 8 as part of a Strengthening Study of RC beams, 5 as part of a Strengthening Study of pre-cracked RC beams, and 7 as part of the Repair Study of pre-cracked RC beams. All RC beams used here have been analytically confirmed that the bending capacity was less than the shear capacity even after strengthening with AFRP sheet. Here, the bending and shear capacities of each strengthened RC beam have been estimated by using multi-section method (fiber model) and modified truss theory, respectively (Japan Society of Civil Engineering 2002).

-The Strengthening Study of RC beams, whose experimental program will be described in Chapter 6 of this dissertation, examined the behavior of flexural pre-tensioned AFRP strengthening systems. The variables examined in the experimental program included the pre-tension force ratio introduced to the AFRP sheet (0, 20, and 40%) and the main reinforcement steel ratio (0.79 and 1.24%).

-The Strengthening Study of pre-cracked RC beams, whose experimental program will be

described in Chapter 7, investigated the load-carrying behavior of pre-cracked RC beams strengthened with pre-tensioned sheet compared to non-pre-cracked ones. Pre-tension force ratio introduced to the AFRP sheet (0 and 40%) and level of prior loading (Level 1 is up to main rebar yielding; Level 2 is up to average point between main rebar yielding and ultimate load) were taken as variables.

-The Repair Study, whose experimental program will be described in Chapter 8, examined the effectiveness of pre-tensioned AFRP systems to restore the capacity of pre-cracked RC beams repaired with pre-tensioned sheet. In this study, pre-tension force ratio introduced to the FRP sheet (0 and 40%), with/without existing cracks and with/without repairing the cracks were taken as variables.

4.3 Material properties

In this research, the AFRP sheet used for flexural reinforcing have a unit mass of 830 g/m^2 and nominal load-carrying capacity of 1.176 kN/m, as shown in **Table 4.1.** AFRP sheet was bonded on the tension-side surface with the same width of the beam. For one direction of the cross-directional AFRP sheet, unit mass and nominal load-carrying capacities were 435 g/m^2 and 588 kN/m, respectively as shown in **Table 4.1**. In addition, for bonding the pre-tensioned AFRP sheet to the cross-directional AFRP sheets, bond for strain relaxation was used, which has a 150 % strain capacity and a young's modulus of 1/60 times smaller than that of the normal epoxy-resin. Epoxy-resin-type putty was used to adjust the horizontal level between the cross-directional AFRP sheet and the bonding surface of the RC beam. The stiffness of putty at a setting of 1.1 GPa was considered as Young's modulus, obtained from material tests. **Table 4.2** shows the mechanical properties of rebar steel (arrangement of stirrups and steel rebar are shown in **Fig.4.2**).

At the commencement of the experiment, average compressive strength of concrete using standard cylinders (shown in **Fig.4.1**) were as follows:

(1) In case of specimens used in strengthened Study, average compressive strengths of concrete was 35.8 MPa;

(2) In case of specimens used in strengthened pre-cracked Study, average compressive strength of concrete was 31.6 MPa and;

(3) In case of specimens used in repair Study, average compressive strength of concrete was 30.2 MPa.

Table 4.1 Mechanical properties of AFRP sheet

Mass (g/m^2)	Nominal tensile capacity (kN/m)	Thickness (mm)	Tensile strength (MPa)	Elastic modulus (GPa)	Ultimate elongation (%)
830*	1,176	0.572	2,060	118	1.75
435/435**	588/588	0.286/0.286			

*: pre-tensioned AFRP sheet, **: cross-directional AFRP sheet

Table 4.2 Mechanical properties of rebar steel

Nominal name of rebar	Yielding strength (MPa)	Ultimate strength (MPa)	Young's modulus (GPa)
D10	356	523	206
D13	377	551	
D16	383	553	
D19	392	559	

(a)

(b)

Fig.4.1 Preparation of RC beams (a) Fresh concrete, (b) Standard cylinders

(a) Stirrups

(b) Rebar steel

Fig.4.2 Arrangement of stirrups and rebar steel

4.4 Experimental procedure

4.4.1 Loading method and measurement items

In this study, the surcharged load (hereinafter, load), the mid-span deflection (herein after, deflection), and the strain distribution of the pre-tensioned AFRP sheet was measured as shown in **Fig.4.3.** These signals were continuously recorded by using digital data-recorder to precisely investigate the debonding process of the sheet. Also, development of cracks and debonding and/or rupturing behavior of the AFRP sheet were continuously recorded by taking photos and video. Strain gauges were bonded to the AFRP sheet at intervals of 100 mm to measure the axial strain distribution of the AFRP sheet during the entire loading procedure as shown in **Fig.4.3.** In addition, strain gauges were bonded on the middle of rebar to measure rebar strain. These loading tests used hydraulic jack of 500 kN capacity. The loading rate is 5 kN/min. It leads to displacement rate of 5 mm/min. A four-point loading flexural test, with 500 mm pure bending span, was conducted. Therefore, the shear span ratio becomes about 7.2 considering the 160 mm effective height of the cross-section in case of the strengthened non-pre-cracked and pre-cracked study. However, in case repaired study, the shear span ratio becomes about 7.5 considering the 180 mm effective height of the cross-section.

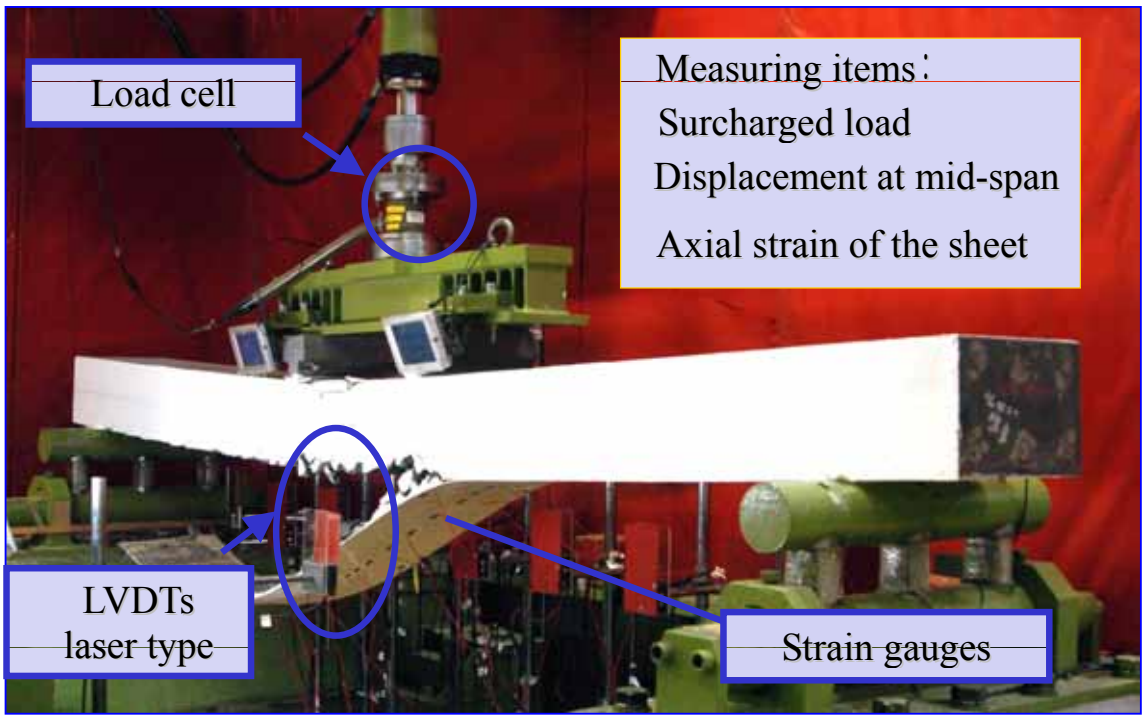

Fig.4.3 Loading method, set up, and measurement items

4.4.2 Outline of pre-loading for making cracks and repairing

Before strengthening the specimens with AFRP sheet in strengthened pre-cracked specimens Study which will be mentioned in Chapter 7, RC beams were pre-loaded for pre-cracking (Level 1: loading up to main rebar yielding; Level 2: loading to the middle point between main rebar yielding and ultimate state (hereinafter, analytical ultimate state)) as shown in **Fig.4.4a**. After that, they were removed from the loading apparatus and then strengthened with AFRP sheet mentioned in Chapter 3. Finally, the specimens were reloaded until reaching complete failure as shown in **Fig.4.4b,c**. The primer was poured inside the pre-cracks to improve the bonding behavior of concrete surface.

However, in case of specimens in repaired study which will be mentioned in Chapter 8, before strengthening with AFRP sheet, Beams were cracked by four-point loading test. The surcharged load was up to reach the middle point of the deflections between numerically estimated main rebar yielding point and the ultimate state (hereinafter, analytical ultimate

state), in which the numerical evaluation method will be explained in Chapter 5. This is the reason that the beams suffered relatively severe damage, even though the rebar yielded and crushing of concrete wasn't reached. After that, they were removed from the loading apparatus and then cracks (hereinafter, existing cracks) were repaired by injecting epoxy-resin type adhesive. Only the cracks with more than 0.2 mm width were repaired. Finally, the specimens were reloaded until reaching complete failure as shown in **Fig.4.4.**

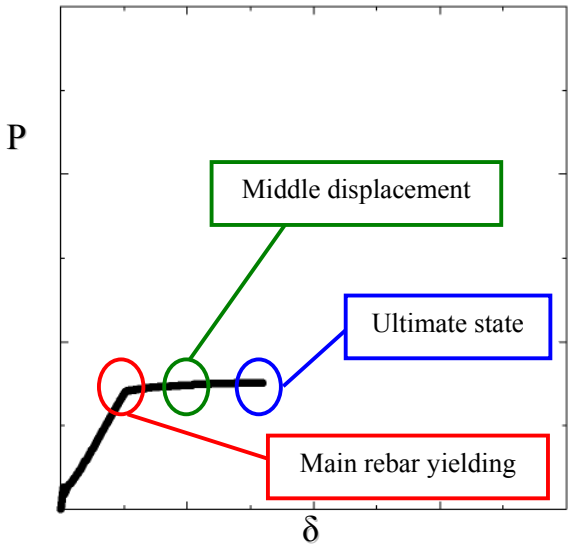

a) Analytical results for control RC beam

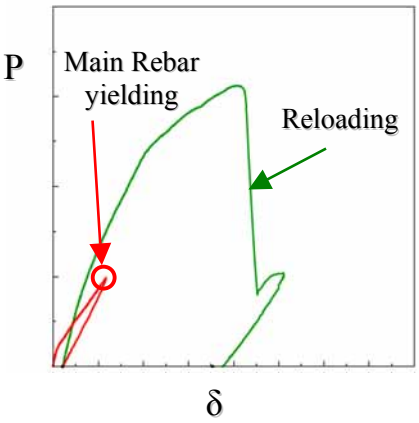

b) Prior loading level 1

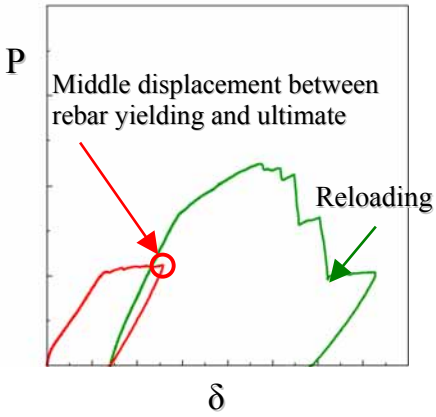

c) Prior loading level 2

Fig.4.4 Loading procedures

4.5 Measurement system

4.5.1 Measurement apparatus

The experimental apparatus that can measure the force act on the RC beam to understand the load-carrying behavior of the RC beam and the study on the flexural performance experimentally is necessary. Moreover, to understand the load-carrying behavior of the RC beam for the force measurement that receives the static force, the load cell, the displacement sensor, the amplifier, and the data recorder, etc. are needed. In the actual experiment, in the reaction support device, a load cell is set up in the side support, and the resultant force output from the load cell is handled as a side support reaction force. In this thesis, the side of support reaction force independently measured is added and the support reaction force is evaluated as a matched combination support reaction force. In addition, strain gauges were bonded to the AFRP sheet at intervals of 100 mm to measure the axial strain distribution of the AFRP sheet during the entire loading procedure. In addition, strain gauges were bonded on the middle of rebar to measure rebar strain as shown in **Fig.4.3**. Also, in the actual experiment, to measure the mid-displacement at the middle of span of the RC beam, the contact less laser type displacement sensor was used as shown in **Fig.4.5**. **Table 4.3** shows the outline of the specification of laser type sensor.

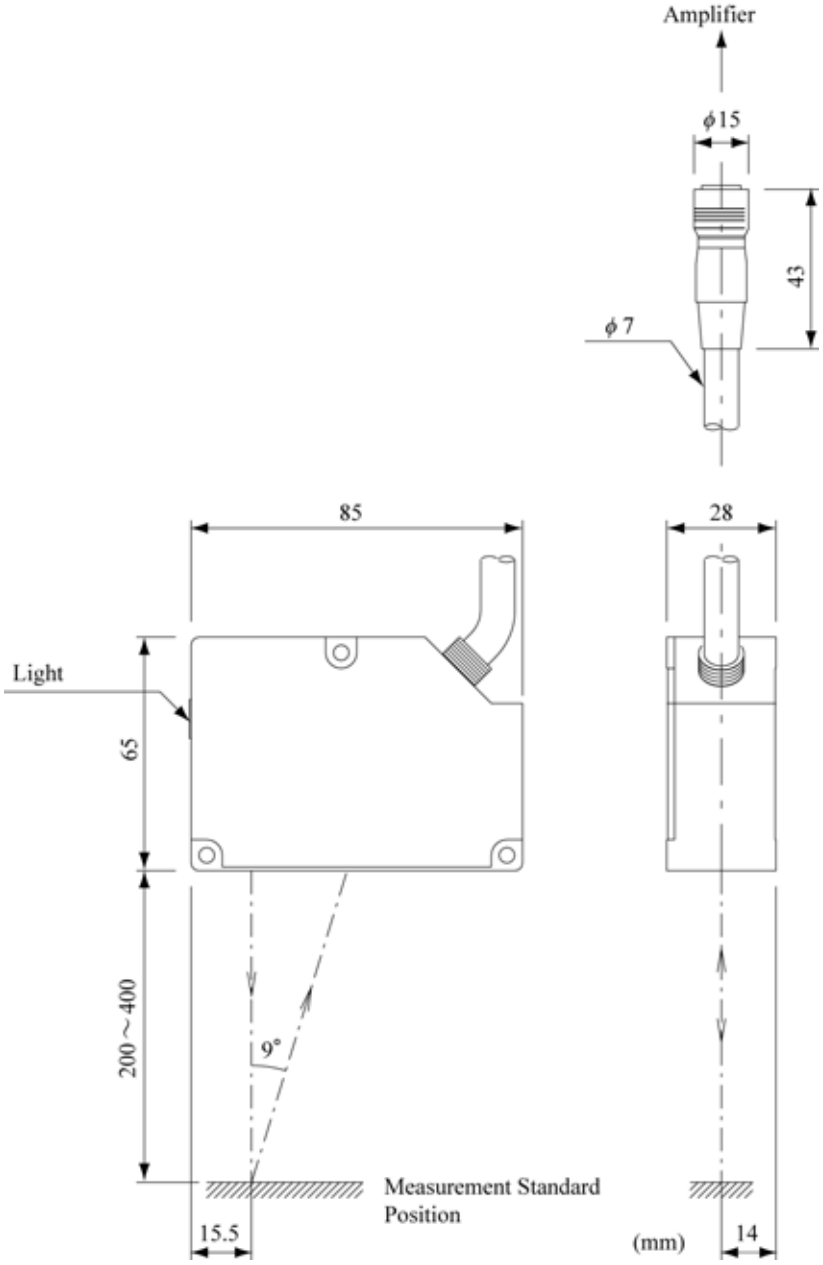

Fig.4.5 Outline of contact less laser type displacement sensor

Table 4.3 Specification kind of contact less laser type displacement sensor (LB300)

Sensor head model (LB-300)	Super-long-range type
Amplifier unit	LB1200
Standard distance	300 mm
Time base range	±100 mm
Source of light	Red semiconductor laser
Wave length Mm (invisibility)	780 ..output.. 20-class or less 3B MW (average 10mW)
Spot diameter	1.2×2.5 Mm (In a standard distance)
Straight line	(white paper) 0.4%of F.S .
Analog voltage output	±5 V (20 mm/V)
Voltage impedance	100 Ohm
Current output	VA-
Temperature drift sensor head.	0.02%of F.S./℃ amplifier unit
Environment use surroundings illuminance	0.02%of F.S./℃
Environment	Lamp and white heat of use surroundings illuminance fluorescent lamp 4,000 Lx or less Ambient temperature of use amplifier unit 0-50℃
Sensor head	0-45℃ Use surroundings humidity 35-85% (No do be dewy.)
Vibration	10-55 Hz amplitude 1.5m
Material	Sensor head aluminum die cast Amplifier unit polycarbonate
Weight	About head sensor 250 g About unit amplifier 530 g

4.5.2 Measurement system flowchart

Fig.4.6 shows flowchart of measurement system. After measuring surcharged load using load-cell, mid-displacement by LVDT laser-type and strains of sheet and rebar using strain gauges, a special amplifier unit is used. Then, the analog to digital conversion and the physical amount conversion (data calibration) are given at the same time as continuously measuring it with ms with a digital data recorder and the data collection is done to the semiconductor memory**.**

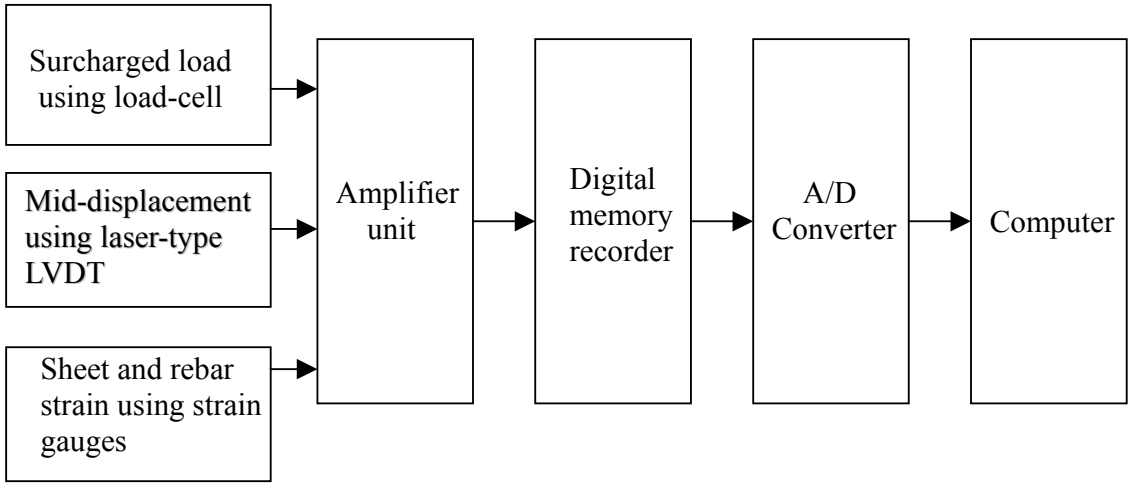

Fig.4.6. Flowchart of measurement system

CHAPTER 5

Analytical approach

5.1 Introduction

Numerical analysis was performed for all RC beams used in this study for comparison with the experimental results. A multi-section method was applied to analytically estimate the load-displacement relation and the axial strain distribution of AFRP sheet used for flexural reinforced each RC beam with different ratios of pre-tension stress and the main reinforcement steel. In this chapter, assumptions taken into consideration to apply this analytical approach will be mentioned, material properties used in this research will be described, and the procedures of calculation of the analytical method explained and described briefly in flowchart.

5.2 Assumptions

In this Analytical approach, it is assumed that:

(1) The ultimate compressive strain of the concrete is 0.35 %, following the standard specifications for concrete structures in Japan (Japan Society of Civil Engineering 2002);

(2) A cross-section of the RC beam remains plane during the whole loading; and

(3) The AFRP sheet is perfectly bonded to concrete until reaching the analytical ultimate state.

In this simulation, the existing cracks and the stiffness of putty used for flattening the bonding surface were not considered

5.3 Material modeling

Stress-strain relationship for the concrete and the steel rebar used in this numerical analysis were determined based on the standard specifications for concrete structures in Japan (Japan Society of Civil Engineering 2002) to predict the flexural behavior of RC beams.

5.3.1 Concrete

For concrete, following Japanese concrete standard, in the tension region, stress increases linearly and cut off at the tensile strength. In the compression region, up to 0.2 % strain, curve is parabola and then keeps constant up to 0.35 % strain and reaches ultimate state. For stress-strain relations shown in **Fig.5.1a**, σ, ε, and f'_c are stress, strain, and strength of the concrete in compression, respectively. In addition, f_t is tensile strength of concrete. When the compressive strain of concrete (ε) is increased up to the ultimate compressive strain of 0.35%, the RC beam is defined to be under analytical ultimate state and the loading point is defined as the analytical ultimate loading point.

5.3.2 Steel reinforcement

Stress-strain relation of steel is assumed as perfect elastic plastic relation with Young's modulus of 206 GPa . f_y and E_s are main rebar yielding strength and Young's modulus of the rebar as shown in **Fig.5.1b**.

5.3.3 AFRP sheet

In the case of AFRP sheets, the axial stress was assumed to be linearly increased up to the breaking strain of 1.75% and to be cut off at zero stress in the tension region. For stress-strain relations shown in **Fig.5.1c**, E_f, f_{fu}, and ε_{fu} are ultimate tensile strength, tensile strain and Young's modulus of the AFRP sheet, respectively.

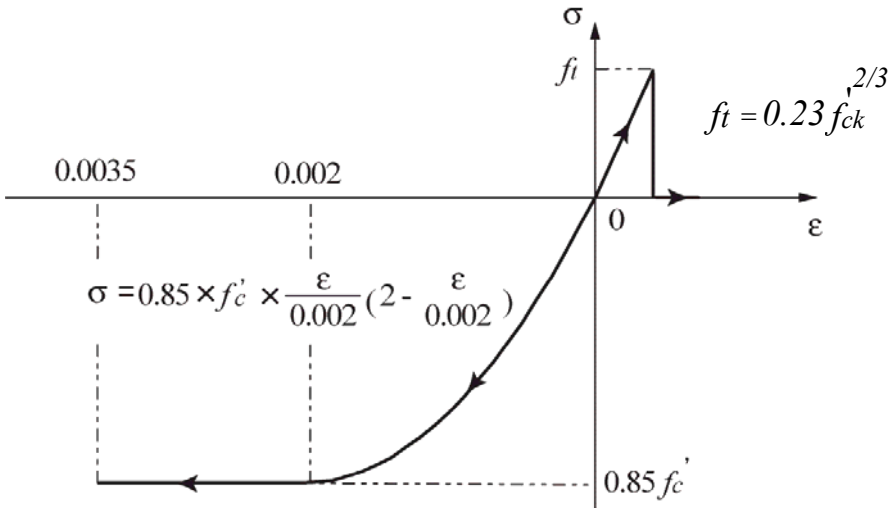

(a) Concrete

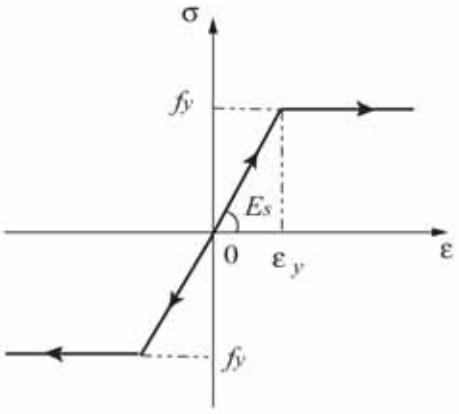

(b) Steel rebar

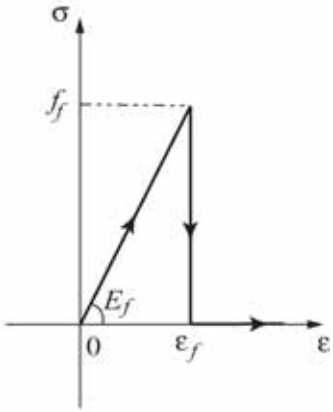

(c) AFRP sheet

Fig.5.1 Stress-strain relation for each material.

5.4 Calculation procedure

A multi-section method is applied to calculate load-displacement relation of the tested beams and axial strain distribution of AFRP sheet. In the calculation procedure using Fortran program, the location of the neutral axis must be determined by trial and error to satisfy the compatibility condition of the variation shown in **Fig.5.2** and the equilibrium condition of the force. In this study, the location of the neutral axis during failure and the strain of AFRP sheet were determined by assuming lower strain edge (ε_l) as shown in **Fig.5.3**. In this analysis, the concrete section was divided into a number of elements of 5 mm thickness and the stress-strain model of concrete was applied (see **Fig.5.1a**). Additionally, a complete elastic material model was applied as in **Fig.5.1b** for the reinforcing bar, and an elastic model, which showed elastic behaviour until the ultimate strain as shown in **Fig.5.1c** was applied for the AFRP sheet. All RC beams used here have been analytically confirmed that the bending capacity was less than the shear capacity even after strengthening with AFRP sheet. Here, the bending and shear capacities of each strengthened RC beam have been estimated by using multi-section method (fiber model) and modified truss theory, respectively (Japan Society of Civil Engineering 2002).

The calculation procedure to predict the load-deflection for a given element within the beam (control and non-pre-tensioned) is given as follows:

- Inputs for the program include the cross-section of the beam, amount of reinforcement and material properties (concrete, steel reinforcement, and AFRP sheet);
- Assume a strain (higher than the initial strain) at the compression fibre of concrete (for pre-tensioned beam) at the given element;
- Set the strain of the lower edge (ε_l);
- By using ε'_c and ε_l, calculate the strain distribution in the lower part of the cross-section of the plane due to calculating the neutral axis depth using force equilibrium equations;
- Confirm lower strain of the edge (ε_l) and calculate the stresses and strains in the

compression, tension steel and AFRP sheet;

- Perform a trial and error procedure by revising the assumed value of the concrete strain, until the total compression and total tension forces are equal;
- Calculate the curvature and bending resistance moment of the given element;
- Repeat the procedure for new values of ε'_c and ε_l.
- When $\varepsilon'_c \geq \varepsilon'_{cu}$ (ε'_{cu} is the ultimate strain of the upper concrete edge (3,500μ)), the calculation procedure stopped because the failure occurred due to concrete crushing.
- The program also allows specifying the prestressing level of the AFRP sheet.

-The calculation procedure for the pre-tensioned strengthened beam is slightly different from the control and the non-pre-tensioned strengthened beams due to initial strains induced in the section. The summary is given as follows.

- Calculate the initial strains in the section due to pre-tensioning;
- Calculate the stresses and the strains at given element.

The above procedure is summarized in a flowchart as shown in **Fig.5.3**, in which ε'_s and ε_s are rebar strains in compression and tension zones, respectively.

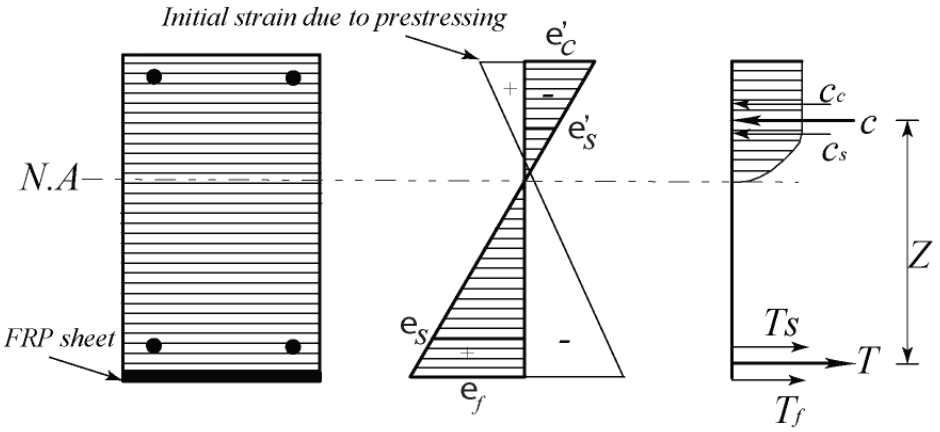

Fig.5.2 Strain and stress distribution of RC beams section

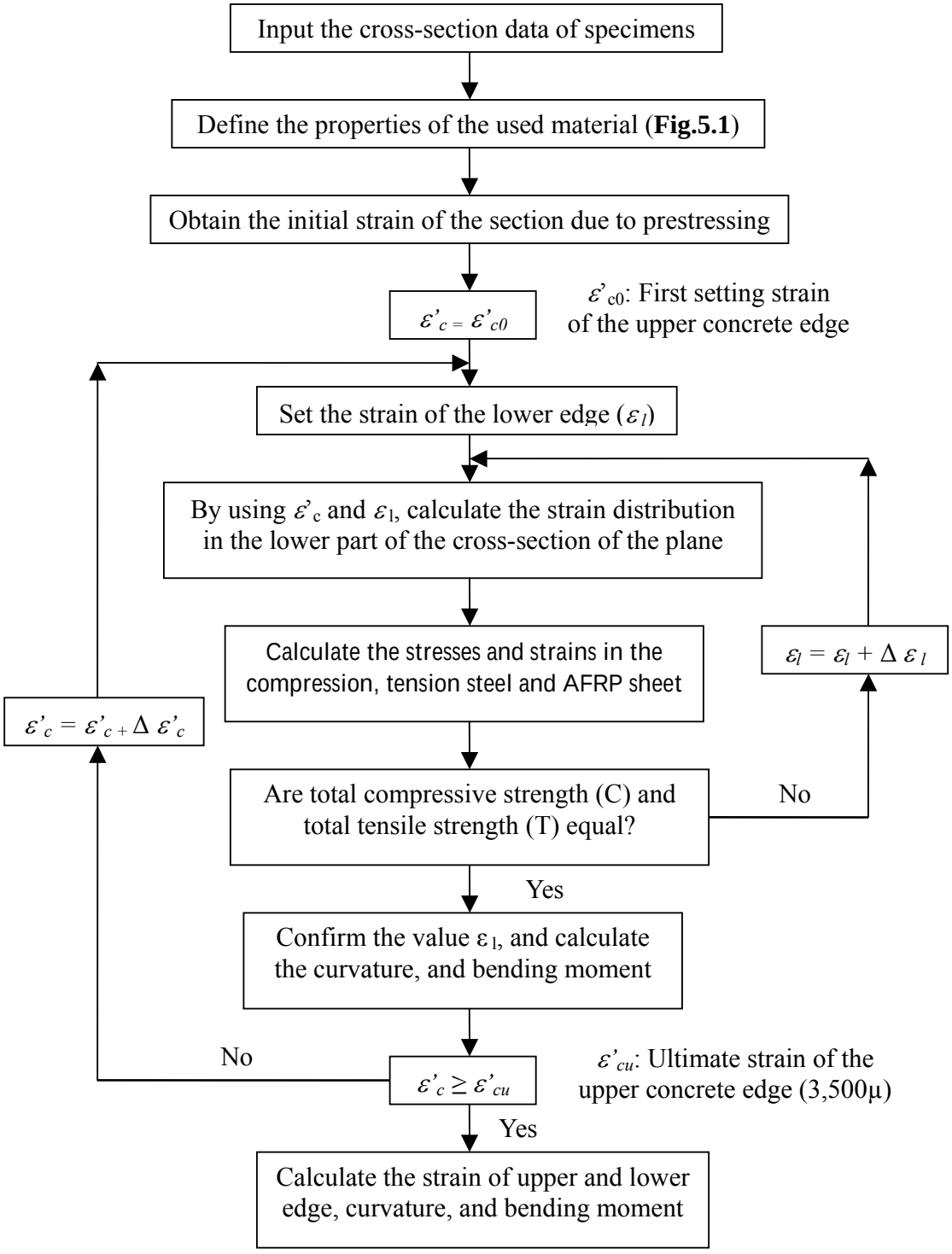

Fig.5.3 Flowchart of the analytical method

CHAPTER 6

Study of strengthened RC beams

6.1 Introduction

In order to develop a rational flexural reinforcing method for RC beams using a pre-tensioned AFRP sheet and to investigate a new proposed anchoring method, the results of eight RC beams tested at the Structural Laboratory of Civil Department at Muroran Institute of Technology, Japan, are presented in this chapter (Kishi et al. 2009). The test results were observed by visual inspection during the test and measured by instrumentation. These results are described in different forms as crack patterns in different stages of loading, load-deformation curves, and axial strain distribution so the sheet was at the ultimate state. The test parameters include pretension stress ratio introduced to the sheet and the main reinforcement steel ratio. These parameters were carefully chosen to obtain different modes of failure as will be discussed in the following sections.

6.2 Outline of specimens

In this study, a total of eight specimens listed in **Table 6.1** were made, in which the pre-tension force ratio introduced to the sheet (0, 20 and 40% of tensile strength of AFRP sheet) and the main reinforcement steel ratio using different diameters of the rebar (D13 and D16 for Beams kind A and B, respectively) were taken as variables. These specimens were designated by the pre-tension force ratio *n*% as Beam A/B-T*n* and control specimens are named as Beam A/B-N without bonding AFRP sheet. The target and actual pre-tension force ratios and the introduced initial strain into the sheet are listed in **Table 6.1**, in which the ratios are obtained by referring to the nominal tensile capacity of the sheet. The beams have a rectangular cross-section of 200 x 300 mm (height x width) and a clear span of

2,800 mm. Layout of the reinforcement and bonding sheets are shown in **Fig.6.1**. Three rebar of diameter 13 mm for Beams type A and three rebar of diameter 16 mm for Beams type B were placed in the lower layer for bending reinforcement. In addition, three rebar of 13 mm diameter were used in the upper layers of all specimens. To prevent premature shear failure, an adequate amount of shear reinforcement was mounted with 10 mm diameter steel stirrups at a spacing of 75 mm as shown in **Fig.6.1**. The ends of the axial rebar were welded to the steel plates of t = 9 mm thickness, set to the ends of the beam, to save the anchoring length of the rebar. AFRP sheet of 300 mm width was pre-tensioned and then bonded onto the tension-side surface, leaving 50 mm between the supporting point and the sheet end as shown in **Fig.6.1**, to preclude the effect of support reaction on the sheet.

Table 6.1 List of specimens

Specimen	Rebar nominal name, (Rebar ratio)	Designed pre-tension force ratio* (%)	Actual pre-tension force ratio* (%)	Introduced initial tensile strain(μ)
A-N	D13 (0.79%)	Non-strengthened		-
A-T0		-	-	-
A-T20		20% (70.6)	19.7% (69.6)	3,439
A-T40		40% (141.1)	37.2% (131.3)	6,494
B-N	D16 (1.24%)	Non-strengthened		-
B-T0		-	-	-
B-T20		20% (70.6)	18.6% (65.7)	3,247
B-T40		40% (41.1)	39.2% (38.2)	6,843

*( ): Pre-tension force (kN)

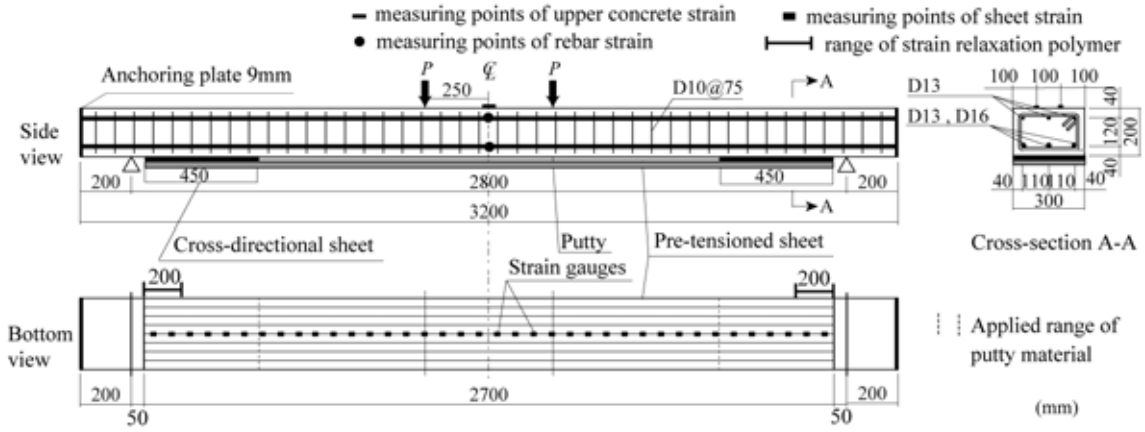

Fig.6.1 Layout of reinforcement and AFRP sheet

6.3 Effect of pre-tension force introduced to the AFRP sheet

The comparisons between experimental and analytical results for the load-displacement relationship at the mid-span of the tested specimens are shown in **Fig.6.2**. In addition, **Table 6.2** presents the experimental and analytical values for the cracking load, the main rebar yielding load, the maximum load, experimental failure modes and the ratio between the experimental and analytical values.

For the tested beam A-N, experimental results (**Fig.6.2.a**) show a decrease in stiffness due to the flexural cracks at the loading level of 10 KN and a displacement of 1.3 mm and then due to the main rebar yielding at a loading level of 40 KN and a displacement of 14 mm. After that, under constant stiffness and an ultimate loading level of 55 KN, a displacement of 70 mm has been reached. Once the failure of the control beam occurs under a compressive force, a subsequent sudden drop of the concrete load-carrying capacity was recorded as shown in **Fig.6.2**.

In case of the control beam B-N, from the experimental results shown in **Fig.6.2.b**, the stiffness decreases due to flexural cracks at the loading level of 6.63 kN and a displacement of 0.77 mm and at main steel reinforcement yielding at the loading level of 60 kN with a displacement of 16 mm. After that, displacement increases, keeping a small increase i in stiffness and then reaching the ultimate state at a loading level of 75 kN with a

displacement of 61 mm. When the compressive strain of concrete reaches 0.35% on the upper fiber, the load consequently drops dramatically as shown in **Fig.6.2b**.

For Beam A-T0 reinforced with non-pre-tensioned AFRP sheets, even though the cracking load seems to be similar to that of the control beam A-N, the flexural stiffness becomes higher after the cracking and also after the main rebar yielding. However, displacement at the ultimate state is almost the same in Beams A-N/T0 as shown in **Fig.6.2a**. In fact, without pre-tension, the addition of the AFRP sheet only slightly affects the beam performance before the first crack. While a significant improvement of the beam performance has been observed after cracking due to the contribution of the AFRP sheets in carrying a portion of the stresses. Thus, the AFRP sheet has induced a redistribution of stresses carried by the steel reinforcement. This may lead to a significant increase in the load-carrying capacity when the main rebar yields. Based on the experimental results of Beam A-T0, the yielding of the main rebar occurs at a load 87% higher than that of the beam A-N (**Table 6.2**). Moreover, a 141% increase in the ultimate load of the control beam A-N was obtained for beam A-T0 when the AFRP sheet without pre-tension is used.

In case of Beam B-T0, the cracking load is little higher than that of Beam B-N. However, flexural stiffness increases notably after reaching the cracking and internal reinforcement yielding as well. Displacement at the ultimate state is nearly unchanged. Thus, the addition of AFRP sheets without pre-tension has little effect on the beam performance before the first crack forms. However, because AFRP sheet carries a portion of tensile stresses after cracking occurs, the beam performance enhances. As a result, the AFRP sheet contributes to the load-bearing capacity of the beams since tensile stresses carried by internal reinforcement are redistributed to the AFRP sheet thereby increasing the loading level at yielding of internal reinforcement. From experimental results of Beam B-T0, the yielding of the internal reinforcement is reached at a load 52% higher than that of Beam B-N as presented in **Table 6.2**. In addition, an 88% increase in the ultimate load of Beam B-N is obtained in Beam B-T0 when AFRP sheet without pre-tension is applied.

For the tested beams A-T20/40 reinforced with pre-tensioned AFRP sheets, the loading level in the region from crack-opening to the ultimate state has a tendency to increase

according to an increment of pre-tension force in the AFRP sheet. When the pre-tensioned AFRP sheet is used, the main rebar is relieved of tensile stresses and placed slightly into compression. It has been observed that the AFRP sheets due to the pre-tensioning carries a great portion of the tensile stresses. As a result, the load-carrying capacity of the beams reinforced with the pre-tensioned AFRP sheet increases after yielding of the main rebar. Thus, the experimental data for the pre-tensioned sheet has revealed that the loading level of the main rebar yielding increases by 130% and 220% for the beams A-T20 and A-T40, respectively, compared to the control beam A-N (**Table 6.2**). This clearly demonstrates the effect of the pre-tensioned sheet in applying an axial compressive force over the whole depth of the section and in applying a moment, which tends to place the top of the section in tension and cause additional compression at the base of the beam. This leads to an increase in the value of the external load required for producing a visible flexural cracking, hence the cracking load increases considerably (204 and 450 % for pre-tension force ratio in the sheet of 20 and 40%, respectively, compared to Beam A-N). Furthermore, from the experimental results summarized in **Table 6.2**, the increase of the ultimate load is higher when the pre-tensioned AFRP sheets were bonded to the beams compared to Beam A-N (up to 210 and 240% for beams A-T20/40, respectively). This increase may be due to a change in the failure mode of Beam A-T0 from sheet debonding to sheet rupture in Beams A-T20/40. Due to the initial camber of the beams reinforced with pre-tensioned sheet, an improvement of the cracking load has been observed. This may be due to the initial pre-tension introduced to the AFRP sheet and the relatively larger tensile force carried by the AFRP sheet. The cracks control not only decreased the deflection but also improved the durability of the concrete structure since its deterioration is strongly related to the width of the cracks. Therefore, it could be concluded that the pre-tensioned AFRP sheet may be successfully applied in the cracked section members. Following failure, the strengthened beams with the sheet retained a reserve capacity, comparable to the strength of the control beam as shown in **Fig.6.2a** in experimental results.

In the case of Beams B-T20/40, the loading level in the range from cracking to the ultimate state tends to increase according to an increment of the pre-tension force in the AFRP sheet

as shown in **Fig.6.2b**. Due to pre-tensioning the AFRP sheet, tensile stresses in the main steel rebar are further reduced and a greater portion of the tensile stresses carried in the beams is shifted from the main steel rebar to the AFRP sheet even before the beams are subjected to external loading. Thus, in comparison to the control beams, a significant increase in the load-carrying behavior is obtained. For example, experimental values illustrate that when pre-tensioned sheet is applied, cracking load increases by 485 and 689 % for Beams B-T20/40, respectively and yielding of main steel reinforcement takes place at loads that are 95 and 138% for Beams B-T20/40, respectively, higher than those of the Beam B-N as shown in **Table 6.2**. As a result, the load-carrying capacity of the beams increases after the yielding of internal reinforcement. Moreover, from experimental results, the ultimate loads increase by 117 and 141 % when pre-tensioned AFRP sheet is bonded to Beams B-T20/40, respectively. This may be occur due to a change in the modes of failure from sheet debonding in Beam B-T0 to sheet rupture in Beams B-T20/40 as will be explained later. Following failure, the strengthened beams with the sheet retained a reserve capacity, comparable to the strength of the control beam as shown in **Fig.6.2b** in experimental results.

At the ultimate state, it is clear that the displacement has a tendency to decrease since a part of the AFRP sheet strain is used for the pre-tensioning process. Thus, the specimens could have a brittle failure behavior. However, displacement at any loading level was significantly lower with the addition of the non-pre-tensioned AFRP sheets and was further reduced when the pre-tensioned sheet is bonded as shown in **Fig.6.2**. These results have proven the ability of the pre-tensioned AFRP sheet to control cracking in RC beams. This could be explained by the fact that the sheet in the reinforced beam generate a tensile force along the deformed concrete section and create an equilibrium among the internal forces with much less deformation compared to that of the control one.

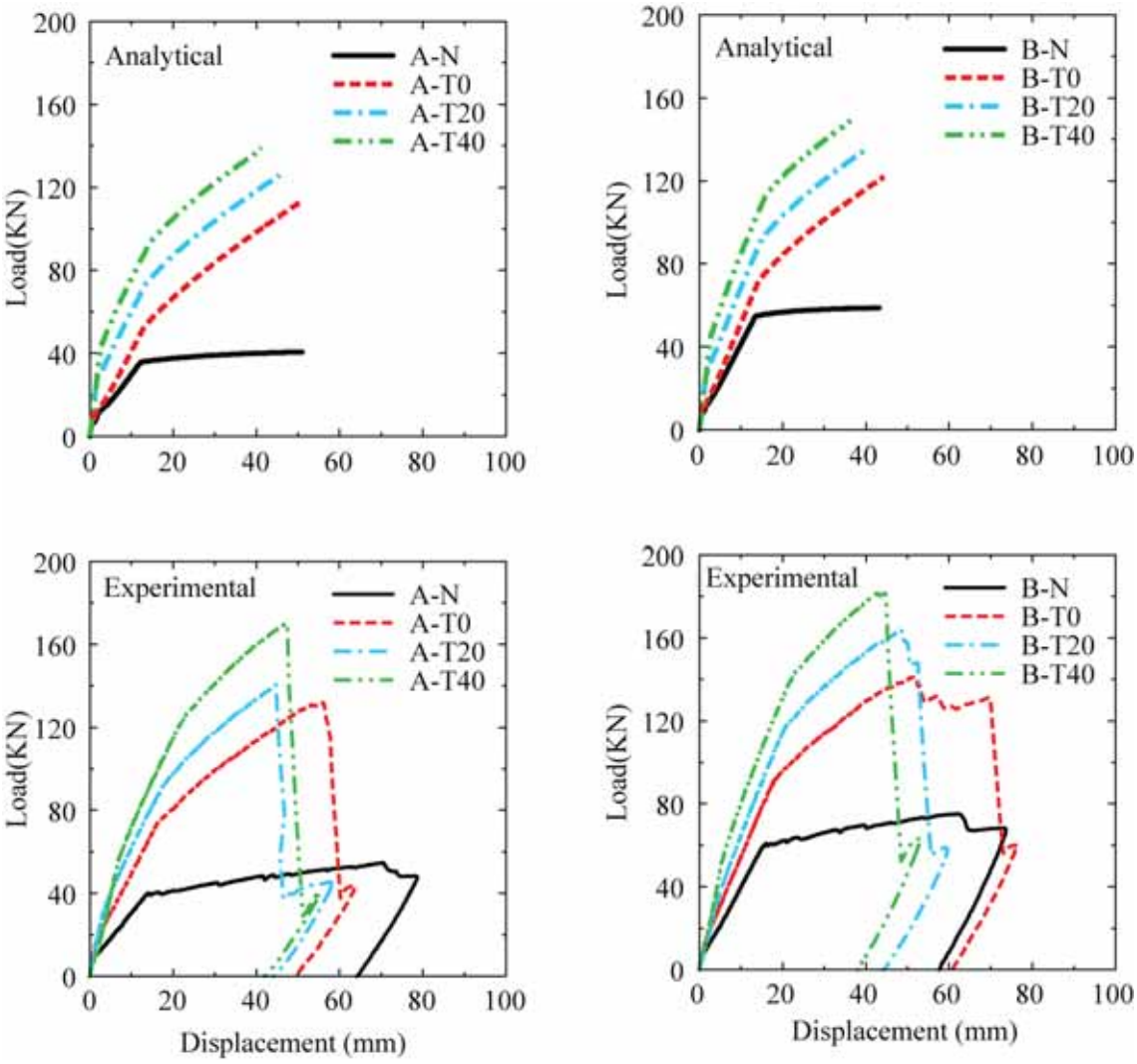

(a) Beams A (b) Beams B

Fig.6.2 Experimental and analytical results of load-displacement relations with the same steel rebar ratio and with different pre-tension force

6.4 Effect of main steel reinforcement ratio

Fig.6.3 and **Table 6.2** show that due to the increase of the main steel reinforcement ratio in Beams B, the flexural stiffness of these beams is higher than that of the Beams A. This confirms that the flexural stiffness and the load-carrying capacity of the tested specimens increase as the tensile reinforcement ratio increases. Moreover, for the specimens reinforced with the pre-tensioned AFRP sheet, the pre-tension level, regardless of the tensile reinforcement ratio, determines the initial crack load. Beyond that, the failure behavior depends on the ratio of the tensile reinforcement. Experimental results have also revealed that the specimens with a low reinforcement ratio (Beams A) have a higher increase in flexural capacity than that of specimens with a high reinforcement ratio (Beams B) compared to control ones (i.e. as the steel ratio lowers, the effectiveness of strengthening with pre-tensioned AFRP sheets increases.). It is found that the maximum load increases by 141, 157, and 210% for the Beams A-T0/20/40, respectively, whereas in case of Beams B-T0/20/40, the maximum load increases by 88, 117, and 141%, respectively as compared to the control beams. Generally, Beams B have shown a similar trend to that of Beams A.

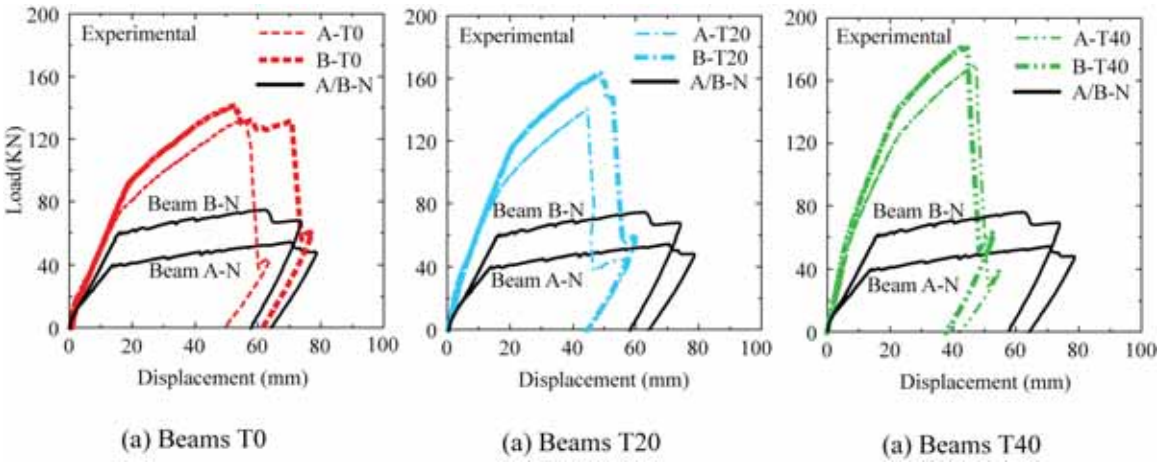

Fig.6.3 Comparisons of load-displacement relations of beams reinforced by bonding AFRP sheet with the same pre-tension force and with different rebar steel ratio

6.5 Comparison between the experimental and analytical results

From the analytical results shown in **Table 6.2** and **Fig.6.4** (In this simulation, the stiffness of putty used for flattening the bonding surface were not considered), the loading level at the cracking, main rebar yielding and the ultimate state are upgraded as a result of introducing pre-tension force to the AFRP sheet. This trend seems to be similar to that found in the experimental results. From **Table 6.2**, the comparisons between the experimental and analytical results have shown that the loading level obtained from experiments at the ultimate state is slightly higher (around 15%) than those of the analytical results for the strengthened specimens (Beams T*n*). These results may indicate that the pre-tensioned AFRP sheet may offer adequate bonding up to the analytical ultimate state of the RC beams without any anchoring devices. Moreover, the difference for beams reinforced with the pre-tensioned AFRP sheet (A/B-T20/40) is lower than that of control beams (28% and 35% for Beams A/B-N, respectively) (**Table 6.2**). Thus, the flexural behavior of beams reinforced with pre-tensioned AFRP sheet can be successfully evaluated using multi-section method. The ratio between the experimental and the predicted results was found to be higher than 1.1, except in case of the beam B-N at cracking, for which the ratio is 0.83 (**Table 6.2**). It may be expected that the ratio of 1.1 could be used as a safety factor in designing the RC beams with the pre-tensioned AFRP sheet using a muli-section method employing putty material. Thus, the flexural behavior of these beams can be analytically predicted as proven in the present study.

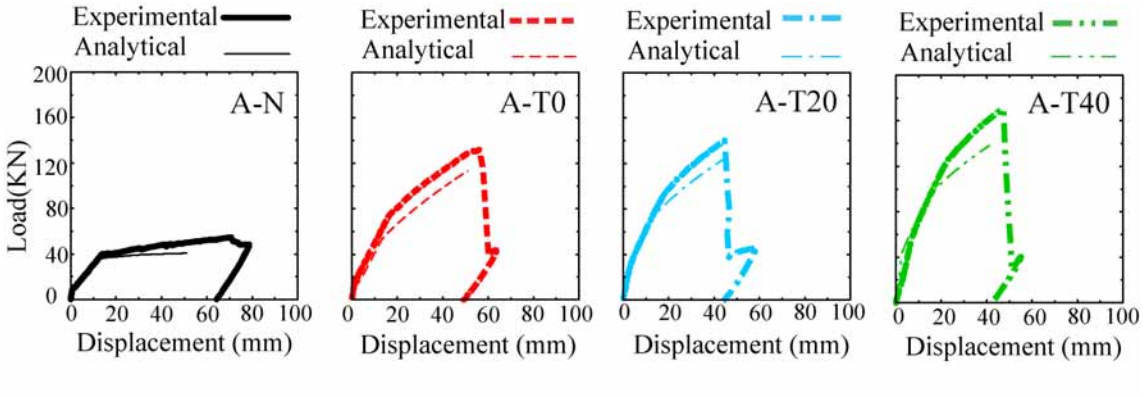

(a) Beams A

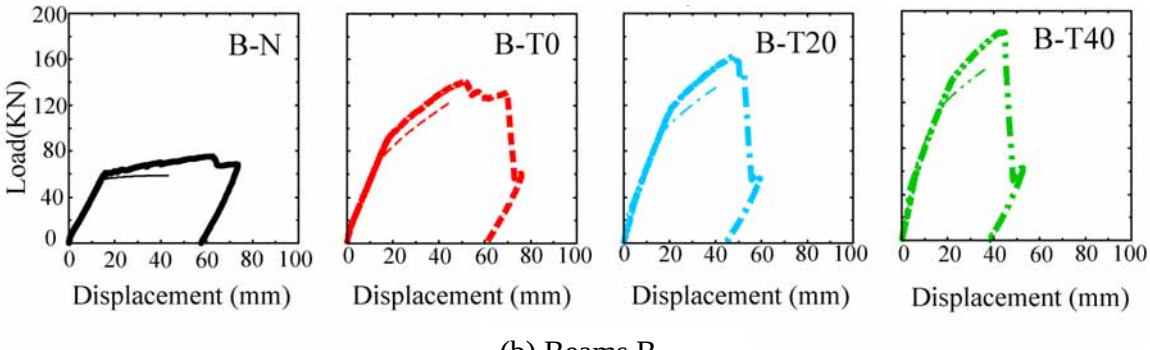

(b) Beams B

Fig.6.4 Comparisons of load-displacement relations between experimental and analytical results

Table 6.2 List of experimental and analytical results

Specimens	Cracking load			Yeild load			Maximum load			Experimental failure mode
	$P_{exp.}$ (kN)	$P_{ana.}$ (kN)	$P_{exp.}/P_{ana.}$	$P_{exp.}$ (kN)	$P_{ana.}$ (kN)	$P_{exp}/P_{ana.}$	$P_{exp.}$ (kN)	$P_{ana.}$ (kN)	$P_{exp.}/P_{ana.}$	
A-N	10.2	6.40	1.59	39.3	35.6	1.12	54.6	40.6	1.35	Concrete crushing
A-T0	18.4	8.13	2.26	74.7	52.5	1.42	131.8	113.5	1.16	Sheet debonding
A-T20	31.0	26.9	1.15	92.4	74.0	1.25	140.5	125.9	1.12	Sheet rupture
A-T40	56.2	42.1	1.33	128.6	93.3	1.38	169.6	138.4	1.23	Sheet rupture
B-N	6.63	7.98	0.83	60.3	54.7	1.10	75.2	58.7	1.28	Concrete crushing
B-T0	14.2	9.38	1.51	91.9	71.7	1.28	141.6	121.9	1.16	Sheet debonding
B-T20	38.8	26.4	1.47	117.9	91.3	1.29	163.6	135.3	1.21	Sheet rupture
B-T40	52.3	43.7	1.20	143.6	112.5	1.28	181.5	148.8	1.22	Sheet rupture

Numerical analysis predicted upper concrete crushing failure modes for all specimens

6.6 Axial strain distribution of the AFRP sheet at ultimate state

In order to investigate the influence of different ratio of the pre-tensioned stress level in the sheet and the main steel reinforcement on the behavior of the RC beams, a comparison of the axial strain distribution of the AFRP sheet between the experimental and the analytical results at the ultimate state are presented in **Fig.6.5**. From this figure, it can be concluded that both experimental and analytical strain distributions in the equi-bending span are almost similar. However, some variations in the experimental strains are observed, probably due to the local effects of cracks on the bond behavior.

On the other hand, from the experimental results in the equi-shear spans of the beams, the distribution of sheet strains near the loading points seems to be larger than that obtained from the numerical analysis. This indicates that the non-pre-tensioned AFRP sheets may be partially debonded due to the peeling action resulting from the opening of the critical diagonal crack (CDC) developed in the lower concrete cover near the loading points, which was found to be similar to the experimental results obtained by Kishi et al. (2000). The axial strain distribution of the AFRP sheet shows that the numerical analysis estimates a

short debonding region compared to that obtained from the experimental results because the plateau of the strain distribution is shorter than that found experimentally. This is because of the assumption in the numerical prediction using a multi-section method that the AFRP sheet is perfectly bonded to the concrete surface until reaching the analytical ultimate state. Generally, a similar trend has been found in both the predicted and experimental curves.

Fig.6.5 shows that the maximum strains of AFRP sheet are approximately 1.25, 1.15 and 0.90 % for Beams A-T0/20/40, respectively. As a result, the ultimate displacements of the beams decrease (51.1, 45.6 and 41.2 mm for A-/T0/20/40, respectively) due to increasing pre-tension force in the sheets. The same trend can be observed for Beams type B (44.4, 40.4 and 36.4 mm for B-/T0/20/40, respectively). Based on these results, it could be confirmed that the strain of AFRP sheet at the ultimate state, generated by the external loading, decreases by pre-tensioning the sheet and decreases additionally due to an increase of the pre-tension stress level. Therefore, the failure behavior of the RC beams becomes more brittle because part of the strain of AFRP sheet is used for the initial pre-tension.

Effective use of the AFRP sheet was due to the pre-tensioning process. Since the usable of the strains of AFRP sheets in the beams reinforced with the pre-tensioned AFRP sheet are higher than those in beams reinforced with the non-pre-tensioned AFRP sheet. Taking into account the high strength of the AFRP sheet, the application of the pre-tensioned AFRP sheet provides an efficient use of the AFRP sheets by adding the initial strains and consequently higher strains accompany higher ultimate loads (if adequate anchorage is provided) are attained in the sheet at the ultimate state. For instance, in Beam A-T40, the additional strain of AFRP sheet of 0.90% due to external loading at ultimate state added to the initial pre-tension strain of 0.65% (**Table 6.1**) giving a total strain of AFRP sheet of 1.55%, close to the ultimate strain of AFRP sheets (1.75%). On the other hand, the ultimate strain in the same beam reinforced with non-pre-tensioned AFRP sheet (A-T0), resulted only from the external loading (1.25%). These results indicate the effectiveness of a proposed anchoring method without metal system.

From comparisons between Beams A and B (**Fig.6.5**), it is confirmed that the strain of the AFRP sheet increases with a decreasing tensile reinforcement steel ratio. Because at the

ultimate state, the strains of AFRP sheets in the Beams A-T0/20/40 are 1.25, 1.15, and 0.90% but is lower for the Beams B (1.15, 1.0, and 0.80% for B-T0/20/40, respectively). Thus, strengthening effectiveness of using pre-tension sheets is higher when the lower ratio of main rebar is used as the AFRP sheet carries a greater portion of the tensile stresses. A similar result was obtained by Sang et al. 2008.

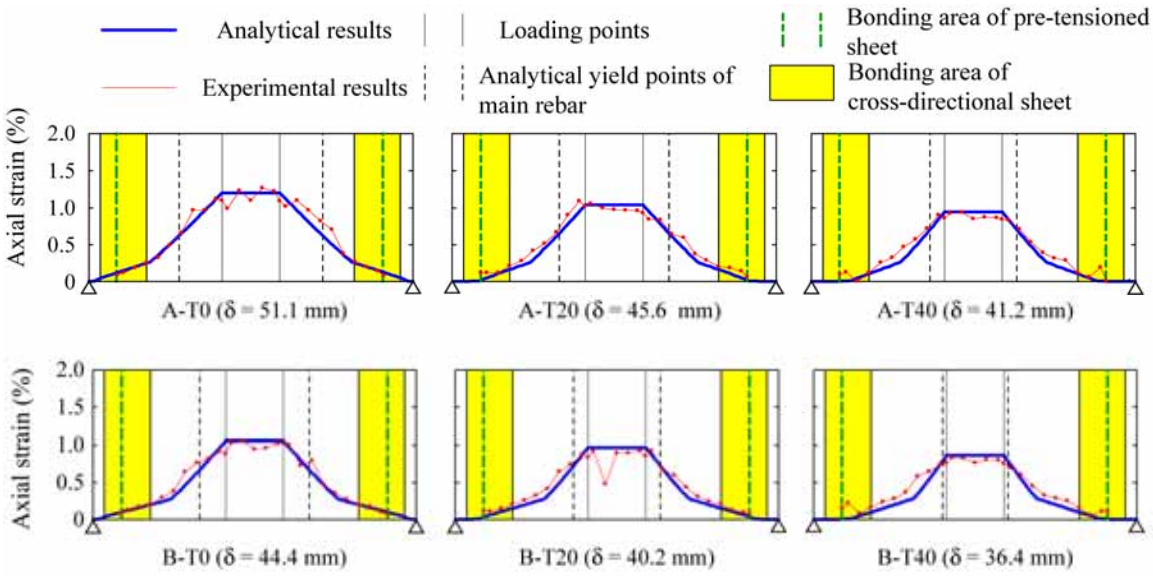

Fig.6.5 Comparisons of axial strain distribution between experimental and analytical results for AFRP sheet at ultimate state.

6.7 Crack pattern and failure modes

Fig.6.6 shows the condition of Beams A at the moment before full sheet debonding for Beam A-T0 and before sheet rupture for Beams A-T20/40 and **Fig.6.7** illustrates the condition of Beams B just before sheet debonding for Beam B-T0 and before the sheet rupture for Beams B-T20/40. From these figures, since the diagonal cracks have occurred in the bottom fiber of the cover concrete near the loading point and the debonding of the AFRP sheets was developed accompanied with a layer of putty due to crack-opening, it could be stated that in the case of the beams reinforced with the non-pre-tensioned AFRP

sheets, the AFRP sheets were debonded due to the peeling action of the CDC. This occurred because of CDC widening, which led to concrete blocks at the tip of CDC push out the AFRP sheets downward. These concrete blocks were formed due to the interaction between the bending and diagonal cracks. Beyond this stage, the cracks progressed horizontally towards the supports. However, for Beams A/B-T20/40 reinforced with pre-tensioned AFRP sheet, the sheet was partially debonded in the equi-shear span as shown in **Figs.6.6.b and 6.7.b**. Although the flexural cracks were distributed over the equi-bending spans of the beams reinforced with pre-tensioned sheets (A/B-T20/40) no sheet debonding was observed. At the stage when the AFRP sheet has shown no significant contribution in the resisting moment of the beams, an immediate loss of the load-carrying capacity has been observed.

In general, from **Figs.6.8 and 6.9** for the strengthened beams, it has been seen that the cracks uniformly propagated along the entire span and the level of damage was significantly lower than that of the control beams. Moreover, when the pre-tensioned sheet is used, a low level of damage of the beam was observed. Many cracks with small widths were observed on the strengthened beams, especially in the case of the beams reinforced with the pre-tensioned AFRP sheet. On the other hand, for control beams, a low amount of cracks were observed, which were much wider. Furthermore, the crack formation in Beams A/B-T20/40 was delayed due to the external pre-tension force in the AFRP sheet. Since the confining effect by the pre-tensioning may help to keep the cracks closed, allowing a significant transfer of force through aggregate interlock across the surface of the crack. The confining effect may have also increased the load-carrying capacity of the beam, hence delaying the opening of the cracks. These observations support the conclusion that the pre-tensioned sheet accompanied with an adequate anchoring method can effectively redistribute the applied stress, confirmed by the similar experimental observations obtained by Dong et al. 2009, in which a metal anchorage system was used.

As the AFRP sheet is applied to the concrete surface, the ultimate strength of the strengthened beams is governed by the tensile strength of AFRP sheet or the concrete’s shear and tensile strengths. At the ultimate state, either the sheet ruptures or failure occurs where severe stresses condition may exist in the concrete cover between the AFRP sheet

and the main rebar. **Figs.6.8 and 6.9** show views of the different modes of failure in the present study. The first pattern occurred in the control beams A/B-N shown in **Figs.6.8a and 6.9a**, in which the beams failed by the concrete crushing caused by a concentration of stresses under the loading points at the upper zone. The second failure mode observed in the beams reinforced with the non-pre-tensioned sheet (Beams A/B-T0) was sheet debonding as shown in **Figs.6.8b and 6.9b**. From these figures, it is observed that after full debonding of the AFRP sheet for Beam A/B-T0, some blocks of the concrete cover and the layer of putty material stacked to the AFRP sheet beneath the internal reinforcement. This could indicate that the putty material is very strong and has a high bond behavior with both the AFRP sheet and concrete. Thus, the debonding of the sheet is mainly due to the tensile failure of concrete near the bonding interface between concrete and putty. The third mode of failure was observed in the beams reinforced with the pre-tensioned sheet, regardless of the pre-tension stress level, where the sheet eventually ruptured due to excessive stress concentrations at the tips of flexural cracks at the equi-bending span as shown in **Figs.6.8c,d and 6.9c,d** for Beams A/B-T20/40. These results may demonstrate the ability of this new anchoring method to maintain the pre-tensioned sheet completely bonded to the concrete surface until reaching the ultimate state.

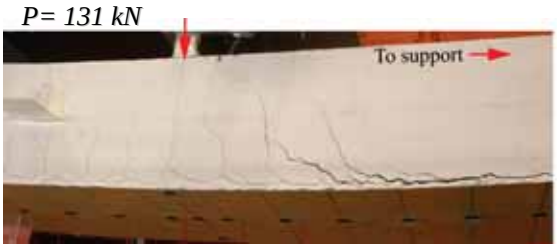

(a) Beam A-T0

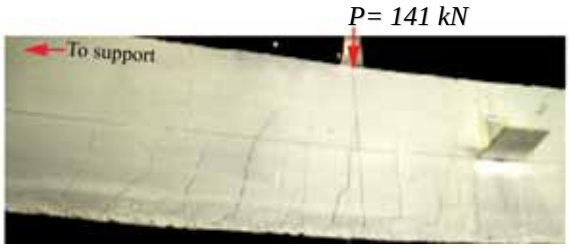

(b) Beam A-T20

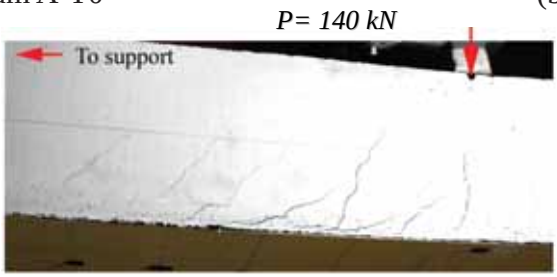

(c) Beam A-T40

Fig.6.6 Photos for Beams A at the moment (a) before full debonding; and (b),(c) before sheet rupture

(a) Beam B-T0

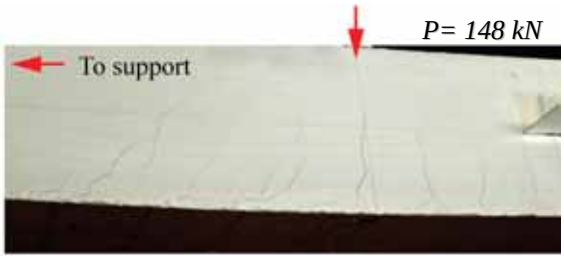

(b) Beam B-T20

(c) Beam B-T40

Fig.6.7 Photos for Beams B at the moment (a) before full debonding; and (b),(c) before sheet rupture

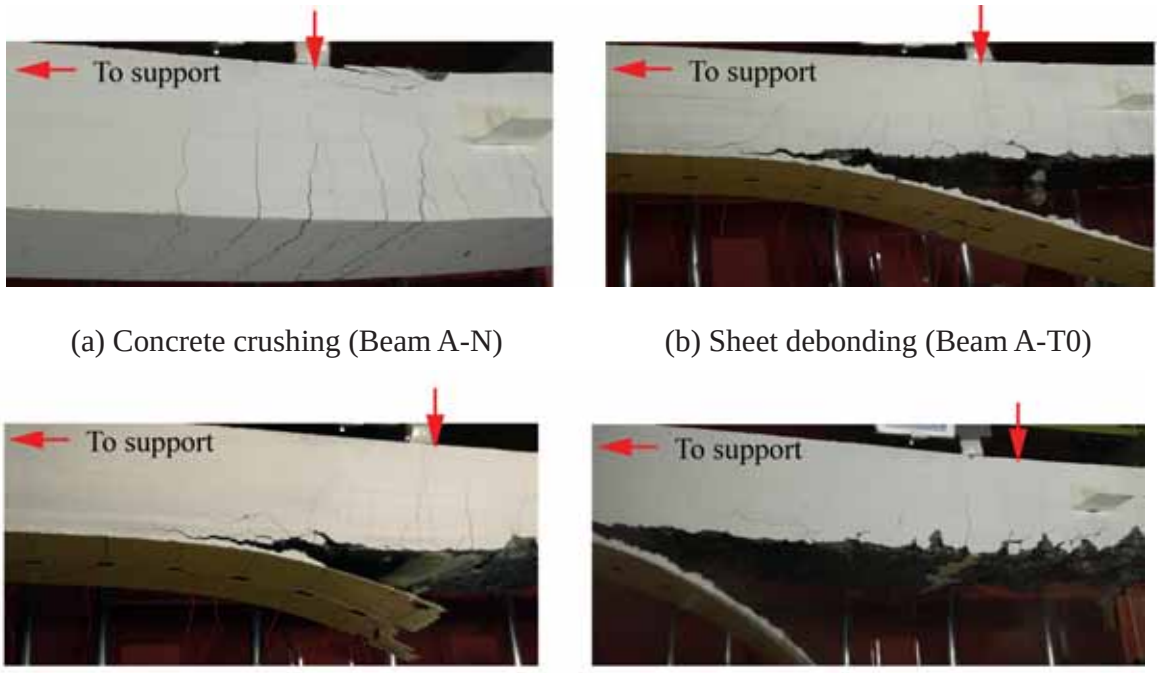

(a) Concrete crushing (Beam A-N)

(b) Sheet debonding (Beam A-T0)

(c) Sheet rupture (Beam A-T20)

(d) Sheet rupture (Beam A-T40)

Fig.6.8 Modes of failure for Beams A

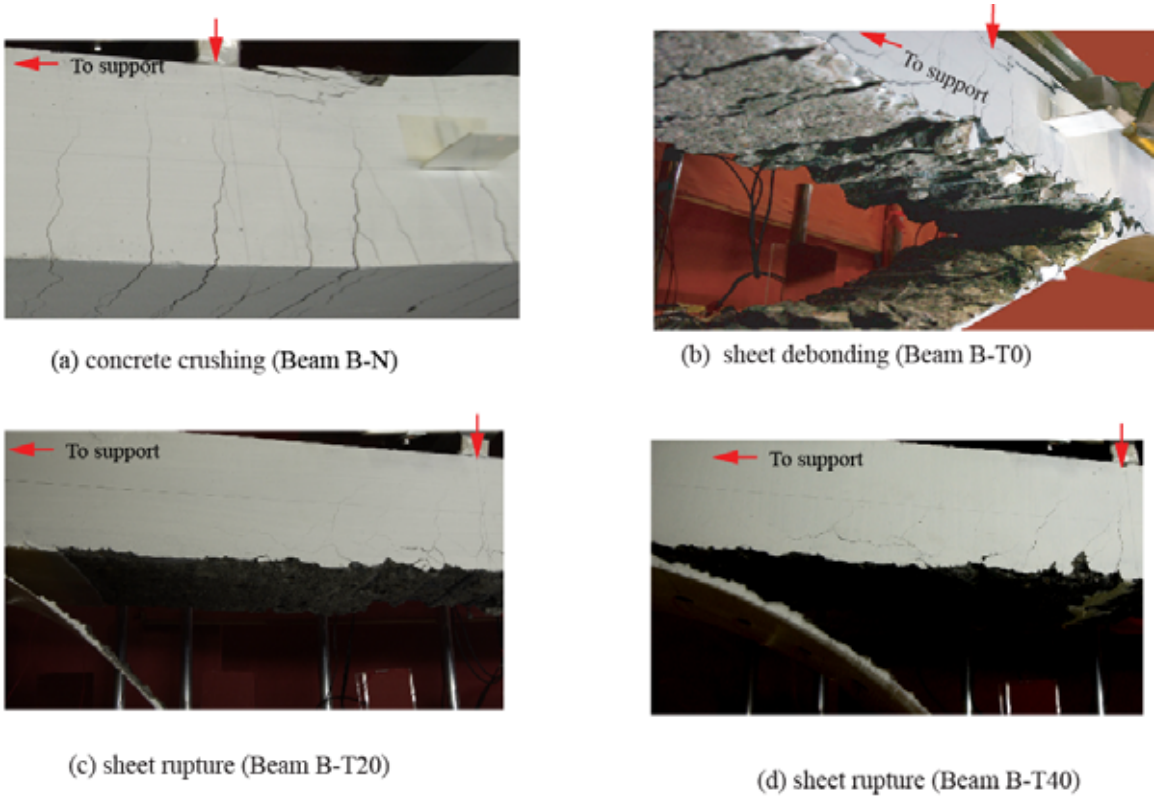

(a) concrete crushing (Beam B-N)

(b) sheet debonding (Beam B-T0)

(c) sheet rupture (Beam B-T20)

(d) sheet rupture (Beam B-T40)

Fig.6.9 Modes of failure for Beams B

6.8 Summary

This chapter presents the Strengthening Study of RC beams to examine the behavior of flexural pre-tensioned AFRP strengthening systems without anchoring devices, hence to investigate the new anchoring method proposed in this research. The variables used in the experimental program included the pre-tension force ratio introduced to the AFRP sheet (0, 20, and 40%) and the main reinforcement steel ratio (0.79 and 1.24%). From this study, the results show that the proposed anchoring method is effective and feasible because the load-carrying capacity increased considerably. A good agreement between experimental and analytical methods was achieved until reaching ultimate state with somewhat perfect bonding between the AFRP sheet and concrete surface.

CHAPTER 7

Study of strengthened pre-cracked RC beams

7.1 Introduction

This chapter presents the experimental and analytical results of four pre-cracked RC beams reinforced with non-pre-tensioned and pre-tensioned AFRP sheets as well as control beam without reinforcing AFRP sheet (Abdel Aziz et al. 2010b). These specimens were tested at the Structural Laboratory of Civil Department at Muroran Institute of Technology, Japan to investigate a rational flexural reinforcing method for pre-cracked RC beams using a pre-tensioned AFRP sheet without anchoring devices. The test results were observed by visual inspection during the test and measured by instrumentation. These results are described in different forms as crack patterns in different stages of loading, load-deformation curves, and axial strain distribution of the sheet after releasing the hydraulic jack and at the ultimate state. The test parameters include pretension force ratio introduced to the sheet and the prior loading level for pre-cracking. These parameters were carefully chosen to obtain different modes of failure as will be discussed in the following sections.

7.2 Outline of specimens

The specimens used in this experiment are listed in **Table 7.1**. These specimens were designated using two parameters: level of prior loading for pre-cracking (L1: loading up to main rebar yielding; L2: loading to the middle point between main rebar yielding and analytical ultimate state) and introduced pre-tension force ratio n (%) referring to the nominal tensile strength of the AFRP sheet as beam L1-Tn. Control beam is named beam N without reinforcement of the sheet. In this study, two values for the pre-force ratio were considered: n = 0 and 40 (%). Dimensions of the RC beams and layouts of the

reinforcement and AFRP sheet are shown in **Fig.7.1**. The beams have a rectangular cross-section of 200 mm height and 300 mm width. Clear span is 2,800 mm. Three rebar of diameter 16 mm for all beams were placed in the lower layer for bending reinforcement. Also, another three rebar of 16 mm diameter were used in the upper layers of all specimens. To prevent premature shear failure, an adequate amount of shear reinforcement was mounted with 10 mm diameter steel stirrups at a spacing of 80 mm. The ends of the axial rebar were welded to the steel plates of t = 9 mm thickness, set to the ends of the beam, to save the anchoring length of the rebar. AFRP sheet of 220 mm width was pre-tensioned and then bonded onto the tension-side surface, leaving 150 mm between the supporting point and the sheet end as shown in **Fig.7.1.** The target and actual pre-tension force ratios and the introduced initial strain into the sheet are listed in the **Table 7.1**, in which the ratios are obtained by referring to the nominal tensile capacity of the sheet. In this study, the same procedures applied in these specimens were used for pre-tensioning and bonding AFRP sheet but the pre-tensioned AFRP sheet was saved by 100 mm on each end, compared to specimens in Chapter 6.

Table 7.1 List of specimens

Specimen	Level of prior loading	Designed pre-tension force ratio* (%)	Actual pre-tension force ratio* (%)	Introduced initial strain (μ)
N	-	Non-Strengthened		-
L1-T0	Level 1	0	0	0
L1-T40		40(141)	36.5(129)	6,205
L2-T0	Level 2	0	0	0
L2-T40		40(141)	39.5(140)	6,732

* ( ): pre-tension force (kN)

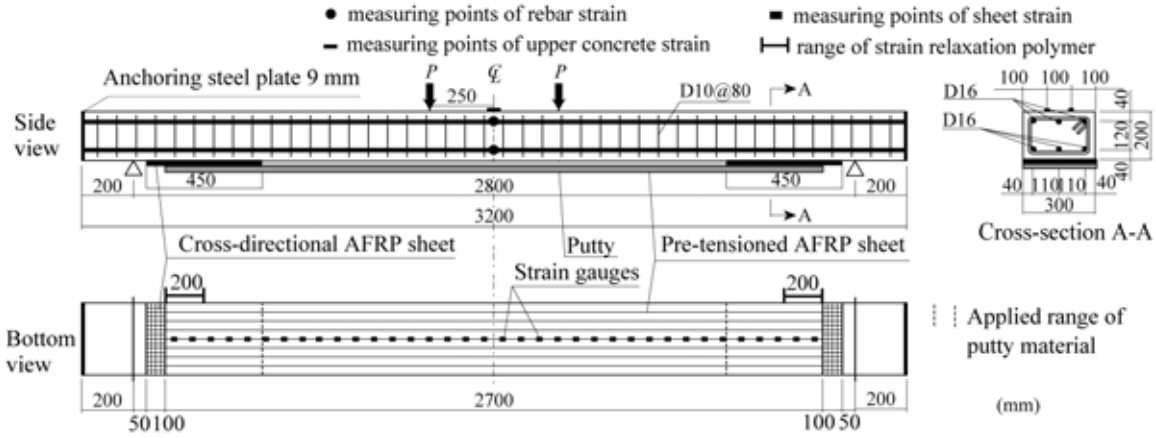

Fig.7.1 Layout of reinforcement and AFRP sheet for RC beam

7.3 Loading procedures

Before strengthening the specimens with AFRP sheets, RC beams were pre-loaded for pre-cracking using two loading levels (L1: loading up to main rebar yielding; L2: loading to the middle point between main rebar yielding and ultimate state (hereinafter, analytical ultimate state)) obtained from analytical results for control RC beam N as shown in **Fig.7.2**. After that, they were removed from the loading apparatus and then strengthened with AFRP sheet. Finally, the specimens were reloaded until reaching complete failure. The primer was poured inside the pre-cracks to improve the bonding behavior of concrete surface.

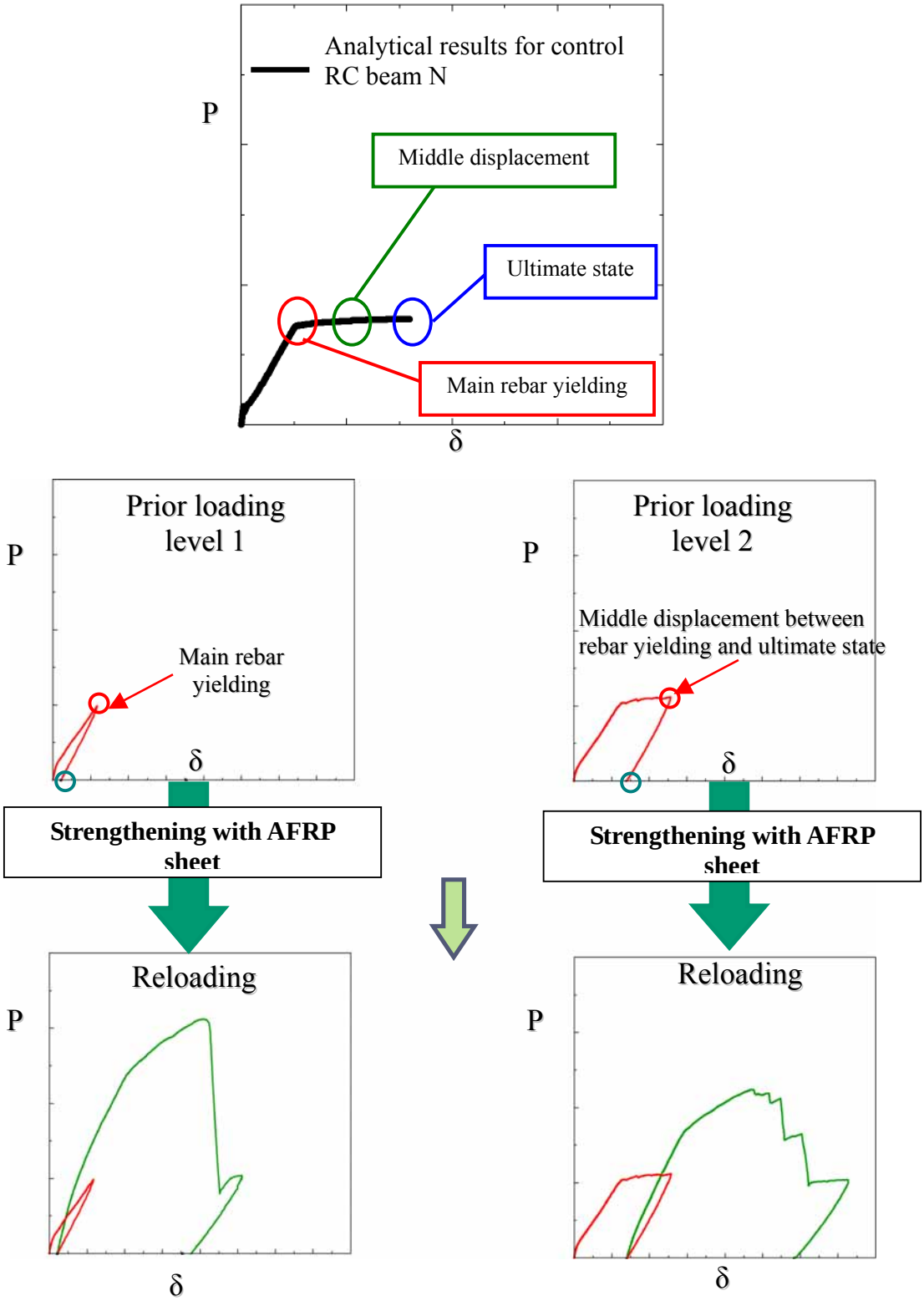

Fig.7.2 Loading procedures

7.4 Experimental results of prior loading

The experimental results at the prior loading for pre-cracking are listed in **Table 7.2**. In this study, beams L1 and L2 were prior subjected to the load up to main rebar yielding and the middle point between main rebar yielding and the beam reaching the ultimate state, respectively. Thus, from this table, it is seen that at the maximum loads of prior loading for Beams L1 (around 50 kN) are less than those in Beams L2 (around 55 kN), maximum displacement of Beams L1 are approximately half the value of those in Beams L2(around 25 mm), strains of main rebar in Beams L1 are about one quarter of value of those in Beams L2(around 6,500 μ), and strains at the upper fiber of concrete in Beams L1 are about half the value of Beams L2 (around 2,000 μ).

On the other hand, after unloading, the residual displacement in Beams L1 are very small (around 2.4 mm) compared to those in Beams L2 (around 13 mm), residual strains of main rebar in Beams L1 are too small (around 300 μ) comparable to of those in Beams L2 (average around 5,000 μ), and residual strains at the upper fiber of concrete in the case of Beams L1 are about one tenth of Beams L2 (around 1,000 μ).

From these results, it is observed that the deflections, main rebar strains, and the upper fiber strains of concrete at the maximum loads of prior loading and after unloading are similar between the two beams of L1. However, in the case of beams L2, main rebar strains are significantly different to each other, even though deflections and the upper fiber strains of concrete are almost similar between them. This may be the reason that the main rebar strains are severely affected by the opening of cracks, since the main rebar has been extremely plasticized and residual deflection has been very large in case of Beams L2-T0/40 due to subjected to high prior loading level.

Table 7.2 Results of prior loading

Specimens	At max. load of prior loading				After unloading		
	Max. load (kN)	Max. Disp. (mm)	Strain of main rebar (μ)	Strain at upper fiber of concrete (μ)	Residual disp. (mm)	Residual strain of main rebar (μ)	Residual Strain at upper concrete fiber (μ)
L1-T0	49.4	13.1	1,884	-1,075	2.6	312	-118
L1-T40	49.4	11.7	1,747	-769	2.2	285	-75
L2-T0	56.0	25.7	9,469	-2,210	13.8	7,664	-1,081
L2- T40	55.2	25.5	3,644	-2,135	13.7	2,256	-1,048

7.5 Crack patterns after prior loading

Crack patterns for each beam occurred due to prior loading are shown in **Fig.7.3**. From this figure, it is observed that the flexural cracks have occurred in the side-surface of the entire span of every beam. The maximum width of cracks is about 0.7 mm, which occurred in the equi-bending span. In the case of Beams L1, which were subjected to low prior loading level (just until reaching the yielding point of main reinforcement steel), the damage was less than that of Beams L2, which were subjected to high prior loading level (until reaching the middle point between yielding of main reinforcement steel and analytical ultimate state). It is found that in Beams L2, many flexural cracks with bigger length observed in both equi-bending and equi-shear spans are more than those found in Beams L1, in which most of the cracks were observed in the equi-bending spans.

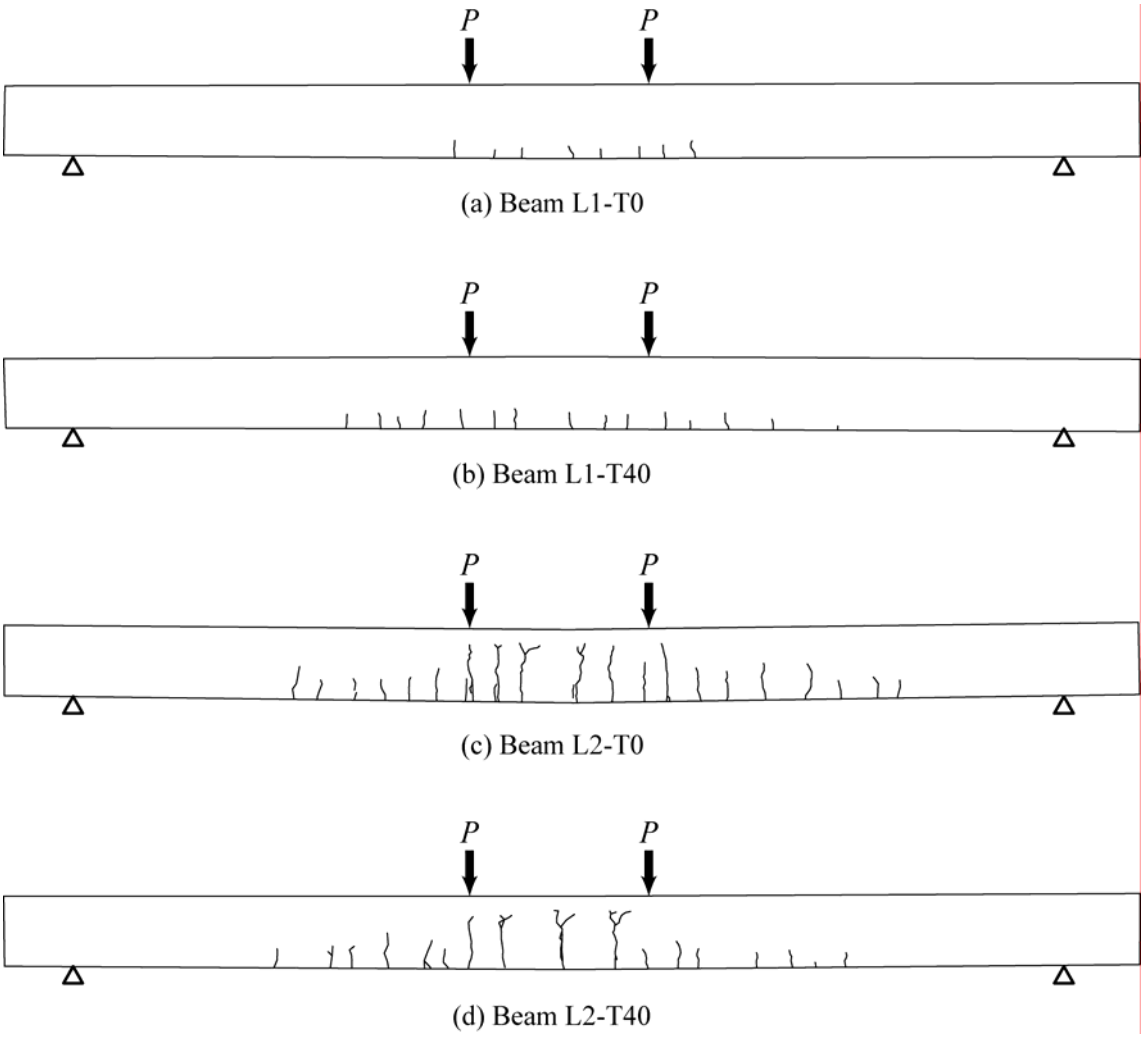

Fig.7.3 Crack patterns after prior loading

7.6 Axial strain distribution of AFRP sheet after release of hydraulic jack

Fig.7.4 shows the axial strain distribution of AFRP sheet immediately after releasing 50 and 100% of actual pre-tension force introduced to the sheet through the hydraulic jack. From this figure, it is clear that as 50% of the pre-tension force was released from the jack, the sheet strains at its ends are about 0.25% for Beams L1/L2-T40. In the case of releasing the

full pre-tension force, strains at the ends of AFRP sheet are almost 0.5% for Beams L1/L2-T40. However, at mid-span, the AFRP sheet strain is minimal (about zero) and almost constant. Then, it increases slowly in the region of bonding cross-directional AFRP sheet to pre-tensioned AFRP sheet using a strain relaxation polymer. Therefore, the strain increases dramatically and reaches its highest value at the end of the pre-tensioned AFRP sheet. This proves that the strain of AFRP sheet increases as the releasing rate of the jack increases and the highest value of the sheet strain occurs at its ends, close to that generated from the jack. In addition, these strains decrease in the region of strain relaxation polymer use. In the actual experiment, the sheet did not peel-off, rather it bonded fully to concrete after the pre-tension force was released from the jack. From these results, it is confirmed that the suggested method for anchoring and bonding pre-tensioned AFRP sheet to pre-cracked RC beams is practicable.

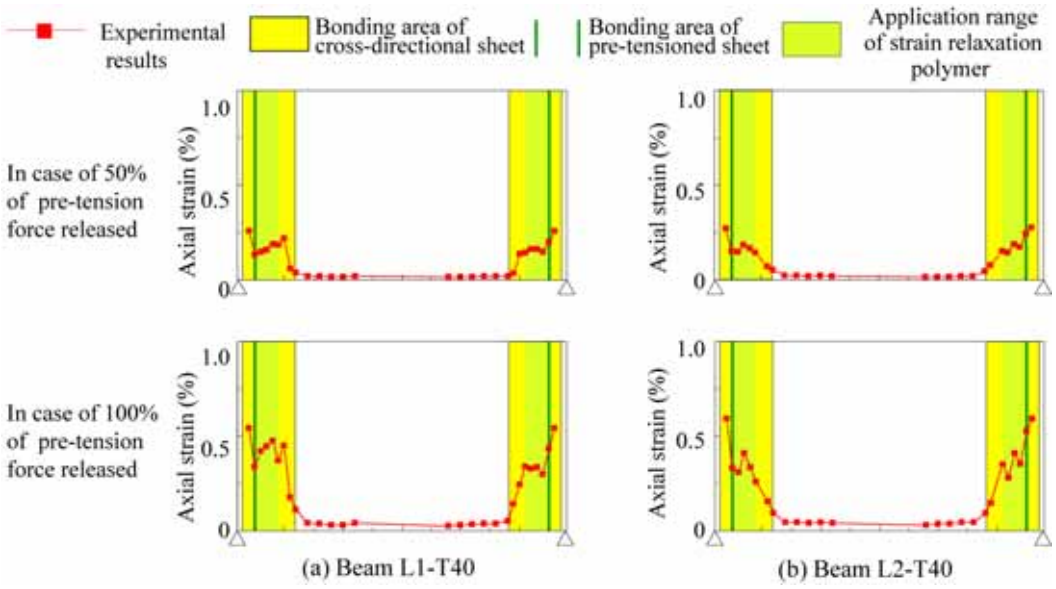

Fig.7.4 Axial strain distribution of AFRP sheet due to release of hydraulic jack.

7.7 Results after reloading up to failure

After removing the prior loading, the beams were strengthened with AFRP sheet, then they were reloaded until reaching complete failure and the following results were obtained;

7.7.1 Effect of pre-tension force introduced to the sheet

Fig. 7.5 shows the comparisons of the load-displacement relationship of beams reinforced by bonding AFRP sheet with the same prior loading level and with different pre-tension force introduced to AFRP sheet. In addition, **Table 7.4** presents the experimental and analytical values for the yield load of the main rebar and the maximum load, experimental failure modes and the ratio between the experimental and analytical values.

From this figure and table, in the case of the control beam N, from the experimental results, the stiffness decreases due to flexural cracks at the loading level of around 10 kN and a displacement of 1.0 mm and at main steel reinforcement yielding at the loading level of 49 kN and a displacement of 13 mm. After that, displacement increases, keeping a small stiffness and then reaching the ultimate state at a loading level of 55 kN and a displacement of more than 60 mm. When the compressive strain of concrete reaches 0.35% on the upper fiber, the load consequently drops dramatically.

In addition, from this figure and table, it is seen that compared to the control beam N, yield and maximum loads of Beam L1-T0 are increased by 58 and 123%, respectively, and these loads also are increased by 145 and 188% for Beam L1-T40, respectively. The same trend occurs in the case of Beam L2-T0/40 but with a slight difference (71 and 107% for the yield and maximum loads of Beam L2-T0/40, respectively) and 168 and 162% increase in the yielding and maximum loads of Beam L2-T40, respectively, compared to the control beam N. This decrease in the improvement of flexural behavior of the beams L2-T0/40 is due to high prior loading level for pre-cracking.

From these results, it can be observed that without pre-tension, the addition of the AFRP sheet only slightly affects the beam performance before the first crack as in Beams L1/L2-T0. However, a significant improvement of the beam performance has been observed after cracking due to the contribution of the non-pre-tensioned sheet in carrying a portion of the

stresses. Thus, the AFRP sheet has induced a redistribution of stresses carried by the steel reinforcement. This may lead to a significant increase in the load-carrying capacity when the main rebar yields. On the other hand, when the pre-tensioned AFRP sheet is used, the main rebar is relieved of tensile stresses and placed into compression. It has been observed that the AFRP sheets, due to the pre-tensioning, carry a great portion of the tensile stresses. As a result, the load-carrying capacity of the pre-cracked RC beams reinforced with the pre-tensioned AFRP sheet (L1/L2-T40) increases after yielding of the main rebar.

This clearly demonstrates the effect of the pre-tensioned sheet in applying an axial compressive force over the whole depth of the section and in applying a moment, which tends to place the top of the section in tension and cause additional compression at the base of the beam. This leads to an increase in the value of the external load required to produce a visible flexural cracking, hence the cracking load increases considerably.

Moreover, due to the initial camber of the beams reinforced with pre-tensioned sheet, an improvement of the cracking load has been observed. This may be due to the initial pre-tension introduced to the AFRP sheet and the relatively larger tensile force carried by the AFRP sheet. The cracks control not only decreased the deflection but also improved the durability of the concrete structure since its deterioration is strongly related to the width of the cracks. Therefore, it could be concluded that the pre-tensioned AFRP sheet may be successfully applied in the cracked section members.

At the ultimate state, it is clear that the displacement has a tendency to decrease since a part of the AFRP sheet strain is used for the pre-tensioning process as in Beams L1/L2-T40. Thus, the specimens could have a brittle failure behavior (sheet debonding and sheet rupture before upper concrete crushing for Beams L1/L2-T40, respectively) but in the case of the beams reinforced with non-pre-tensioned sheet, the failure occurs after concrete crushing (sheet debonding and sheet rupture after upper concrete crushing for Beams L1/L2-T0, respectively). In addition, displacement at any loading level was significantly lower with the addition of the non-pre-tensioned AFRP sheet and was further reduced when the pre-tensioned sheet is bonded as shown in **Fig.7.5**. These results have proven the ability of the pre-tensioned AFRP sheet to control cracking in pre-cracked RC beams. This could

be explained by the fact that the sheet in the reinforced beam generates a tensile force along the deformed concrete section and creates equilibrium among the internal forces with much less deformation compared to the control.

From these results, it is confirmed that in the cases of pre-cracked RC beams reinforced with pre-tensioned AFRP sheet (L1/2-T40), the flexural stiffness is increased from the beginning of loading to the ultimate state in comparison with control beam N and the beams reinforced with normal AFRP sheet (L1/2-T0), in spite of the magnitude of prior loading.

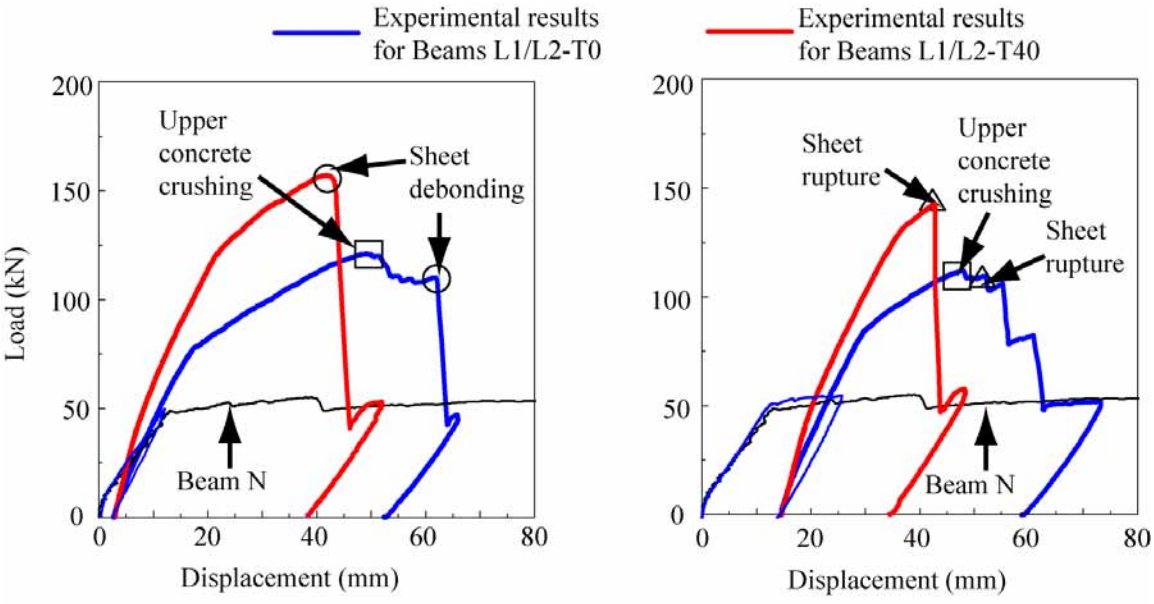

(a) Beams L1 (b) Beams L2

Fig.7.5 Comparisons of load-displacement relations of beams reinforced by bonding AFRP sheet with the same prior loading level and with different pre-tension force

7.7.2 Effect of prior loading level

Fig.7.6 shows the comparisons of the load-displacement relationship of beams reinforced by bonding AFRP sheet with the same pre-tension force introduced to AFRP sheet and with different prior loading level. In this figure, the experimental results for the beams

reinforced with AFRP sheet are shifted to the origin point to be able to compare directly the load-deflection curves between two beams with different pre-cracking levels. From this figure and **Table 7.3**, it is observed that: (1) maximum loads of beams L1 (121 and 156 kN for Beams L1-T0/40, respectively) are larger than those from numerical results (115 and 143 kN for Beams L1-T0/40, respectively); but (2) the maximum loads of beams L2 (112 and 142 kN for Beams L2-T0/40, respectively) are smaller than those of beams L1 and are similar or a little smaller than those from numerical ones. This implies that: (1) beams L2-T0 may reach the compressive failure of concrete because the residual strain of the upper fiber concrete after prior loading was around 1,100 μ, as described in **Table 7.1**; and (2) in the case of beam L2- T40, the sheet ruptured by increasing the sheet strain at the pre-cracked area locally even though the residual strain was reduced by bonding pre-tensioned AFRP sheet (around 1050 μ).

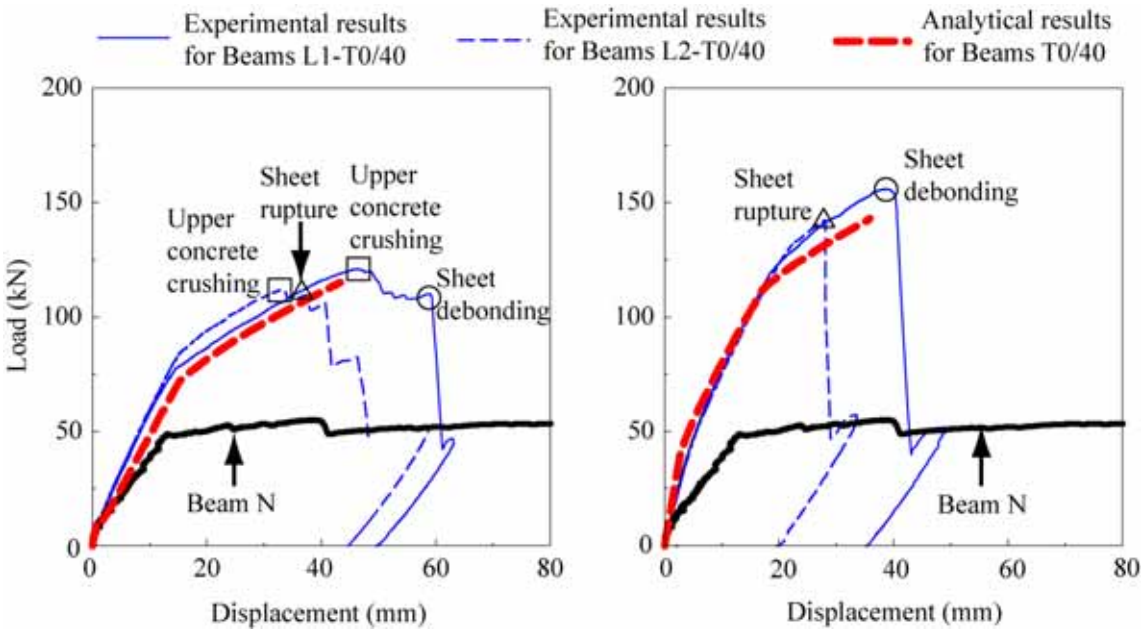

(a) Beams T0 (b) Beams T40

Fig.7.6 Comparisons of load-displacement relations of beams reinforced by bonding AFRP sheet with the same pre-tension force and with different prior loading level

7.7.3 Comparison between the experimental and analytical results

Fig.7.7 shows the comparisons of the load-displacement relationship between experimental and numerical results including residual displacement due to prior loading, in which the numerical ones are indicated only for strengthened pre-cracked RC beams with pre-tensioned AFRP sheet (i.e. in this simulation, the existing cracks and the stiffness of putty used for flattening the bonding surface were not considered).

Comparing with the experimental and numerical results, it is seen that the whole of initial stiffness, the second stiffness after cracking and the third one after main rebar yielding are almost similar to each other for all cases.

From the analytical results shown in **Table 7.3** and **Fig.7.7**, the loading level at the cracking, main rebar yielding and the ultimate state are upgraded as a result of introducing pre-tension force to the AFRP sheet. This trend seems to be similar to that found in the experimental results. From **Table 7.3**, the comparisons between the experimental and analytical results have shown that the loading level obtained from experiments at the ultimate state is slightly higher (around 7% for yielding and ultimate states) than that of the analytical results for Beams L1-T0/40. These results may indicate that the pre-tensioned AFRP sheet may offer adequate bonding up to the analytical ultimate state of the pre-cracked RC beams subjected to low prior loading level (reach yielding point of main rebar). Thus, the flexural behavior of these beams reinforced with pre-tensioned AFRP sheet can be successfully evaluated using multi-section method. However, the maximum loads of experimental results for Beams L2-T0/40 are lower than those of analytical ones but at yielding point of main rebar the experimental results are more than those of analytical ones (about 17%) (**Table 7.3**). Thus, it is observed that numerical results can better match the experimental results for non pre-cracked beams but not for pre-cracked beams. Therefore, it is not recommended to use these numerical analyses using the multi-section method to predict the flexural behavior of pre-cracked RC beams strengthened with pre-tensioned AFRP sheet subjected to high prior loading level (reach more than yielding point of main rebar) due to sever damage in the beam as in Beams L2-T0/40.

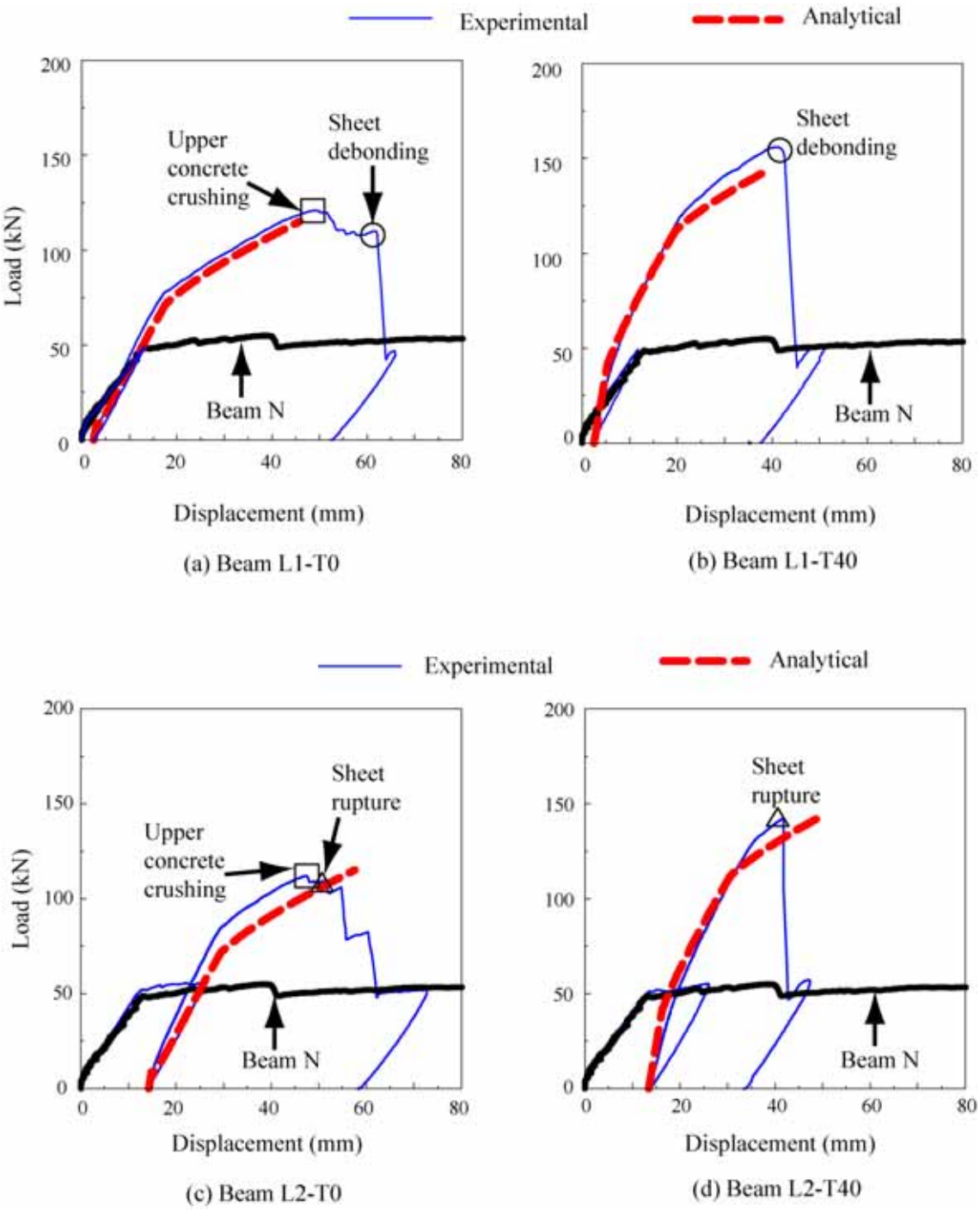

Fig.7.7 Experimental and analytical results of load-displacement relations

Table 7.3 List of experimental and analytical results after reloading

Specimens	Yeild load			Maximum load			Experimental failure mode
	$P_{exp.}$ (kN)	$P_{ana.}$ (kN)	$P_{exp.}/P_{ana.}$	$P_{exp.}$ (kN)	$P_{ana.}$ (kN)	$P_{exp.}/P_{ana.}$	
N	48.9	55.7	0.88	54.2	59.1	0.92	Concrete crushing
L1-T0	77.5	71.9	1.08	121	115	1.05	Sheet debonding
L1-T40	120	112	1.07	156	143	1.09	Sheet debonding
L2-T0	83.5	71.9	1.16	112	115	0.97	Sheet rupture
L2- T40	131	112	1.17	142	143	0.99	Sheet rupture

Numerical analysis predicted upper concrete crushing failure modes for all specimens

7.7.4 Axial strain distribution of the AFRP sheet at ultimate state

The comparisons of the axial strain distribution of AFRP sheet at the analytical ultimate state between experimental and numerical results are shown in **Fig.7.8**. In addition, the comparisons for the case of beams L2-T0/40 are performed for the results at the real ultimate state because the deflection at the real ultimate state was smaller than that at the analytical ultimate state, as shown in **Fig.7.7**. From this figure, it is observed that the experimental results for all beams considered here are in good agreement with the numerical results. Then, it is confirmed from these results that the AFRP sheet was fully bonded to concrete surface in spite of with/without introducing pre-tension force into the sheet. In the case of beam L2-T40, the sheet ruptured even though the axial strains of AFRP sheet in the equi-bending span were almost 5,000 μ (if adding the initially introduced strain (around 7000 μ), it becomes almost 12,000 μ) as shown **Fig.7.8d**. It may be due to the affection of pre-cracks because the large strains occurred locally in the equi-bending span as shown in **Fig.7.8e**.

In general, for all beams, it is observed that the experimental and analytical strain distributions in the equi-bending span are similar but local effects of the pre-cracks on the bond behavior may produce some variations in the experimental strains of the sheet.

In addition, Beams L1/L2-T0 and L1-T40 show a higher distribution of the AFRP sheet strain in the equi-shear span near the loading points in the experimental results over the analytical ones. This demonstrates that the AFRP sheet may be partially debonded due to the peeling action of the opening critical diagonal crack (CDC) developed in the lower

concrete cover near the loading points. This difference between experimental and analytical results is most likely due to the fact that in numerical analysis, it is assumed that the AFRP sheet is fully bonded to the concrete surface up to the analytical ultimate state. However, beam L2-T40 reached the ultimate state with sheet rupture after passing the maximum load; however the cracks have not been opened and the sheet did not tend to be debonded due to the peeling action of CDC.

Fig.7.8 shows that AFRP sheet can be used efficiently by applying pre-tensioning. The pre-tensioned AFRP sheet application provides the efficient use of AFRP sheet by adding the initial strains. Thus, when an adequate anchorage method is applied, higher strains of the sheet accompanying higher ultimate loads are obtained. For example, in Beam L1-T40, the additional AFRP sheet strain of 0.75% due to the loading at beam failure added to the initial pre-stress strain of 0.62%, giving a total AFRP sheet strain of 1.37%, which is equal to 78% of the ultimate strain of the sheet (see **Table 7.2**). On the other hand, the same beam reinforced with non-pre-tensioned AFRP sheet (L1-T0) only has the ultimate strain due to external loading (1.0%). This implies that a proposed anchoring method is effective because the usable AFRP sheet strains of the beams reinforced with pre-tensioned AFRP sheet are higher compared to those of the beams reinforced with non-pre-tensioned AFRP sheet.

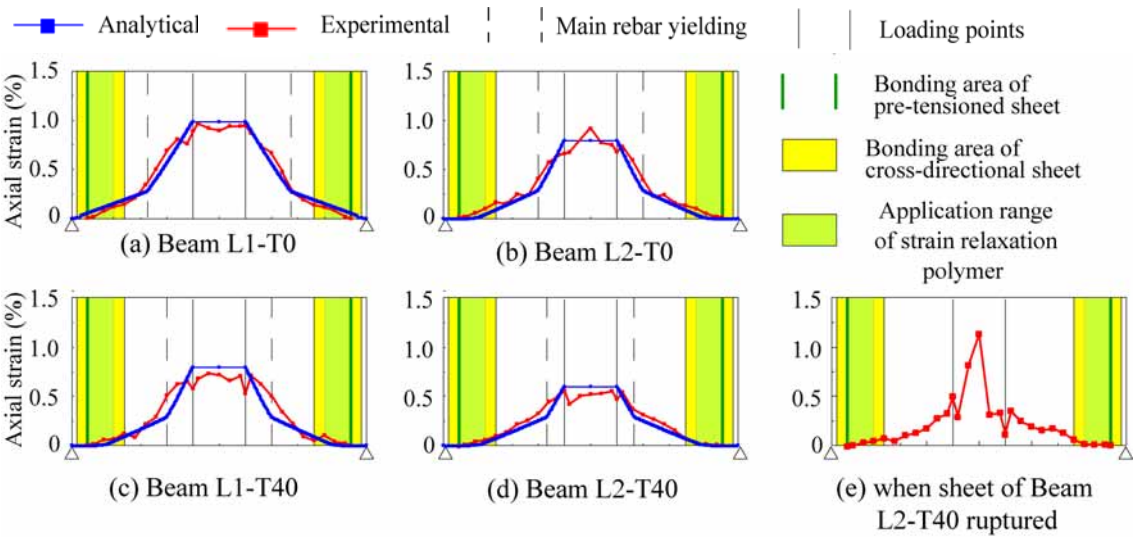

Fig.7.8 Comparisons of axial strain distributions of AFRP sheet between experimental and numerical results.

7.7.5 Crack pattern and failure modes

Fig.7.9 shows the crack distributions formed on the lateral-side surface of the beam near the ultimate state. From this figure, it is observed that Beams L1/2-T0 reached the ultimate state with sheet debonding and/or rupturing after the upper concrete reached the compressive failure. In the case of Beam L1-T0, the sheet was debonded due to the peeling action of the critical diagonal crack (CDC), which occurred near the loading points in the equi-shear span. This occurred because of CDC widening, resulting in concrete blocks at the tip of the CDC and pushing the AFRP sheet downward. These concrete blocks formed at a section of combined flexural and shear cracks initiated near the loading points. After that, the cracks developed horizontally towards each support.

On the other hand, even though the loading levels of Beams L1/2-T40 are larger than those of beams L1/2-T0, the upper fiber of concrete of Beams L1/2-T40 has not been under compressive failure and/or cracks have not been significantly opened. This means that the residual upper fiber strains of concrete were decreased and cracking is restrained due to bonding the pre-tensioned AFRP sheet.

In addition, in the case of Beams L1/L2-T40, shear cracks cannot be seen due to a higher pre-tensioned stress level applied to the sheet, seeing as how this factor resulted in an improved shear capacity of the pre-cracked RC beams. Consequently, the CDC was controlled and as a result, only the flexural cracks appeared as shown in **Figs.7.9b,d** for Beams L1/L2-T40. Even though flexural cracks were distributed over the entire side-surface of these beams, sheet debonding had not yet been initiated as shown in **Figs.7.9b,d**.

In the case of strengthened beams, the cracks caused by prior loading can be restrained, especially in the case of beams reinforced with pre-tensioned AFRP sheets. However, in the case of control beam N, which failed due to the concrete crushing caused by a concentration of stresses under the loading points at the upper zone, fewer cracks of greater width were observed, implying that as pre-tensioned AFRP sheet is applied, a greater portion of stresses are transferred from internal reinforcement to the pre-tensioned sheets. Similar behavior was noted by Weight et al. 2001.

Also, it is observed that applying pre-tensioning to the sheet delays the crack formation in Beams L1/L2-T40 because the pre-tension force led to the confining effect thereby preventing the opening of cracks. This is probably due to permitting great forces to transfer across the aggregate interlock through the face of the cracks, resulting in upgrading the flexural capacity of the pre-cracked RC beams.

From **Fig.7.10**, it was observed by authors at the experiment that: (1) the sheet of Beam L1-T40 was abruptly debonded due to the peeling action of the CDC immediately after passing the loading level of P = 152 kN as shown in **Fig.7.10b**; and (2) Beam L2-T40 reached the ultimate state with sheet rupture after passing the maximum load, however the cracks have not been opened and the sheet did not tend to be debonded due to the peeling action of CDC as shown in **Fig.7.10d**.

In the case of Beam L1-T0, the failure mode was sheet debonding due to the peeling action of CDC as shown in **Fig.7.10a**. However, the sheet was ruptured in Beam L2-T0 because of the high local effect of pre-cracking due to the high prior loading level, as shown in **Fig.7.10c**.

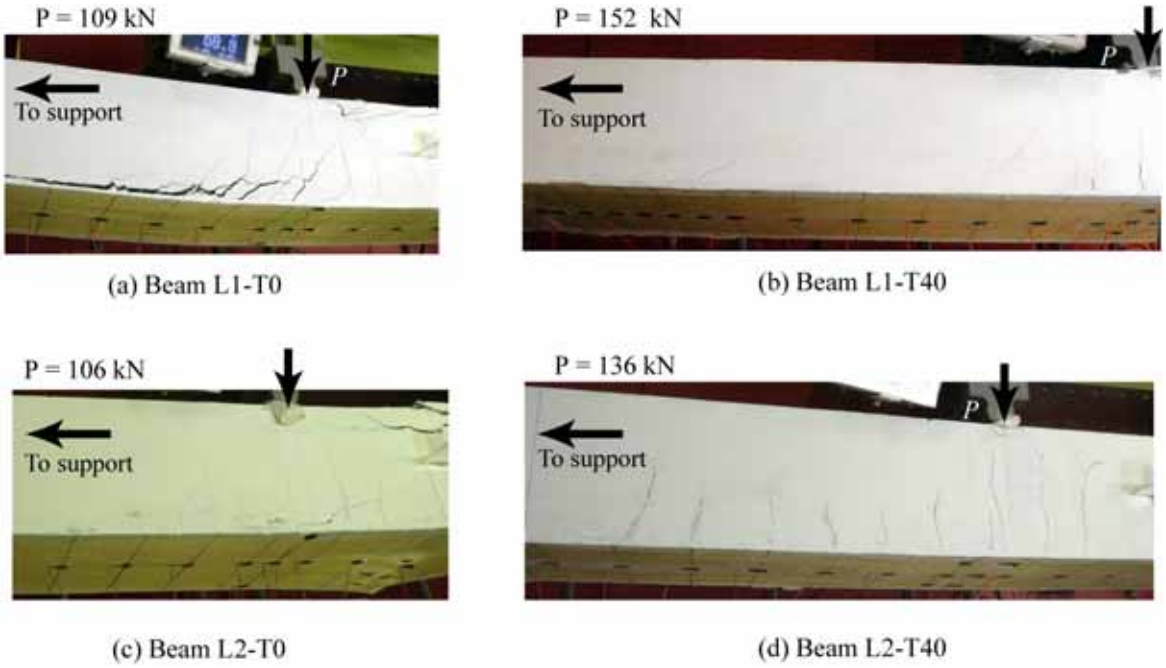

Fig.7.9 Crack distributions on side-surface of beam: (a, b): just before full debonding; and (c, d): just before sheet rupture.

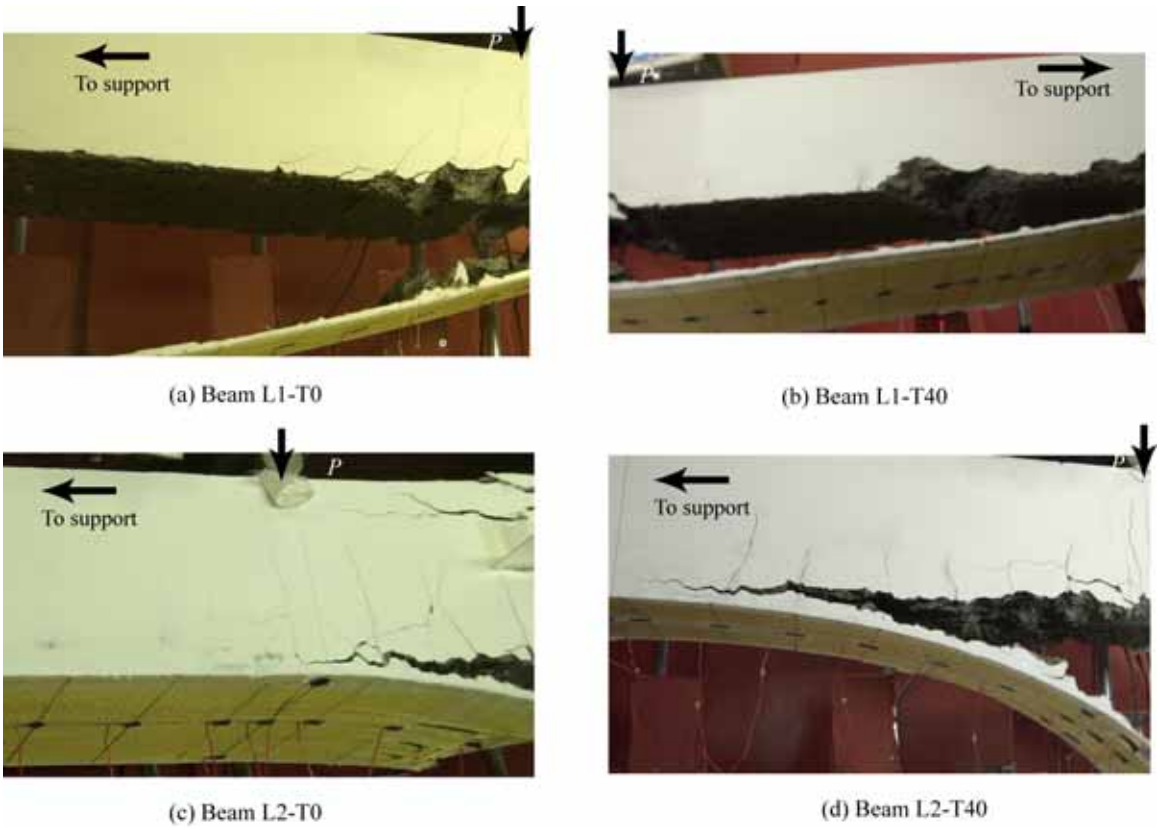

Fig.7.10 Failure modes; (a,b) Sheet debonding, and (c,d) Sheet rupture

7.8 Summary

In this chapter, Strengthening Study of pre-cracked RC beams has investigated the load-carrying behavior of pre-cracked RC beams strengthened with pre-tensioned sheet compared to non-pre-cracked ones. Pre-tension stress ratio introduced to the AFRP sheet (0 and 40%) and the level of prior loading (Level 1 is up to main rebar yielding; Level 2 is up to the average point between main rebar yielding and ultimate load) were taken as variables. From this study, it is observed that due to introducing pre-tension force into the sheet, flexural capacity and durability of the pre-cracked RC beams can be improved and the width of cracks can be decreased. This implies that a new anchoring method is effective and feasible. Numerical results can better match the experimental results for non-pre-cracked beams but not for pre-cracked beams subjected to high prior loading up to the middle point between the main rebar steel yielding and the ultimate state because the existing cracks and the stiffness of putty used for flattening the bonding surface were not considered in numerical analysis.

CHAPTER 8

Study of repaired pre-cracked RC beams

8.1 Introduction

In this chapter, an investigation of the effects of repairing the cracks on the load-carrying behavior of the existing RC members strengthened by bonding pre-tensioned AFRP sheet onto the tension-side surface is explained by conducting four-point loading tests of the RC beams. The tests were performed using beams with/without existing cracks and beams with/without repairing of the cracks as variables. These specimens were tested at The Structural Laboratory of Civil Department at Muroran Institute of Technology, Japan to investigate a rational flexural reinforcing method for pre-cracked RC beams using a pre-tensioned AFRP sheet with a simple anchoring method. The test results were observed by visual inspection during the test and measured by instrumentation. These results are described in different forms as crack patterns in different stages of loading, load-deformation curves, and axial strain distribution of the sheet at the ultimate state. The parameters were carefully chosen to obtain different modes of failure, as will be discussed in the following sections.

8.2 Test specimens

The test specimens used in this study are listed in **Table 8.1**. These specimens were categorized as: (1) with/without existing cracks (N: without and D: with cracks); (2) with/without repairing existing cracks (N: without and DR: with repaired cracks); and (3) with/without the introducing pre-tension force into the AFRP sheet (N: without and P: with introducing pre-tension force). Each specimen was denoted by connecting these categories with a hyphen sequentially. The control beam is named Beam O, which is without existing

cracks and not reinforced with AFRP sheet. The control beam has also been referred to as Beam N-N-N. In this study, prior loading level is until reaching the middle point between the main rebar yielding and the analytical ultimate state. The beams have a rectangular cross-section of 220 × 220 mm (width × depth) and a clear span of 3,200 mm. The layout of the reinforcement, AFRP sheet, and measuring points are shown in **Fig.8.1**. Each of the two deformed steel bars of 19 mm and 16 mm diameters are placed in the upper and lower fibers, respectively and are welded to steel plates of t = 9 mm thickness at the ends of the beams, to save the anchoring length of the rebar. To prevent premature shear failure, stirrups of 10 mm diameter are placed every 100 mm. AFRP sheet of 220 mm width was pre-tensioned and then bonded onto the tension-side surface, leaving 80 mm between the supporting point and the sheet end as shown in **Fig.8.1**. The target and actual pre-tensioning force ratios and the introduced initial strain into the sheet is listed in **Table 8.1**, in which the ratios are obtained by referring to the nominal tensile capacity of the sheet.

Table 8.1 List of specimens

Specimen	W/O Existing cracks	W/O Repairing cracks	Designed pre-tension force ratio* (%)	Actual pre-tension force ratio* (%)	Introduced initial strain (μ)
O(N-N-N)	-	-	Non-strengthened		
N-N	Without	-	0		
D-N	With	Without			
DR-N		With			
N-P	Without	-	40 (104)	40.1 (104)	7,008
D-P	With	Without		30.5 (78.9)	5,337
DR-P		With		34.8 (89.9)	6,081

*: ( ) Pre-tension force (kN)

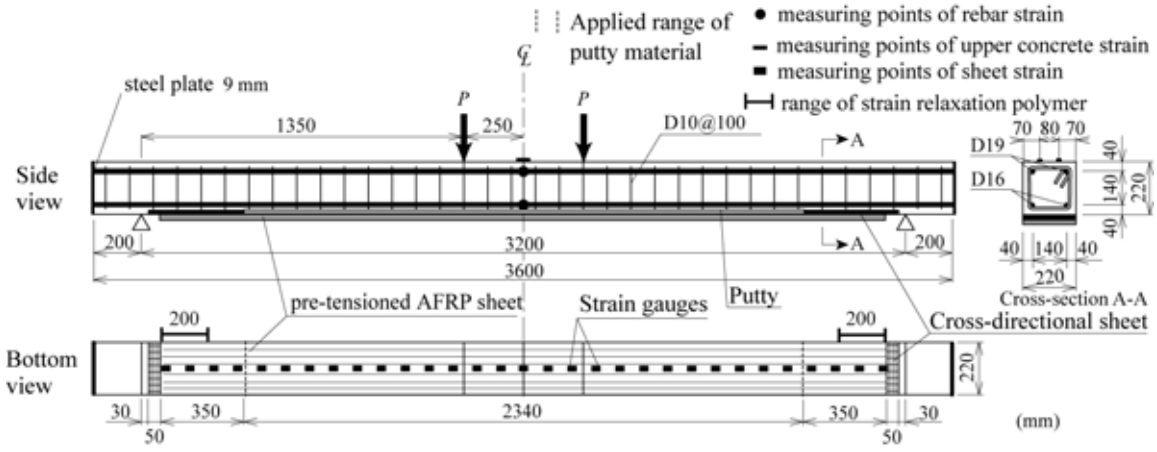

Fig.8.1 Layout of reinforcement and AFRP sheet

8.3 Loading procedures and repairing the cracks

In this study, before strengthening with AFRP sheets as mentioned before in Chapter 3, Beams D were pre-cracked by four-point loading tests. The surcharged load was able to reach the middle point of the deflections between the numerically estimated main rebar yielding point and the ultimate state (hereinafter, analytical ultimate state), in which the numerical evaluation method was explained in Chapter 5. This is the reason that the beams suffered relatively severe damage, even though the rebar yielded and crushing of concrete was not reached. After that, they were removed from the loading apparatus and then cracks (hereinafter, existing cracks) of the Beams DR were repaired by injecting epoxy-resin type adhesive. Finally, the specimens were reloaded until complete failure as shown in **Fig.8.2**. **Fig.8.3** shows the steps of repairing the cracks, in which the cracks surfaces were prepared by sawcut to improve the bonding capacity of the surface (**Fig.8.3a,b**). Then, the surfaces of cracks were coated with putty material to prevent injected epoxy-resin from going out from inside of cracks during injection process and pipe used for injection was installed inside the cracks (**Fig.8.3c**). After that, only cracks with more than 0.2 mm width were repaired by injecting epoxy-resin using injection device (**Fig.8.3d**). Finally, the installation pipe and injection device were removed from the crack after curing the epoxy- resin.

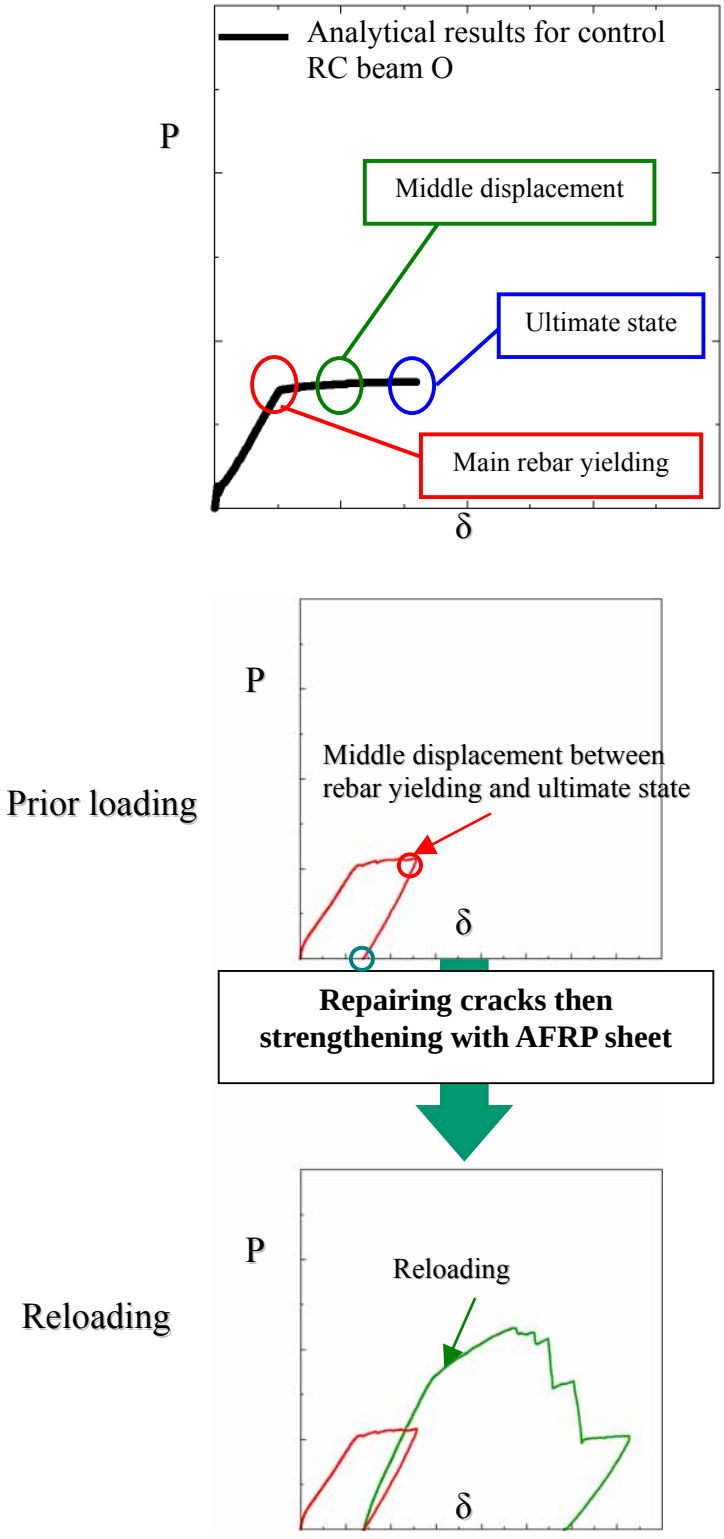

Fig.8.2 Loading procedures

(a) Preparing the cracks surfaces

(a) After preparing the cracks surfaces

(c) Coating the cracks surfaces with putty

(d) Injecting epoxy-resin inside the cracks

Fig.8.3 Steps of repairing the cracks

8.4 Experimental results of prior loading and after reinforcing with AFRP sheet

The experimental results at the maximum deflection (around 31.5 mm) under preloading for making cracks, after unloading, and after reinforcing with/without pre-tensioned AFRP sheet are listed in **Table 8.2**. From this table, it is observed that at maximum load of prior loading, the concrete strain at the upper fiber is around 2,000 μ and main rebar strain at the mid-span is larger than the yielding strain (1,850 μ). However, after unloading, the residual concrete strain at the upper fiber is around 1,000 μ and a residual deflection is about 17 mm. In the case of the beams reinforced with pre-tensioned AFRP sheet (Beams D-P and DR-P), the deflection was restored after reinforcing due to introduced prestress into the lower fiber of the beam, which leads to form a compression zone at the base of the beam; hence the confinement of pre-cracks occurs. The restored deflections for Beam D-P and DR-P are 12 mm and 6 mm, respectively. This implies that for the case of the crack-repaired Beam DR-P, the recovery becomes smaller than the case of non crack-repaired Beam D-P, due to the cracks filled with grouting chemicals.

On the other hand, in the case of the beams reinforced with non-pre-tensioned AFRP sheet (D-N and DR-N), the restored deflections are still the same values of preloading and reloading cases (17 mm) because non-pre-tensioned sheet has no effect on the pre-cracks.

Table 8.2 Results of prior loading

Spec-imen	At max. load of prior loading				After unloading			After reinforcing
	Load (kN)	Disp. (mm)	Strain at upper fiber concrete (μ)	Strain of main rebar (μ)	Residual disp. (mm)	Residual strain at upper fiber concrete (μ)	Residual strain of main rebar (μ)	Disp.* (mm)
D-N	37.8	31.6	-2,014	5,066	17.1	-950	3,486	17.1
DR-N	35.8	31.4	-2,038	2,272	16.9	-995	383	16.9
D-P	37.6	31.6	-2,359	2,645	17.2	-1,274	1,737	12.0
DR-P	37.0	31.3	-1,725	3,113	16.5	-796	1,924	6.0

*: ( ) restoring displacement due to reinforcing with pretensioned AFRP sheet

8.5 Crack patterns after prior loading

Crack patterns for each beam that occurred due to preloading are shown in **Fig.8.4**. From this figure, it is observed that the flexural cracks have occurred in the side-surface of the entire span of every beam due to prior loading. The maximum width of cracks is about 0.7 mm, which occurred in the equi-bending span. In this figure, the repaired cracks injected with epoxy-resin after reinforcement with AFRP sheet are marked by thick lines.

It is clear from this figure that the specimens have suffered severe damage through almost the entire span because of a high prior loading level, in which the surcharged load is until reaching the middle point between the main rebar yielding and the analytical ultimate state.

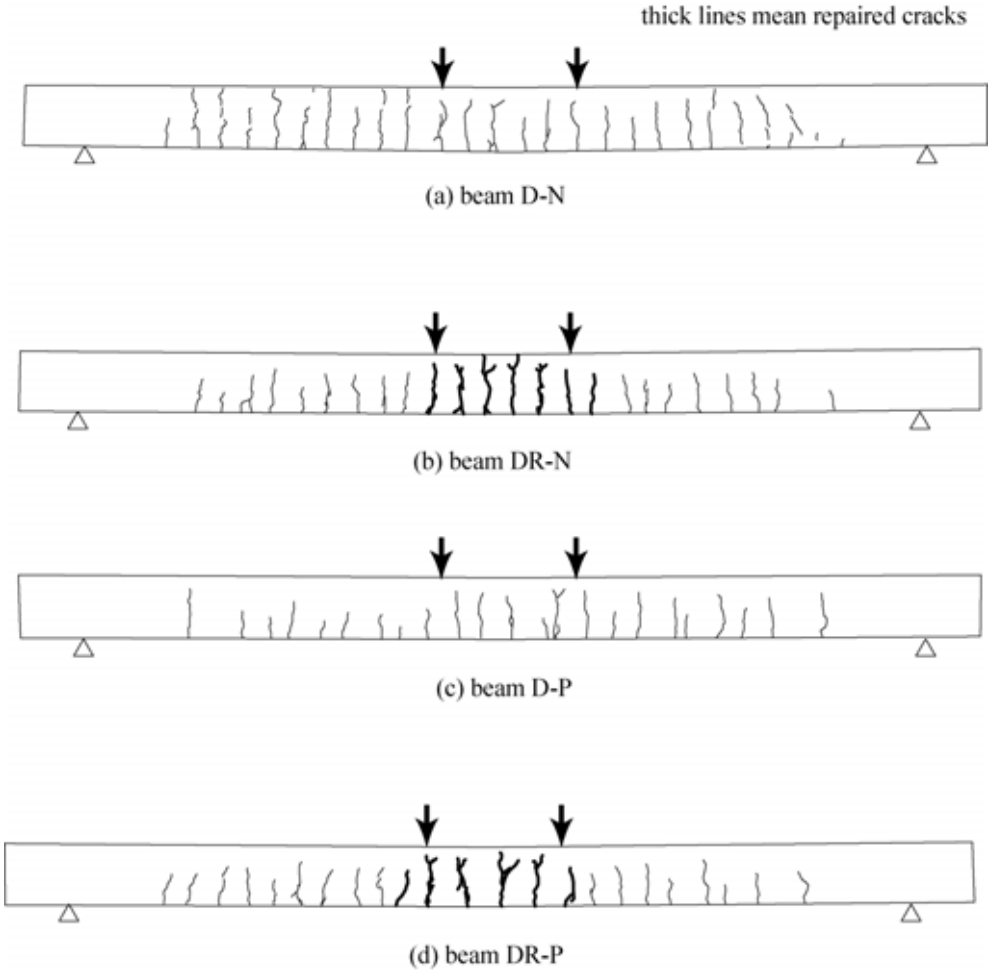

Fig.8.4 Crack patterns after prior loading

8.6 Results after reloading up to failure

After removing the prior loading, the beams were strengthened with AFRP sheet, then they were reloaded until reaching complete failure and the following results were obtained;

8.6.1 Effect of pre-tension force introduced to the sheet

Fig.8.5 shows comparisons of load-displacement relations of beams reinforced by bonding AFRP sheet with different pre-tension force and with/without repairing the cracks caused by prior loading to investigate the effectiveness of introducing pre-tension force to the sheet. For the control beam O, experimental results show a decrease in stiffness due to the flexural cracks at the loading level of 6 KN and a displacement of 1.1 mm and then due to the main rebar yielding at a loading level of 33 KN and a displacement of 15 mm. After that, under a slight increase in the stiffness, an ultimate loading level of 43 KN, and a displacement of 67 mm have been reached as presented in **Table 8.3**. Once the failure of the control beam occurs under a compressive force, a subsequent sudden drop of the concrete load-carrying capacity was recorded as shown in **Fig.8.5**.

In the case of Beam N-N reinforced with non-pre-tensioned AFRP sheet, the cracking load is a little higher (38%) than that of Beam O. However, flexural stiffness increases notably after reaching the cracking and main rebar yielding as well. Displacement at the ultimate state is nearly unchanged as shown in **Fig.8.5a**. Thus, the addition of AFRP sheet without pre-tension has little effect on the beam performance before the first crack forms. However, because AFRP sheet carries a portion of tensile stresses after cracking occurs, the beam performance is enhanced. As a result, the AFRP sheet contributes to the load-bearing capacity of the beams since tensile stresses carried by main rebar are redistributed to the AFRP sheet thereby increasing the loading level at the yielding of the main rebar. From experimental results of Beam N-N, the yielding of the main rebar and ultimate loads are reached at a load 55 and 78%, respectively, higher than that of Beam O as presented in **Table 8.3**. Whereas in the case of Beam N-P reinforced with pre-tensioned AFRP sheet, the yielding of the main rebar and ultimate loads are reached at a load 147% higher than that of Beam O as shown in **Table 8.3**. Moreover, due to the introduction of pre-tension force in

the sheets bonded to Beam N-P, cracking load increases by 328% compared to that of Beam N-N.

In addition, from **Fig.8.5b** and **Table 8.3**, it is seen that compared to the control beam O, cracking, yield, and maximum loads of Beam D-N are increased by 15, 58, and 88%, respectively, and these loads are also increased considerably by 450, 160, and 198% for Beam D-P, respectively.

In the case of Beam DR-N, cracking, yield, and maximum loads are increased by 15, 56, and 98%, respectively; whereas the increase in these loads is 440, 165, and 161%, respectively, for Beam DR-P comparable to control beam O as shown in **Fig.8.5c** and **Table 8.3**. This increase in the improvement of flexural behavior of the Beam DR-P is due to the introduction of pre-tension force to the sheet

From these results, it is observed that in the case of the tested beams (N-P, D-P and DR-P) reinforced with pre-tensioned sheet, the loading level in the region from crack opening to the ultimate state has a tendency to increase due to the introduction of pre-tension force in the AFRP sheet. The cracking loads of the beams reinforced with pre-tensioned sheet (N-P, D-P and D-RP) are increased by 210, 380%, and 372, respectively, compared to Beams N-N, D-N, respectively, and DR-N. When the pre-tensioned AFRP sheet is used, the main rebar is relieved of tensile stresses and placed slightly into compression. It has been observed that the pre-tensioned AFRP sheet carries a great portion of the tensile stresses. As a result, the load-carrying capacity of the beams reinforced with the pre-tensioned AFRP sheet increases after yielding of the main rebar. Thus, the experimental data for the pre-tensioned sheet has revealed that the loading level of the main rebar yielding increases by 60, 65 and 70% for the beams N-P, D-P, and DR-P, respectively, compared to the beams reinforced with non-pre-tensioned sheet (N-N, D-N, and DR-N), respectively (**Table 8.3**). This clearly demonstrates the effect of the pre-tensioned sheet in applying an axial compressive force over the whole depth of the section and in applying a moment, which tends to place the top of the section in tension and cause additional compression at the base of the beam. This leads to an increase in the value of the external load required to produce a visible flexural cracking, hence the cracking load increases considerably. Furthermore,

from the experimental results summarized in **Table 8.3**, the increase of the ultimate load is higher when the pre-tensioned AFRP sheet was bonded to the beams, compared to Beams N-N D-N, and DR-N (up to 39 and 43, and 32 % for Beams N-P, D-P, and DR-P, respectively). Due to the initial camber of the beams reinforced with pre-tensioned sheet, an improvement of the cracking load has been observed. This may be due to the initial pre-tension introduced to the AFRP sheet and the relatively larger tensile force carried by the AFRP sheet. The cracks control not only decreased the deflection but also improved the durability of the concrete structure since its deterioration is strongly related to the width of the cracks. Therefore, it could be concluded that the pre-tensioned AFRP sheet may be successfully applied in the cracked section members.

At the ultimate state, it is clear that the displacement has a tendency to decrease since a part of the AFRP sheet strain is used for the pre-tensioning process as in Beams N-P, D-P, and DR-P. Thus, the specimens could have a brittle failure behavior. In addition, displacement at any loading level was significantly lower with the addition of the non-pre-tensioned AFRP sheet and was further reduced when the pre-tensioned sheet is bonded, as shown in **Fig.8.5**. These results have proven the ability of the pre-tensioned AFRP sheet to control cracking in pre-cracked RC beams. This could be explained by the fact that the sheet in the reinforced beam generates a tensile force along the deformed concrete section and creates equilibrium among the internal forces with much less deformation compared to the control.

From these results, it is observed that: (1) reinforcing with pre-tensioned AFRP sheet, the load-carrying capacity of the beams can be increased by more than 30 % compared to the case of reinforcing with normal sheet (Beams N); and (2) cracking and rebar yielding loads can be effectively increased by reinforcing with pre-tensioned AFRP sheet (more than 200 and 60% for yield and cracking loads, respectively, compared to the case of reinforcing with normal sheet)

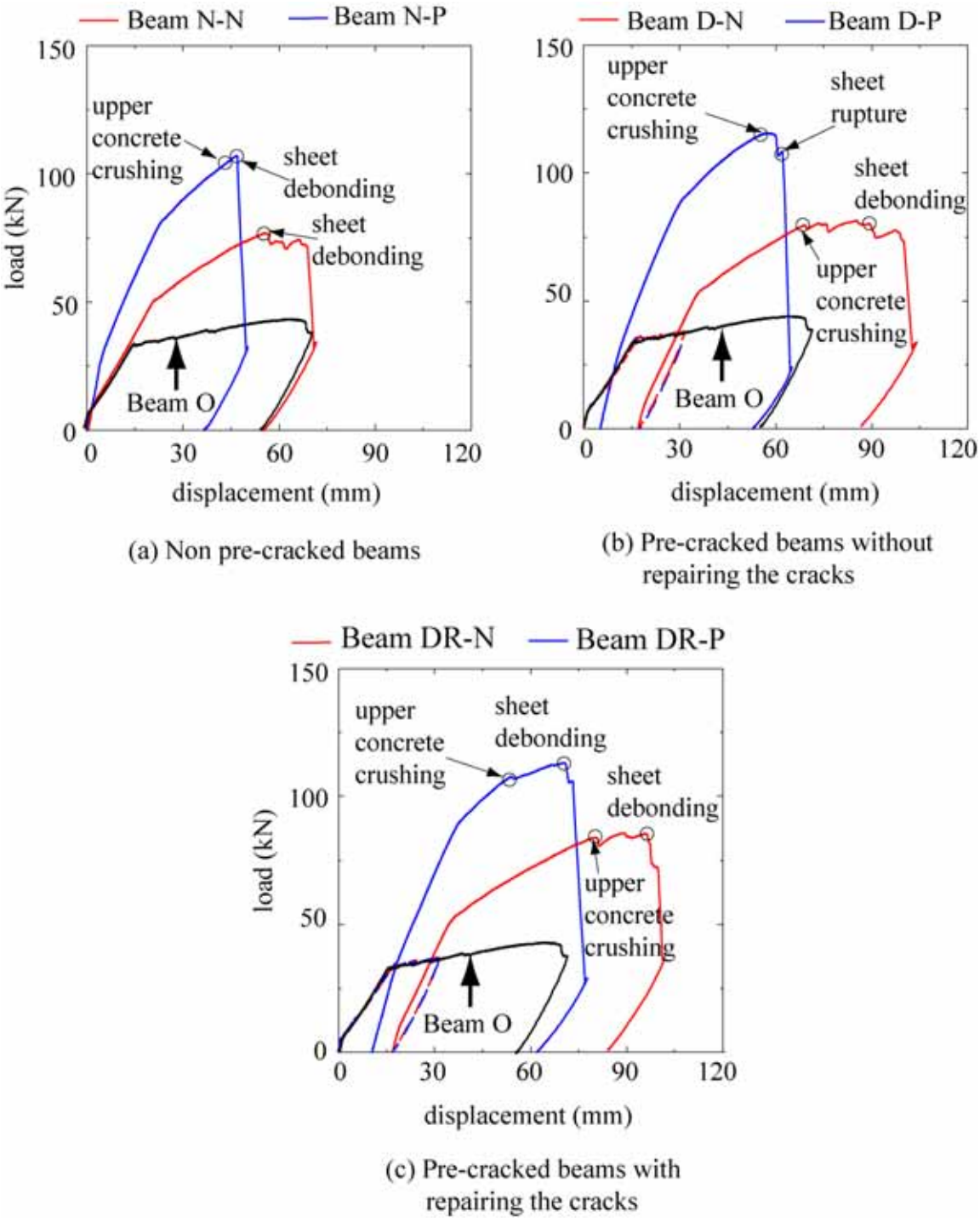

Fig.8.5 Comparisons of load-displacement relations of beams reinforced by bonding AFRP sheet with different pre-tension force.

8.6.2 Effect of repairing the cracks

Fig.8.6 shows comparisons of load-displacement relations of beams reinforced by bonding AFRP sheet with different pre-tension force and with/without repairing the cracks caused by prior loading to investigate the effectiveness of repairing the cracks by epoxy-resin injection.

Comparing the results for the case with/without repairing existing cracks, load-carrying capacity is almost similar for both cases. In the case of the beams reinforced with non-pre-tensioned AFRP sheets (D-N and DR-N), repairing the cracks has no effect on failure modes but the ultimate load increases by about 6%, as shown in **Fig.8.6a** and **Table 8.2.**

However, the beam in the case without repairing cracks and reinforced with pre-tensioned sheet (D-P) broke down with sheet rupture. On the other hand, the beam in the case with repairing cracks and also reinforced with pre-tensioned sheet (DR-P) reached the ultimate state in the sheet debonding failure mode after upper concrete crushing, as shown in **Fig.8.6b**. This implies that in the case of Beam DR-P, the opening of the existing cracks is rationally restrained by repairing and then the local strains in the sheet around the cracks are also controlled not to be large, irrespective of pre-tension stress ratio introduced to the sheet.

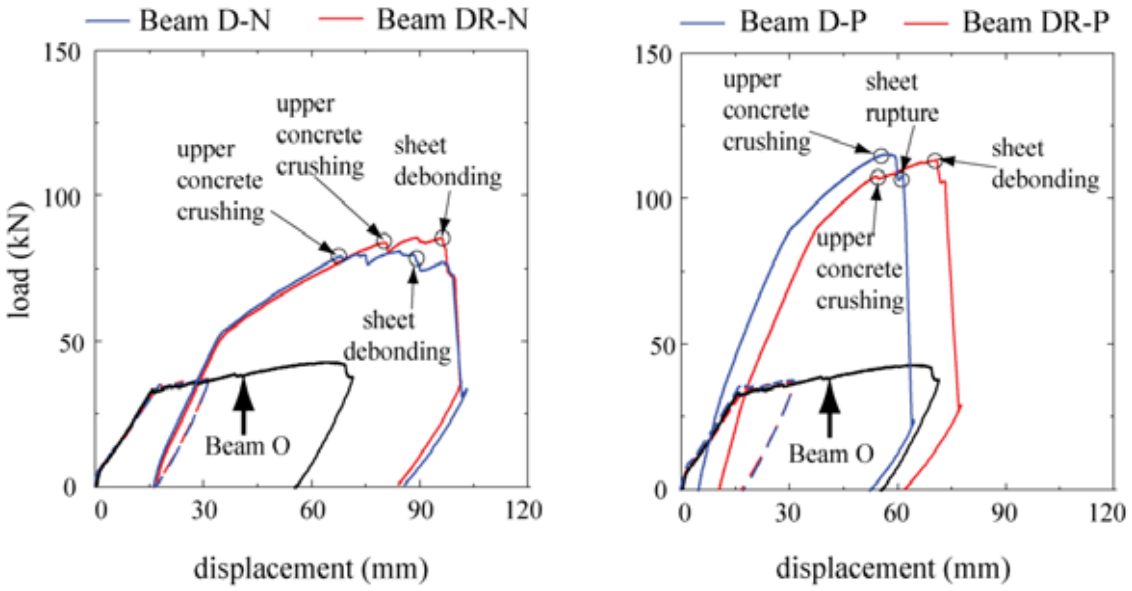

(a) Beams reinforced with normal sheet (b) Beams reinforced with pre-tensioned sheet

Fig.8.6 Comparisons of load-displacement relations of beams reinforced by bonding AFRP sheet with the same pre-tension force and with /without repairing the cracks

8.6.3 Comparison between the experimental and analytical results

Comparisons of the load-deflection relationship between experimental and numerical results for each beam are shown in **Fig.8.7**. In this figure, experimental results are shown from preloading through loading after reinforcing with AFRP sheet. Numerical results were obtained by means of a multi-section method mentioned in Chapter 5. In this simulation, the existing cracks and the stiffness of putty used for flattening the bonding surface were not considered.

From this figure, it is clear that in the case of Beam N-N, the debonding sheet occurs before reaching upper concrete crushing, whereas in Beams D-N and DR-N, the AFRP sheet was debonded after upper concrete crushing. It is observed that because of residual strains in the upper concrete due to prior loading level in Beams D-N and DR-N, the analytical results are less than the experimental ones at the yielding of main rebar but at the ultimate state,

the analytical results are the same in Beam D-N and less than those of the experimental results in Beam DR-N, as shown in **Fig.8.6** and **Table 8.2**. Thus, the load-carrying behavior of Beams D-N and DR-N did not significantly influence by repairing the cracks and bonding non-pre-tensioned AFRP, so their behavior are similar to that found in non-pre-cracked beams (N-N). Therefore, Beams D-N and DR-N reached the analytical ultimate state before sheet debonding and the experimental maximum load exceeds the analytical ones, especially when the pre-cracks are repaired. Moreover, the stiffness inclination of the curve of these beams decreased after yielding the main steel reinforcement. The same trend can be noted for Beams D-P and DR-P reinforced with pre-tensioned AFRP sheet. However, the flexural behavior can be improved more than in the case of reinforcing pre-cracked RC beams with normal sheet. This confirms that the experimental load-carrying behavior of the pre-cracked RC beams reinforced with non-pre-tensioned or pre-tensioned AFRP sheet will be more than those of numerical analysis because the existing cracks and the stiffness of putty used for flattening the bonding surface were not considered in numerical analysis.

Finally, from theses results, it is observed that numerical results can better match the experimental results for non pre-cracked beams but not for pre-cracked beams.

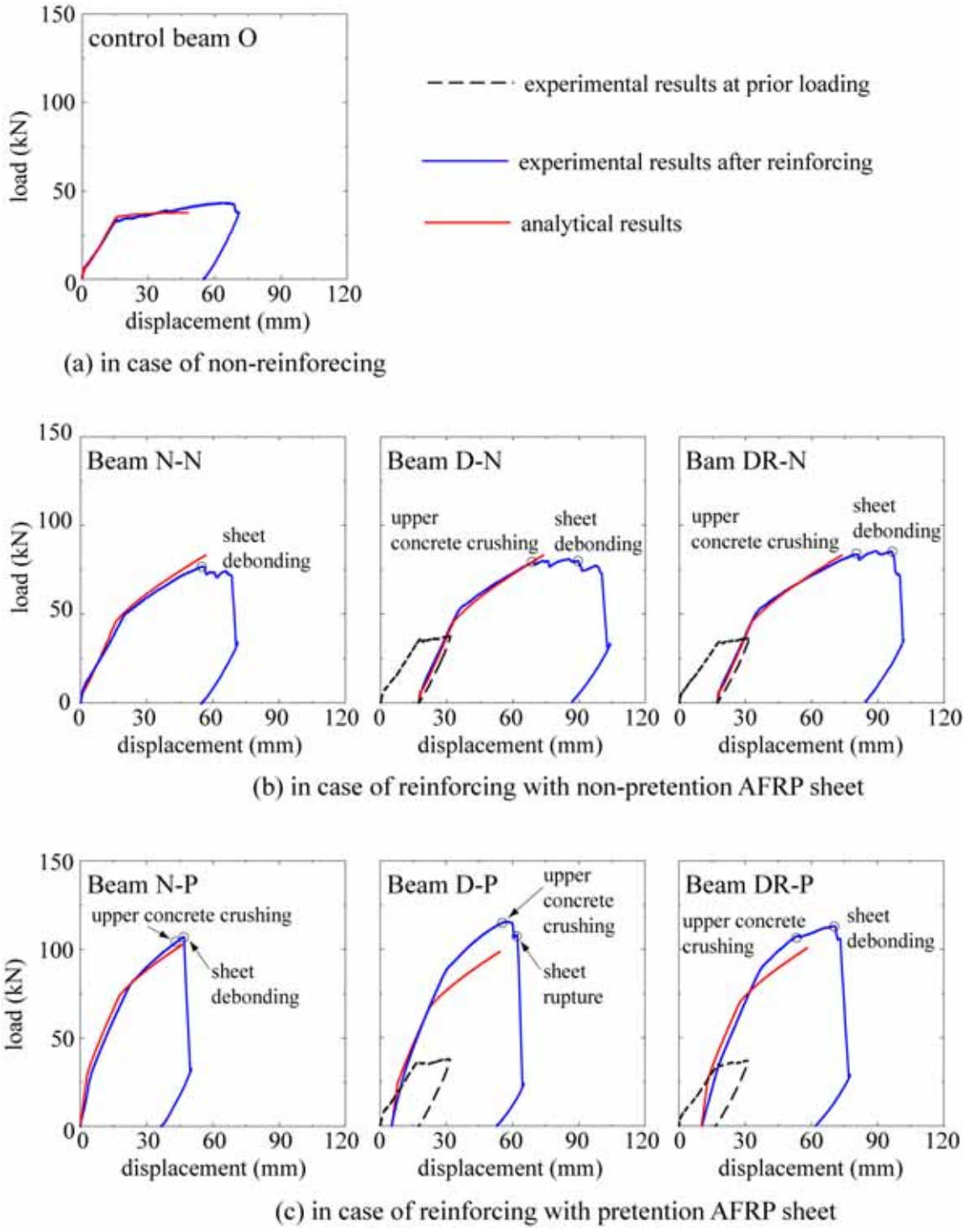

Fig.8.7 Comparisons of load-displacement relations between experimental and analytical results.

Table 8.2 List of experimental and analytical results

Specimens	Cracking load			Yeild load			Maximum load			Experimental failure mode
	$P_{exp.}$ (kN)	$P_{ana.}$ (kN)	$P_{exp.}/P_{ana.}$	$P_{exp.}$ (kN)	$P_{ana.}$ (kN)	$P_{exp}/P_{ana.}$	$P_{exp.}$ (kN)	$P_{ana.}$ (kN)	$P_{exp.}/P_{ana.}$	
O(N-N-N)	5.98	6.63	0.90	32.8	34.8	0.94	43.2	37.7	1.15	Concrete crushing
N-N	8.25	6.63	1.24	50.9	45.8	1.10	76.8	83.2	0.92	Sheet debonding
D-N	6.85	6.63	1.03	51.9	45.8	1.13	81.0	83.2	0.92	Sheet debonding
DR-N	6.85	6.63	1.03	51.1	45.8	1.12	85.5	83.2	1.03	Sheet debonding
N-P	25.6	30.1	0.85	81.1	74.0	1.10	107	103	1.04	Sheet debonding
D-P	32.9	24.8	1.33	85.5	71.9	1.19	116	109	1.06	Sheet rupture
DR-P	32.3	26.9	1.20	86.9	73.2	1.19	113	107	1.06	Sheet debonding

Note: Numerical analysis predicted upper concrete crushing failure modes for all specimens

8.6.4 Axial strain distribution of the AFRP sheet at ultimate state

Comparisons of the strain distribution of the pre-tensioned AFRP sheet between experimental and numerical results at the analytical ultimate state are shown in **Fig.8.8**. In the cases of Beams D-P and DR-P, measured strain distributions at the actual ultimate state are also shown in this figure. From this figure, it is observed that numerical results are almost similar to the experimental results. This means that the bonding capacity of the sheet has been kept sufficiently up to the analytical ultimate state.

From the strain distributions of Beams D-P and DR-P at the actual ultimate state, it is observed that more than 15,000 μ strain locally occurred in the equi-bending span of the Beam D-P. Since the initial tensile strain at the introduction of pre-tensioning force was 5,337 μ (see **Table 8.2**), it is confirmed that at the ultimate state, the total strain that occurred in the sheet may reach its breaking point (ultimate tensile strain of the sheet is 17,500 μ, as presented in chapter 4). On the other hand, the maximum strain that occurred in the equi-bending span of the Beam DR-P was almost 10,000 μ. This implied that the beam reached the ultimate state in the sheet-debonding mode due to a peeling action of the sheet because of the strain being flattened and not localized by repairing existing cracks.

Also, in case of Beams N-P without prior loading, the failure mode was sheet debonding

because of a peeling action of the opening critical diagonal crack (CDC) developed in the lower concrete cover near the loading points. This difference between experimental and analytical results is most likely due to the fact that in numerical analysis, it is assumed that the AFRP sheet is fully bonded to the concrete surface up to the analytical ultimate state.

In general, for all beams, it is observed that the experimental and analytical strain distributions in the equi-bending span are similar but local effects of the pre-cracks on the bond behavior may produce some variations in the experimental strains of the sheet. Therefore, the above results imply that a proposed anchoring method is effective and feasible.

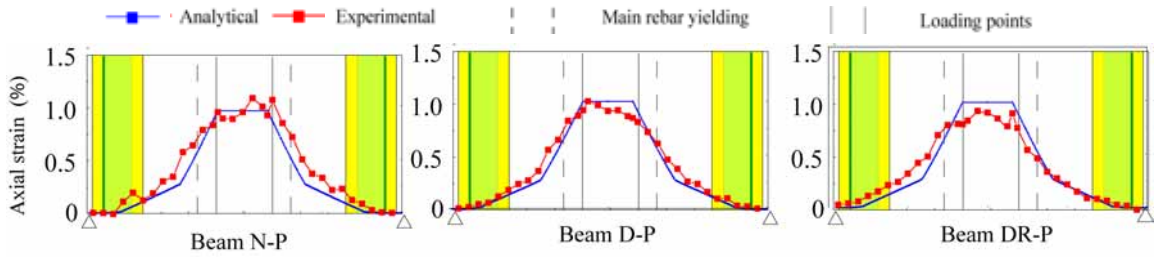

(a) At analytical ultimate state

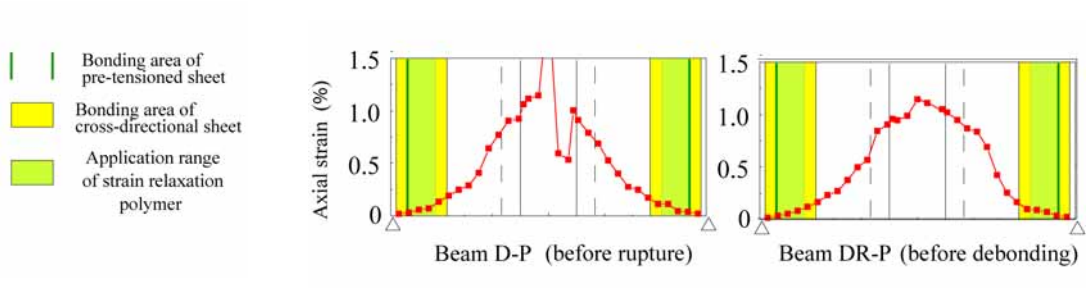

(b) At real ultimate state

Fig.8.8 Comparisons of axial strain distributions of AFRP sheet between experimental and numerical results.

8.6.5 Crack pattern and failure modes

Figs.8.9 and 8.10 show the crack patterns of each beam at the loading step close to the ultimate state for each beam. From this figure, it is observed that: (1) flexural and diagonal shear cracks occurred in the equi-bending and equi-shear spans, respectively, in every beam; and (2) the sheet tends to be partially debonded due to the peeling action of the critical diagonal crack which was proven by Triantafillou and Plevris 1992 and Kishi et al. 2005. This occurred because of CDC widening, resulting in concrete blocks at the tip of the CDC, pushing the AFRP sheet downward. These concrete blocks formed at a section of combined flexural and shear cracks initiated near the loading points. After that, the cracks developed horizontally towards each support, as shown in **Figs.8.9 and 8.10**.

From **Fig.8.9**, in the case of Beam N-N reinforced with non-pre-tensioned sheet without prior loading, the failure mode tends to be due to sheet debonding because of the peeling action of CDC, as shown in **Fig.8.9a**. In addition, by comparing Beams D-N with DR-N, repairing the cracks in Beam DR-N has little effect on crack behavior, failure mode, and load-carrying capacity, as shown in **Figs.8.9b,c**.

In the case of Beam N-P reinforced with pre-tensioned sheet without prior loading, shear cracks can hardly be seen due to the pre-tension force applied to the sheet, seeing as how this factor resulted in an improved shear capacity of the pre-cracked RC beams. Consequently, the CDC was controlled and as a result, only the flexural cracks appeared due to the introduction of pre-tension force to the sheet, as shown in **Fig.8.10a**.

Also, it is observed that the pre-cracked Beams D-P and DR-P were more cracked than Beam N-P and reached compressive failure in the upper fiber area of the equi-bending span. This is due to the compressive strains staying behind in the upper fiber area at the preloading for making cracks. In the case of Beam D-P, existing cracks tend to be more opened and then the sheet was broken by the locally large strains occurring around the widely opened cracks as shown in **Fig.8.10b**. On the other hand, in the case of Beam DR-P, the existing cracks cannot be more opened and new cracks occurred in different places from the existing ones as shown in **Fig.8.10c**. Therefore, it is seen that the repairing of existing cracks is very effective to restrain the early rupture of the pre-tensioned AFRP sheet. Then,

it is very important to repair the existing cracks before reinforcing with the pre-tensioned AFRP sheet in the field.

For beams reinforced with non-pre-tensioned sheet (**Fig.8.11**), it is observed that Beam N-N failed due to sheet debonding near the upper concrete crushing as shown in **Fig.8.11a** but the sheet was debonded after concrete crushing in Beams D-N and DR-N as shown in **Figs.8.11b,c**. Due to crack repair in Beam DR-N, the sheet debonding and upper concrete crushing occurred at a higher displacement than those of Beam D-N but at similar maximum loads.

On the other hand, in the case of beams reinforced with pre-tensioned sheet shown in **Fig.8.12**, it is observed that; Beam N-P failed due to sheet debonding near the upper concrete crushing as shown in **Fig.8.12a** but at higher maximum load than Beam N-N. However, the failure mode of Beam D-P was sheet rupture because of the local effect of cracks caused by prior loading as shown in **Fig.8.12b**. Due to repairing cracks, Beam DR-P failed by sheet debonding, as shown in **Fig.8.12c**.

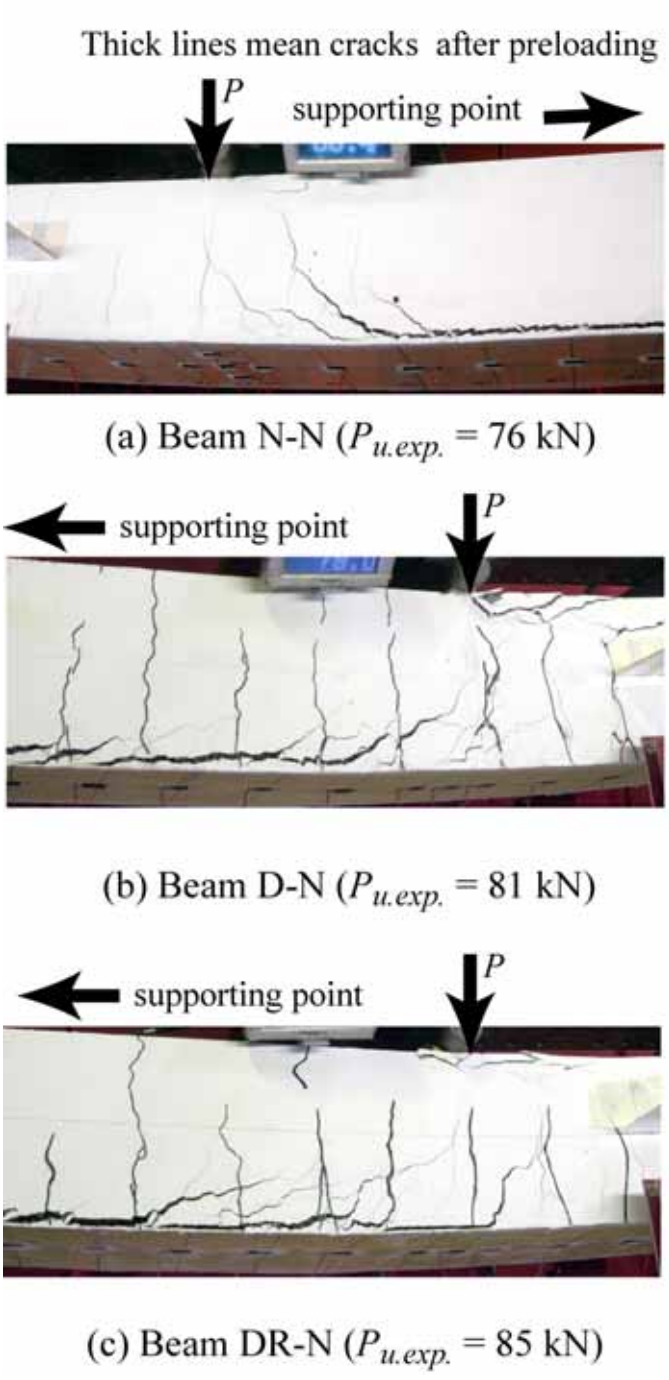

Fig.8.9 Crack distributions on side-surface of beams reinforced with normal sheet

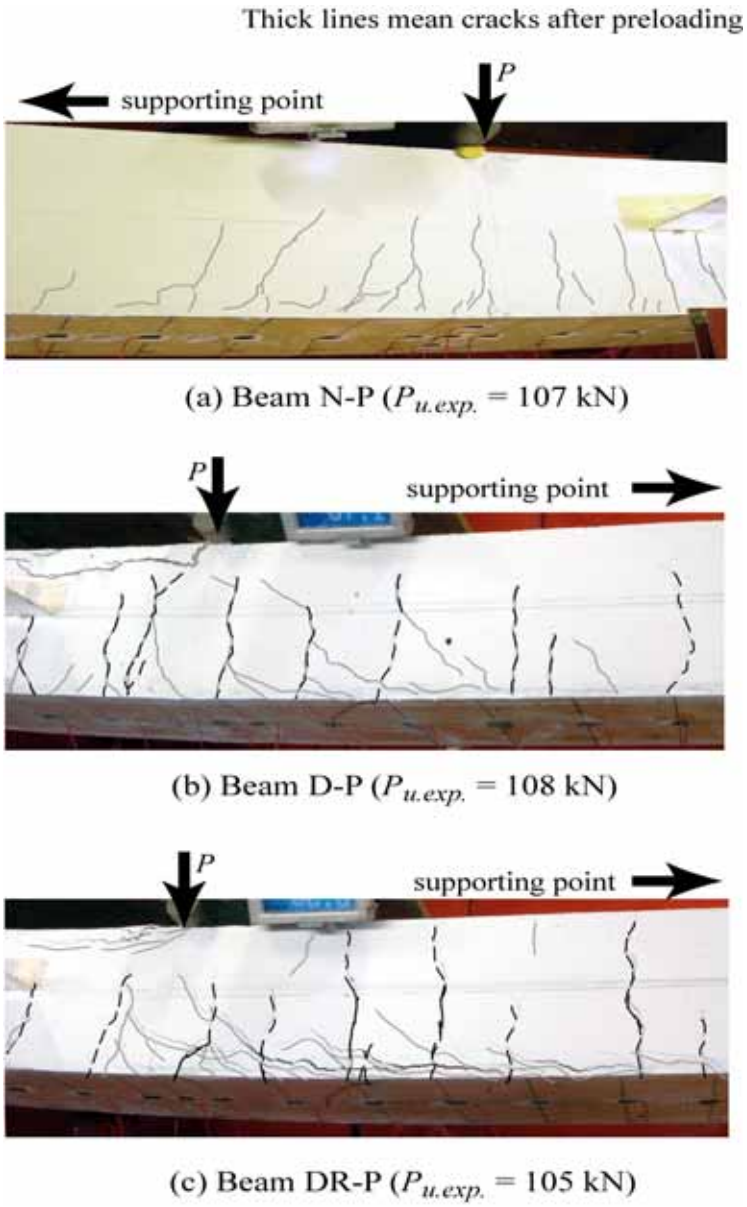

Fig.8.10 Crack distributions on side-surface of beams reinforced with pre-tensioned sheet

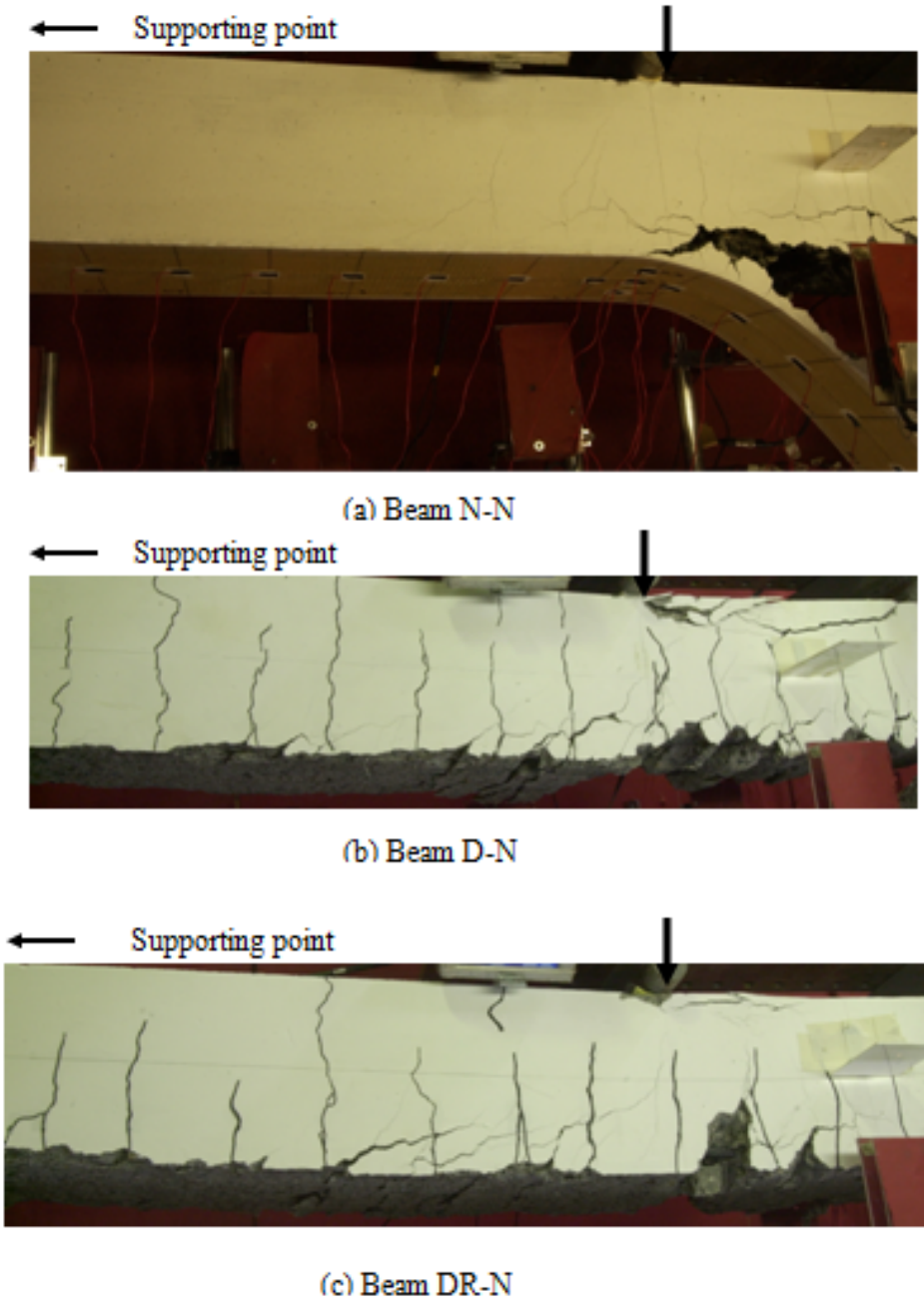

Fig.8.11 Failure modes of beams reinforced with normal sheet
(a) sheet debonding before concrete crushing, and
(b,c) sheet debonding after concrete crushing

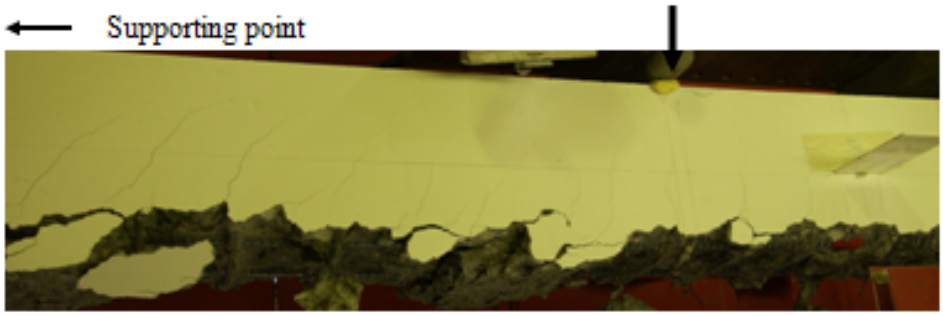

(a) Beam N-P

(b) Beam D-P

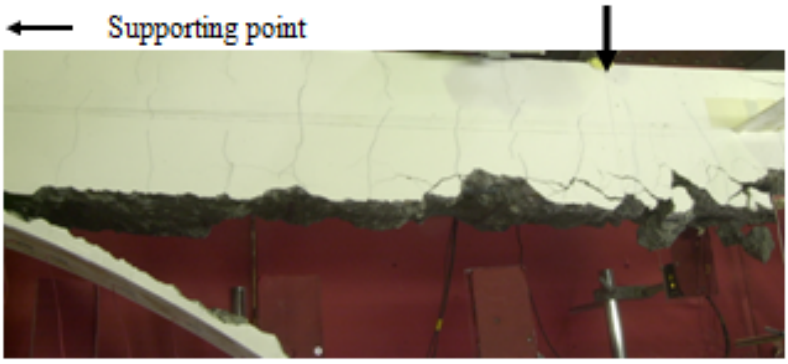

(c) Beam DR-P

Fig.8.12 Failure modes of beams reinforced with pre-tensioned sheets;
(a,c) sheet debonding after concrete crushing, and
(b) sheet rupture

8.7 Summary

This chapter presents Repair Study of pre-cracked RC beams to examine the effectiveness of pre-tensioned AFRP systems to restore the capacity of repaired pre-cracked RC beams reinforced with pre-tensioned sheet. Pre-tension stress ratio introduced to the FRP sheet (0 and 40%), with/without existing cracks and with/without repairing the cracks by injection of epoxy resin were taken as variables. From this study, the following results were obtained: 1) flexural load-carrying capacity of the cracked RC beams can be significantly improved by bonding the pre-tensioned AFRP sheet onto the tension-side surface; 2) by repairing the existing cracks, the sheet rupture can be prevented because of the opening of cracks and also large strains occurring in the sheet due to the opening can rationally be restrained; and 3) numerical results can better match the experimental results for non-pre-cracked beams but not for pre-cracked beams.

CHAPTER 9

Summary and conclusions

9.1 Summary

In order to develop a rational flexural reinforcing method for strengthening and repairing pre-cracked RC beams using a pre-tensioned Aramid Fiber Reinforced Polymer (AFRP) sheets, a new anchoring method was proposed. In this method, to distribute the concentrated anchoring stresses of pre-tensioned AFRP sheet, the base cross-directional non-pre-tensioned AFRP sheets were bonded to the concrete surface around the anchoring area. In addition, to decrease gradients of bonding stresses near the anchoring area, a strain relaxation polymer (with low young's modulus) was used as a bonding material. An applicability of the proposed method for anchoring pre-tensioned AFRP sheet was investigated by conducting a static four-point loading test. The objectives of this research are threefold. First, the overall structural behavior of pre-tensioned FRP strengthened RC beam, effectiveness and feasibility of using a simple anchoring method without metal system were studied. The second objective is to study the effectiveness of using pre-tensioned FRP sheet to strengthen pre-cracked RC beams. The third objective of this research is to investigate the flexural behavior of FRP repaired pre-cracked RC beams.

A total of 20 RC beams were tested in the course of this research; 8 as part of a Strengthening Study of RC beams, 5 as part of a Strengthening Study of pre-cracked RC beams, and 7 as part of the Repair Study of pre-cracked RC beams.

The analytical portion of the research is employed to describe the flexural behavior of all tested beams and for comparison with the experimental results. A multi-section method was applied to analytically estimate the load-displacement relation and the axial strain

distribution of AFRP sheets used to flexural reinforce each RC beam, with different ratios of pre-tension stress in the sheet and the main reinforcement steel ratio.

9.2 Conclusions

The conclusions in this section are divided according to the part of the dissertation as follows;

1- Strengthening Study of RC beams

This study has investigated effectiveness and feasibility of using a simple anchoring method without metal system, for which a static four-point loading test has been conducted. The variables examined in the experimental program included the pre-tension stress ratio introduced to the AFRP sheet (0, 20, and 40%) and the main reinforcement steel ratio (0.79 and 1.24%). Based on the results obtained, the following conclusions can be drawn:

(1) A new anchoring method without permanent mechanical systems at both ends of the pre-tensioned AFRP sheet has been shown to be effective and applicable to prevent any premature peeling failures associated with the high shear stresses present at the ends of the sheets;

(2) Based on the experimental results of beams reinforced with non-pre-tensioned AFRP sheets, the yielding of the main rebar occurs at a load 70 % higher than that of the control beam. Moreover, a 115 % increase in the ultimate load of the control beam was obtained, when the AFRP sheet without pre-tension is used. However, the cracking load is a little higher than that of control beam.

(3) The experimental data for the pre-tensioned sheet have revealed that the cracking load is increased by 345 and 570 % for pre-tension stress ratio in the sheet of 20 and 40%, respectively. In addition, the loading level of the main rebar yielding is increased by 113 % and 179 % for pre-tension stress ratio in the sheet of 20 and 40%, respectively, compared to the control beams. This clearly demonstrates the effect of the pre-tensioned sheet in applying an axial compressive force over the whole depth of the section and in applying a moment, which tends to place the top of the section in tension and cause additional compression at the base of the beam. This leads to an

increase in the value of the external load required for producing visible flexural cracking; hence the cracking load is increased considerably. Moreover, the increase of the ultimate load is higher when the pre-tensioned AFRP sheet was bonded to the beams compared to the control beam (up to 164 and 191 % for pre-tension stress ratio in the sheet of 20 and 40%, respectively). This increase may be due to a change in the failure mode of sheet debonding for beams reinforced with non-pre-tensioned AFRP sheet to sheet rupture in the case of the beams reinforced with pre-tensioned AFRP sheet;

(4) From these results, it is observed that a significant increase of the cracking load, the yield load and the ultimate load of the RC beams. This improvement is mainly due to the reinforcing with the pre-tensioned AFRP sheets. In addition, the load carrying capacity has a tendency to increase according to an increment of the pre-tension force in the AFRP sheet. However, the displacement at the ultimate state tends to decrease;

(5) Similar trends have been noted in both observed and predicted curves using the multi-section method. The effect of the addition of non-pre-tensioned and pre-tensioned sheet is almost similar on both observed and predicted results;

(6) As the main steel reinforcement ratio lowers, the effectiveness of reinforcing with pre-tensioned AFRP sheets increases. When the steel ratio is 0.79 %, the maximum load increases by 141, 157, and 210% for pre-tension stress ratio in the sheet of 0, 20, and 40 %, respectively, whereas in the case of steel ratio of 1.24 %,, the maximum load increased by 88, 117, and 141%, for pre-tension stress ratio in the sheet of 0, 20, and 40 %, respectively, compared to the control beams.;

(7) The beams reinforced with non-pre-tensioned AFRP sheet failed by sheet debonding, starting from the tip of the critical diagonal crack at the lower concrete cover near the loading points. However, the beams reinforced with the pre-tensioned AFRP sheet failed by sheet rupture. This change in failure mode is probably due to pre-tensioning the sheet accompanied with a proposed anchoring method, which results in maintaining the pre-tensioned sheet perfectly bonded to the concrete surface up to the ultimate state.

2- Strengthening Study of pre-cracked RC beams

This study has examined the load-carrying behavior of pre-cracked RC beams strengthened with pre-tensioned sheet compared to non-pre-cracked ones. Pre-tension stress ratio introduced to the AFRP sheet (0 and 40%) and the level of prior loading (Level 1 is up to main rebar yielding; Level 2 is up to the average point between the main rebar yielding and ultimate load) were taken as variables, for which static four-point loading tests were conducted. From these experiments and numerical analyses, the following conclusions can be drawn:

(1) It is seen that compared to the control beam, yield and maximum loads of beams subjected to low preloading level and reinforced with non-pre-tensioned AFRP sheet are increased by 58 and 123%, respectively, and these loads are also increased by 145 and 188% for beams subjected to low preloading and reinforced with pre-tensioned AFRP sheet, respectively. In the case of beams subjected to high preloading level and reinforced with non-pre-tensioned AFRP sheet, yield and maximum loads are increased by 71 and 107% but they are increased by168 and 162, for beams subjected to high preloading level and reinforced with pre-tensioned AFRP sheet, respectively, comparable to the control beam.

(2) Thus, it can be noted that flexural stiffness of the pre-cracked RC beams can be significantly improved by bonding pre-tensioned AFRP sheet on the tension-side surface of the beams. And the tendency of the improvement is similar in spite of the magnitude of the loading level for pre-cracking. Therefore, a proposed anchoring method without anchoring devices has shown to be feasible in case of the pre-cracked RC beams;

(3) Pre-tensioned AFRP sheet has retained enough bonding capacity up to the ultimate state of the beams in the case of prior loading with large residual deflection;

(4) Flexural reinforced pre-cracked beams with normal AFRP sheet tend to reach the ultimate state earlier due to the existing residual upper fiber strain of concrete;

(5) However, when reinforcing the beams with pre-tensioned AFRP sheet, the opening of

the cracks that occurred due to prior loading can be restrained and residual strains can be decreased;

(6) In the case of reinforcing the severely damaged RC beams with pre-tensioned AFRP sheet, repairing the cracks should be carefully treated before reinforcing in order to restrain the sheet rupture and;

(7) It is not recommended to use numerical analysis using a multi-section method to predict the flexural behavior of pre-cracked RC beams strengthened with pre-tensioned AFRP sheet subjected to high prior loading level (more than the yielding point of the main rebar) due to severe damage in the beam because the existing cracks and the stiffness of putty used for flattening the bonding surface were not considered in numerical analysis.

3-Repair Study of pre-cracked RC beams

This study has investigated the effectiveness of pre-tensioned AFRP systems to restore the capacity of repaired pre-cracked RC beams reinforced with pre-tensioned sheet. In this study, pre-tension stress ratio introduced to the FRP sheet (0 and 40%), with/without existing cracks and with/without repairing the cracks were taken as variables.

In this study, in order to investigate the effects of the existing cracks on load-carrying behavior of the reinforced existing RC members with pre-tensioned AFRP sheet, four-point loading tests of the flexural reinforced RC beams with pre-tensioned AFRP sheet were conducted. From this experiment, the following results were obtained:

(1) Due to bonding pre-tensioned AFRP sheets on the tension-side surface of the existing RC beams, flexural load-carrying capacity can be significantly improved;

(2) Even though the existing cracks were not repaired, bonding capacity of the sheet has been kept up to the analytical ultimate state;

(3) In repairing the existing cracks, the opening of cracks and the increase of the strains introduced in the sheet due to those cracks can be effectively restrained and strain around the cracks being flattened not localized so sheet rupture can be prevented;

(4) It is very important for preventing the sheet rupture to repair the existing cracks before

reinforcing with the pre-tensioned AFRP sheet in the field;

(5) The experimental load-carrying behavior of the pre-cracked RC beams reinforced with non-pre-tensioned or pre-tensioned AFRP sheet will be more than those of numerical results because the existing cracks and the stiffness of putty used for flattening the bonding surface were not considered in numerical analysis; and

(6) Numerical results can better match the experimental results for non-pre-cracked beams but not for pre-cracked beams subjected to prior loading up to the middle point between the main rebar steel yielding and the ultimate state.

REFERENCES

1. Carolin, A.: Carbon Fiber Reinforced Polymers for Strengthening of Structural Elements", Doctoral Thesis, Luleå University of Technology, 2003.
2. Nanni, A, "Composites: Coming on Strong", Concrete Construction, vol. 44, 1999, pp. 120.
3. ACI Committee 440: State-of-the-Art Report on FRP for Concrete Structures (ACI440R-96), ACI Manual of Concrete Practice, American Concrete Institute, 1996.
4. Oehlers, D.J.: Reinforced Concrete Beams with Plates Glued to their Soffits", Journal of Structural Engineering, V.118, No. 1, 1990.
5. Swamy, R.N., Hobbs, B., and Roberts, M.: Structural Behavior of Externally Bonded, Steel Plated RC Beams after Long-Term Exposure, the Structural Engineer, Vol. 73, No. 16, 1995.
6. Yeong-Soo Shin and Chadon Lee.: Studied flexural behavior of reinforced concrete beams strengthened with carbon fiber-reinforced polymer laminates at different levels of sustaining load, ACI Struct. J., Vol. 100, Issue 2, March 2003, pp. 231-239.
7. Federico A. Tavarez, Lawrence C. Bank, and Michael E. Plesha.: Analysis of fiber-reinforced polymer composite grid reinforced concrete beams, ACI Struct. J., Vol. 100, Issue 2, March 1, 2003, pp. 250-258.
8. H. Saadatmanesh and M.R. Ehsani: Fiber composite plates can strengthen beams, Concrete International, ACI 123, 1990, pp. 65-71.
9. Omar Chaallal, Munzer Hassan, and Mohsen Shahawy: Confinement model for axially loaded short rectangular columns strengthened with fiber-reinforced polymer wrapping, ACI Struct. J., Vol. 100, Issue 2, March 1, 2003, pp. 215-221.
10. Ayman M. Okeil, Sherif El-Tawil, and Mohsen Shahawy: Short-Term Tensile

Strength of Carbon Fiber-Reinforced Polymer Laminates for Flexural Strengthening of Concrete Girders, ACI Struct. J., Vol. 98, Issue 4, July 1, 2001, pp. 470-478.

11. Houssam Toutanji and Gerardo Ortiz: The effect of surface preparation on the bond interface between FRP sheets and concrete members, J. Composite Structures,Vol. 53, Issue 4, Sep. 2001, pp. 457-462.
12. Mohsen Shahawy, Omar Chaallal, Thomas E. Beitelman, and Adnan El-Saad: Flexural strengthening with carbon fiber-reinforced polymer composites of preloaded full-scale girders, ACI Struct. J., Vol. 98, Issue 5, Sept. 1, 2001, pp. 735-742.
13. Laura De Lorenzis, Brian Miller, and Antonio Nanni: Bond of fiber-reinforced polymer laminates to concrete, ACI Materials Journal/ May-June 2001, pp 256-264.
14. J. G. Teng, S. Y. Cao and L. Lam: Behavior of GFRP-strengthened RC cantilever slabs. Construction and Building Materials,Vol.15, Issue 7,Oct. 2001, pp. 339-349.
15. Zhishen Wu and Jun Yin: Fracturing behaviors of FRP-strengthened concrete structures, Engineering Fracture Mechanics. Vol. 70, Issue 10, July 2003, Pages 1339-1355.

.16 Thanasis C. Triantafillou: Shear strengthening of reinforced concrete beams using epoxy-bonded FRP composites, ACI, Struct. J., Vol. 95, Issue2, March 1, 1998, pp.107-115.

.17 Sergio F. Breña, Regan M. Bramblett, Sharon L. Wood, and Michael E. Kreger: Increasing flexural capacity of reinforced concrete beams using carbon fiber-reinforced polymer composites, ACI, Struct. J., Vol. 100, Issue1, Jan.1, 2003, pp. 36-46.

.18 N. F. Grace, G. A. Sayed, A. K. Soliman and K. R. Saleh: Strengthening reinforced concrete beams using fiber reinforced polymer (FRP) laminates, ACI, Struct. J., Vol. 96, Issue 5, Sep. 1, 1999.

19. Lopiz-Anido R., Gupta R., Ganga Rao H., Halabe H., Kshirsagar S. and Frankin, R.: Evaluation of a new rehabilitation technology for bridge piers with composite materials, IDEA Report NCHRP-33, Transportation Research Board, National Research Council, National Academy of Science, Washington D.C., 1999.

20. Osman Hag-Elsafi, Sreenivas Alampalli and Jonathan Kunin: Application of FRP laminates for strengthening of a reinforced-concrete T-beam bridge structure, J. Composite Structures, Vol. 52, Issues 3-4, May-June 2001, pp. 453-466.
21. Zobel, R.S. and Jirsa, J.O.: Performance of Strand Splice Repair in Prestressed Concrete Bridges, PCI Journal V.43 No.6, 1998, pp. 72-84.
22. Stallings, J.M., Tedesco, J.W., El-Mihilmy, M., McCauley, M.: Field Performance of FRP Bridge Repairs, Journal of Bridge Engineering, Vol. 5, No.5, 2000, pp. 107-113.
23. Schiebel, S., Parretti, R., Nanni, A.: Repair and Strengthening of Impacted PC Girders on Bridge A4845, Missouri Department of Transportation Report RDT01-017/RI01-016, 2001.
24. Tumialan, J.G., Huang, P.C, Nanni, A.: Strengthening of an Impacted PC Girder on Bridge A10062." Final Report RDT01-013/RI99-041, Missouri DOT, St. Louis County, MO, 2001, pp. 41.
25. Di Ludovico, M.: Experimental Behavior of Prestressed Concrete Beams Strengthened with FRP, Report CIES 03-42, University of Missouri-Rolla, MO,2003.
26. Klaiber, F. W., Wipf, T.J., Kempers, B.J.: Field Laboratory Testing of Damaged Prestressed Concrete (P/C) Girder Bridges, Iowa Department of Transportation Report HR-397, 1999.
27. Green, P.S., Boyd, A.J., Lammert, K., and Ansley, M.: CFRP repair of impact damaged bridge girder Volume 1: Structural evaluation of impact-damaged prestressed concrete I girders repaired with FRP materials," Florida Department of Transportation Structures Research Report 922, 2004, pp.194.
28. Di Ludovico, M., Nanni, A., Prota, A., & Cosenza, E.: Repair of Bridge Girders with Composites: Experimental and Analytical Validation, ACI Structural Journal, Vol. 102 Vol.No.5, 2005, pp.639-648.
29. El-Tawil, S. and Okeil, A. M.: LRFD Flexural Provisions For PSC Bridge Girders Strengthened with CFRP Laminates, ACI Structural Journal, Vol. 99, No.2, 2002, pp. 300-310.
30. G.F. Zhang, N. Kishi, H. Mikami, and M. Komuro: A numerical prediction method for

flexural behavior of RC beams reinforced with FRP sheet, Proceedings of International Symposium on Bond Behaviour of FRP in Structures, 2005, International Institute for FRP in Construction.

31. Kishi N., Mikami H., and Zhang G.: Numerical cracking and debonding analysis of RC beams reinforced with FRP sheet, ASCE CC J., Vol.9 No.6, 2005a, pp. 507-514.
32. Mikami H., Kishi N., and Kurihashi Y.: Flexural bonding property of FRP sheet adhered to RC beams, 16th Congeress of IABSE, Lucerne, Swiss, Paper 252, 2000, CD-ROM.
33. Kishi N., Zhang G., Mikami H., Kurihashi Y.: Effects of rebar yielding on failure behavior of flexural reinforced RC beams with FRP sheet, proceedings of FRPRCS-8 University of Patras, Patras, Greece, 2007, July 16-18.
34. Kurihashi Y., Kishi N., Mikami H., Sawada S.: A proposal of design procedure for flexural strengthening RC beams with FRP sheet, proceedings of the first fib congress, composite structures, 2007,pp.157-164.
35. Sawada, S., Kishi, N., Mikami, H., and Kurihashi, Y.: An Experimental Study on Debond-Control of AFRP for Flexural Strengthened RC Beams", Proceedings of FRPRCS-6, 2003, pp.287-296.
36. Zhang GF, Kishi N, and Mikami, H.: Influence of Material Properties of FRPS on Strength of Flexural Strengthened RC Beams. Proceedings of FRPRCS-6, 2003, pp.327-336.
37. Zhang GF, Kishi N, and Mikami, H.: Effects of bonding configuration on shear behavior of RC beams reinforced with aramid FRP sheets, FRPRCS-8 University of Patras, Patras, Greece, July, 2007, pp.16-18.
38. Mahmoud M. Hashem, Youssef L. Zaki, Magdy N. Salib, and Ahmed A. Hamouda: Behavior of pre-cracked RC beams strengthened with CFRP sheets, American Society of Civil Engineering, 6th International Engineering and Construction Conference (IECC'6), Cairo, Egypt, June 28-30, 2010, pp. 809-820.
39. Süleyman Adanur, Ahmet Can Altunışık, and Abdurrahman Keskin: Comparison of analysis results of footbridges using steel and CFRP materials, American Society of

Civil Engineering, 6th International Engineering and Construction Conference (IECC'6), Cairo, Egypt, June 28-30, 2010, pp.581-588.

40. Osman, Shallan, Hesham F. Shaaban, and Maher k.mohamed : Numerical analysis of strengthening flat slab using carbon fiber-reinforced polymer, American Society of Civil Engineering, 6th International Engineering and Construction Conference (IECC'6), Cairo, Egypt, June 28-30, 2010, pp. 615-625.
41. Ramadan Abd-Al Aziz Askar, M. M. A. El- Metawally, and A. Abd- Al khalek. :Behavior of R.C. box girders strengthened using CFRP sheets, American Society of Civil Engineering, 6th International Engineering and Construction Conference (IECC'6), Cairo, Egypt, June 28-30, 2010, pp.569-580 .
42. Triantafillou, T. C. and Deskovic, N.: Innovative pre-stressing with FRP sheets: mechanics of short-term behaviour." J. Eng. Mech., Vol.117, No.7, 1991, pp. 1652-1672.
43. Triantafillou, T. C., Deskovic, N. and Deuring, M.: Strengthening of concrete structures with prestressed fiber reinforced plastic sheets, ACI Struct. J., Vol. 89, No.3, 1992, pp. 235-244.
44. Quantrill RJ, Hollaway LC.: The flexural rehabilitation of reinforced concrete beams by the use of prestressed advanced composite plates, Compos Sci Technol, 58, 1998, pp.1259–1275.
45. Wight R. G., Green, M. F., and Erki, M. A.: Prestressed FRP sheets for poststrengthening reinforced concrete beams, J. Compos. Constr., Vol.5, No.4, 2001, pp. 214–220.
46. El-Hacha R., Wight, R. G., and Green, M. F.: Innovative system for prestressing fiber-reinforced polymer sheets, ACI Struct. J., Vol.100, No.3, 2003b, pp. 305–313.
47. El-Hacha R., Wight, R. G., and Green, M. F.: Prestressed carbon fiber-reinforced polymer sheets for strengthening concrete beams at room and low temperatures." J. Compos. Constr.,Vol. 8, No.1, 2004, pp. 3–13.

48. Huang Y.; WU J., Yen T., Hong C., and Lin Y.: Strengthening Reinforced Concrete Beams Using Prestressed Glass Fiber-Reinforced Polymer Part 1: Experimental Study, Journal of Zhejiang University Science 6A (3), 2005, pp. 166-174.

49. Sang-Kyun Woo, Jin-Won Nam, Jang-Ho Jay Kim, Sang-Hoon Han, Keun Joo Byun: Suggestion of flexural capacity evaluation and prediction of prestressed CFRP strengthened design, Eng. Struct. J. Vol.30, No.12, 2008, pp. 3751-3763.

50. Dong-Suk Yang, Sun-Kyu Park, Kenneth W. Neale: Flexural behaviour of reinforced concrete beams strengthened with prestressed carbon composites, J.Compos. Struct., Vol. 88 No.4, 2009, pp. 497-508.

51. Stöcklin I., and Meier, U.: Strengthening of concrete structures with prestressed and gradually anchored CFRP strips I., Proc. of FRPRCS-5, London, 2001, pp. 291-296.

52. Stöcklin I., and Meier, U.: Strengthening of concrete structures with prestressed and gradually anchored CFRP strips II., Proc. of FRPRCS-6, Singapore, 2001, pp. 1321-1330.

53. Czaderski C., and Motavalli, M.: 40-year-old full-scale concrete bridge girder strengthened with prestressed CFRP plates anchored using gradient method, J. Composites, Part B, Vol. 38, No.7–8, 2007, pp. 878–886.

54. Mohammad Reza Aram, Christoph Czaderski, and Masoud Motavalli: Effects of gradually anchored prestressed CFRP strips bonded on prestressed concrete beams." J. Compos. for Constr., Vol.12, No.1, 2008, pp. 25-34.

55. Ferrier E., Ennaceur C., Bigaud D., and Hamelin P.: Prestressed externally bonded FRP reinforcement for RC beams, Proc. of FRPRCS-5, London, 2004, pp. 271-280.

56. Kim Y. J., Chen Shi, and Mark F. Green: Flexural strengthening of RC beams with prestressed CFRP sheets: development of nonmetallic anchor systems, J. Compos. for Constr., Vol.12, No.1, 2008a, pp. 35-43.

57. Kim Y. J., Chen Shi, and Mark F. Green: Flexural strengthening of RC beams with prestressed CFRP sheets: using nonmetallic anchor systems, J. Compos. for Constr. Vol.12, No.1, 2008b, pp. 44-52.

58. Kim, Y. J., Jesse M. Longworth, R. Gorden Wight, and Mark F. Green: Flexure of two-way slabs strengthened with prestressed or non-prestressed CFRP sheets, J. Compos. for Constr., Vol.12, No.4 August, 2008c, pp. 366-374.

59. Piyong Yu, Pedro F. Silva, and Antonio Nanni: Description of a mechanical device for prestressing of carbon fiber-reinforced polymer sheets - Part I, ACI Struct. J., Vol.105, No.1, 2008, pp. 3-10.

60. Piyong Yu, Pedro F. Silva, and Antonio Nanni: Description of a mechanical device for prestressing of carbon fiber-reinforced polymer sheets - Part II, ACI Struct. J., Vol.105, No.1, 2008, pp.11-20.

61. Ikeda, S., Kishi, N., Mikami, H., and Zhang, G: Experimental study of flexural strengthened PC beams with pre-tensioned FRP sheet, JCI Annual J., Vol.29, No.3, 2007, pp 1501-1506, in Japanese.

62. N. Kishi, H. Mikami, Y. Kurihashi, and S. Sawada: Flexural behavior of RC beams reinforced with NSM AFRP RODS, Proceedings of International Symposium on Bond Behavior of FRP in Structures, 2005b, pp. CD ROM.

63. Carolin, A. Nordin, M. and Taljsten, B., Concrete beams strengthened with near surface mounted reinforcement of CFRP, Proceedings of the International Conference on FRP Composites in Civil Engineering, Hong Kong, China, 2001, pp. 1059- 1066.

64. Hassan T. and Rizkalla, S.: Investigation of bond in concrete structures strengthened with near surface mounted CFRP strips, ASCE, Journal of Composites for Construction, Vol. 7, No.3, 2003, pp.248-257.

65. Hassan, T., Rizkalla, S.: Bond mechanism of NSM FRP bars for flexural strengthening of concrete structures, ACI Structural Journal, Vol. 101, No. 6, Nov.-Dec., 2004.

66. El-Hacha, R., Rizkalla, S.: Near-surface-mounted fiber-teinforced-polymer reinforcements for flexural strengthening of concrete structures," ACI Structural Journal, Vol. 101, No. 5, Sep.-Oct., 2004.

67. Yost J.R., Gross S.P., and Dinehart D.W.: Near surface mounted CFRP reinforcement for structural retrofit of concrete flexural members," Proceedings of the 4th

international conference on Advanced Composite Materials in Bridges and Structures (ACMBS 2004), Calgary, Alberta, Canada, 2004.

68. Barros J.A.O., and Fortes A.S.: Flexural strengthening of concrete beams with CFRP laminates bonded into slits, Cement and Concrete Composites Journal, Vol. 28, No. 2, 2005, pp. 471-480.
69. Barros J.A.O., Ferreira D. R.S.M., Fortes A.S., and Dias S.J.E.: Assessing the effectiveness of embedding CFRP laminates in the near surface for structural strengthening, Construction and Building Materials Journal, 20, 2006, pp. 478-491.
70. Aidoo J., Harries K.A., and Petrou M.F.: Full-scale experimental investigation of repair of reinforced concrete interstate bridge using CFRP materials, American Society of Civil Engineers (ASCE), Journal of Bridge Engineering, Vol. 11, No. 3, 2006, pp. 350-358.
71. Nordin H. and Taljsten B.: Concrete beams strengthened with prestressed near surface mounted CFRP, American Society of Civil Engineers (ASCE), Journal of Composites for Construction, Vol. 10, No. 1, 2006, pp. 60-68,.
72. Triantafillou, T. C., and Plevris, N.: Strengthening of RC beams with epoxy-bonded fibre-composite materials, Materials and Structures, Vol. 25, 1992, pp. 201-211.
73. Renata Kotynia, Hussien Abdel Baky, Kenneth W. Neale, M.ASCE, and Usama A. Ebead: Flexural strengthening of RC beams with externally bonded CFRP Systems: Test Results and 3D Nonlinear FE Analysis, Journal of Composites for Construction, Vol. 12, No. 2, April 1, 2008, pp.190-201.
74. Aram, M. R., Christoph Czaderski, and Masoud Motavilli: Debonding failure modes of flexural FRP-strengthened RC beams, Journal for Composites Part B, 2007, pp.
75. Gibson, R.F.: Principles of composite material mechanics," McGraw-Hill Science, New York, USA, 1994.
76. Nanni, A.: Fiber reinforced plastic materials]. The First Middle East Workshop on Structural Composites, Sharm El-sheikh, Egypt, 14-16 June, 1996.
77. Larralde, J. and Hamid, A.A.: Utilization of advanced composite materials in civil engineering applications", Fifth International Colloquium on Concrete in Developing

Countries, Cairo, Egypt, Jan. 1994, PP. 896-907.

78. ACI Committee 440: State-of-the-Art Report on FRP for Concrete Structures (ACI 440R-96), ACI Manual of Concrete Practice, American Concrete Institute, 1996.

79. Abdelrahman, A.A., and Rezkallah, S.H.: Advanced composites for concrete structures,The Fifth international colloquium on concrete in developing countries, Egypt, 1996.

80. American Concrete Institute (ACI), State-of-The-Art Report: Fiber reinforced plastic (FRP) reinforcement for concrete structure, Reported by ACI Committee 4140, 1995.

81. Moukwa, M.: Molecular structure and properties of thermosetting resins used in advanced composites materials, Advanced Composites Materials in Bridges and Structures (ACMPS-II). Proceedings of the Second International Conference, Montreal, Quebec, Canada, 1996, pp. 83-90.

82. Saadatmanesh, H., and Ehsani, M. R.: 'RC beams strengthened with GFRP plates. I: Experimental study, J. Struct. Eng., ASCE, Vol.117, No.11, 1991, pp. 3417–3433.

83. Kim, Y. J., Chen Shi, and Mark F. Green: Ductility and cracking behavior of prestressed concrete beams strengthened with prestressed CFRP sheets, J. Compos. for Constr., Vol.12, No.3, 2008d, pp. 274-283.

84. Kim, Y. J., Green, M. F., and R. Gordon Wight: Live load distributions on an impact-damaged prestressed concrete girder bridge repaired using prestressed CFRP sheets, J. Compos. for Constr., Vol.11, No.2 March, 2008e, pp. 202-210.

85. Kim, Y. J., Green, M. F., Fallis, G. J.: Repair of bridge girder damaged by impact loads with prestressed CFRP sheets." J. Compos. for Constr., Vol.13, No.1, Jan. 2008f, pp. 15-23.

86. Kim, Y. J., Bizindavyi, L., and Green, M. F.: Applicability of steel anchor plates for prestressing multilayered CFRP sheets, 4th Int. Conf. on Advanced Composite Materials in Bridges and Structure, CD-ROM, ACMBS-IV, CSCE, Calgary, Alta, Canada, 2004.

87. Kim, Y. J., Green, M. F., Fallis, G. J., Wight, G. R., and Eden, R.: Damaged bridge girder strengthening: Field application of prestressed fiber-reinforced polymer

sheets." PCI J., Vol.28 No.11, 2006, pp. 47–52.

88. Japan Society of Civil Engineers: Standard specifications for concrete structures-2002," Structural performance verification, Tokyo, Japan, 2002.

89. Kishi N., Mikami H., Kurihashi Y. and Abdel Aziz M. Aly.: Load carrying behavior of flexural reinforced RC beams with pre-tensioned AFRP sheets, proceedings of FRPRCS-9 Sydney, Australia, 2009, July 13-15.

90. S. Sawada, N. Kishi, H. Mikami, Abd-Al Aziz M. ALY, Y. Kurihashi: Static loading test of the flexural reinforced PC beams with pre-tensioned AFRP sheet, Proceedings of JSCE 2009 annual meeting, 2009, pp. 1093-1094.

91. Abdel Aziz M. ALY, Kishi N., Mikami H., and Kurihashi Y.: Effect of pre-tension force of AFRP sheet on load-carrying behavior of reinforced RC beams, Proceedings of JSCE 2010 annual meeting, V-597, 2010a, pp.1193-1194.

92. Abdel Aziz M. ALY, Kishi N., Kurihashi Y.,and Mikami H.,: Flexural strengthening effect due to bonding pre-tensioned AFRP sheet to pre-cracked RC beams using a simple anchoring method, American Society of Civil Engineering, 6th International Engineering and Construction Conference (IECC'6), Cairo, Egypt, June 28-30, 2010b, pp.893-900.

93. Y. Kurihashi, N. Kishi and Abdel Aziz M. Ali: Load-carrying capacity of flexural reinforced PC beams with pre-tensioned AFRP sheet, Proceedings of CICE, Beijing, China, Sept., 27-29, 2010.

Publications